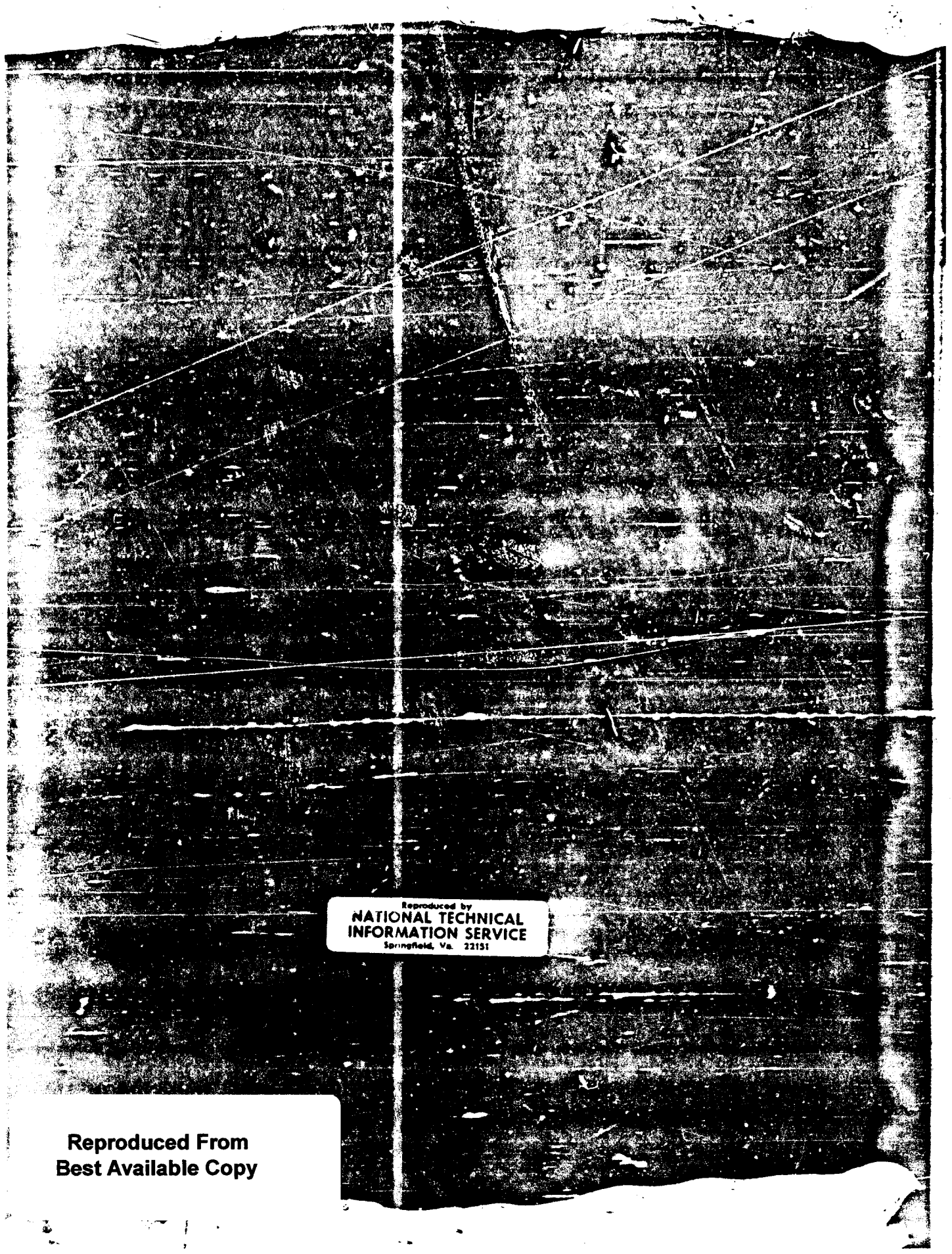

GAS TURBINE CYCLE CALCULATIONS: EXPERIMENTAL VERIFICATION OF OFF-DESIGN-POINT PERFORMANCE PREDICTIONS FOR A TWO-SPOOL TURBOJET WITH VARIOUS AIR BLEEDS

by

M.S. CHAPPELL AND W. GRABE

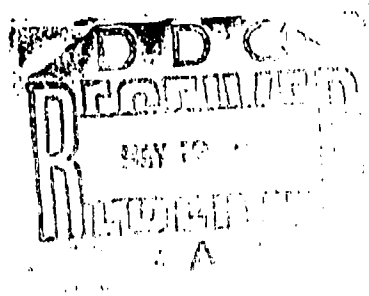

E.P. Cockshutt, Head
Engine Laboratory

D.C. MacPhail
Director

SUMMARY

As part of a continuing program of gas turbine cycle calculations, the Engine Laboratory of the National Research Council of Canada has proposed a simplified method for calculating off-design-point performance of turbojet and turbofan engines, both at sea level static and at altitude flight conditions. This method specifically implies constancy of component efficiencies and linearity of corrected mass flow with corrected engine speed.

During a series of tests on a J-75 two-spool turbojet engine, experimental data were gathered at part-throttle conditions, and subsequently with compressor bleed extraction and with propelling nozzle area change.

In general, the calculation routine yielded very good predictions of the part-throttle performance of the datum engine. It was far less successful, however, in forecasting the effects of compressor bleed extraction, propelling nozzle area change, and combinations of these perturbations to the basic cycle.

TABLE OF CONTENTS

ILLUSTRATIONS

ILLUSTRATIONS (Cont'd)

ILLUSTRATIONS (Cont'd)

APPENDICES

GAS TURBINE CYCLE CALCULATIONS: EXPERIMENTAL VERIFICATION OF OFF-DESIGN-POINT PERFORMANCE PREDICTIONS FOR A TWO-SPOOL TURBOJET WITH VARIOUS AIR BLEEDS

1.0 INTRODUCTION

The Engine Laboratory is engaged in a continuing program of generating Gas Turbine Cycle Calculation routines of sufficient flexibility and rigour to have wide applicability for aircraft performance studies. References 1, 2, 3, and 5 are members of the series of reports describing these cycle analysis programs. In particular, Reference 1 describes the performance prediction program for turbojet and turbofan engines operating at part-throttle, both at sea level static and at altitude flight conditions. The predictions are based on constant component efficiencies and a linear relation between corrected air mass flow and corrected L.P. compressor speed. Further details are given in Section 4.0.

As part of another investigation (Ref. 6) a two-spool turbojet engine was installed in the Laboratory's No. 4 Test Cell during the summer of 1970 (Fig. 1). This provided an opportunity to compare the performance predictions of the Off-Design-Point (O.D.P.) program (Ref. 1) with experimental data. In addition to the comparison of measured and predicted part-throttle performance, the current investigation compares the observed and calculated effects of substantial bleed extraction from the H.P. compressor delivery plenum, of variations in propelling nozzle area, and of combinations of these two perturbations to the basic engine cycle.

2.0 EXPERIMENTAL ARRANGEMENT

2.1 Engine and Installation

The experimental data for this verification were measured on a J-75/P-3 two-spool turbojet. This early version of the J-75 engine series comprised a ten-stage L.P. compressor driven by a two-stage turbine, and a seven-stage H.P. compressor driven by a single-stage turbine. Twin anti-surge bleeds were fitted between the compressor spools to vent approximately 6% of the L.P. compressor mass flow at L.P. spool speeds below about 78%, (Fig. 2). The main combustor was of the can-annular type. The engine was fitted with an afterburner and a two-position propelling nozzle (Fig. 3), however the afterburner was not used during this test program.

The engine was installed in No. 4 Test Cell during the summer of 1970, as illustrated in Figure 1.

2.2 Provisions for Bleed Extraction

The term "Main Bleed" as used in this report refers to the extraction of H.P. compressor delivery air for purposes not directly related to the operation of the J-75 engine. This bleed was in addition to the anti-surge bleeds (described in Section 2.1) that were necessary for the proper functioning of the engine.

Main bleed air was extracted from the diffuser between the H.P. compressor delivery annulus and the combustor inlet plenum. Four separate ports were fitted as standard equipment on the J-75 engine. Two 3-inch diameter offtakes were provided

TABLE I

INSTRUMENTATION

STATION	PARAMETER MEASURED	SENSOR TYPE AND LOCATION	READOUT		
			INSTRUMENT TYPE	RANGE	ESTIMATED ACCURACY
		THERMODYNAMIC PARAMETERS			
0	Barometric Pressure	Mercury Barometer	Direct Reading	26 to 32"Hg	0.005"Hg
1	Test Cell Depression	Open Tube on Test Cell Wall 10 Feet Forward of Engine	Manometer	0 to 20"H_2O	0.05"H_2O
2	Intake Static Pressure	4 Wall Taps (Ganged) at the Bellmouth Exit	Manometer	0 to 80"H_2O	0.05"H_2O
	Intake Total Temperature	4 Thermistor Probes at the Bellmouth Exit	Direct Reading Galvanometer	-40 to +150°C	0.1°C
3	L.P. Compressor Delivery Total Pressure	2 5-Point Radially Averaging Rakes (Ganged)	Bourdon Gauge	0 to 147 psig	0.1 psi
	L.P. Compressor Delivery Total Temperature	2 Single FE/CON Thermocouple Probes (at 1/3 and 2/3 Radii) Readout Separately	Bristol Pyrometer	0 to 450°C	1.0°C
4	H.P. Compressor Delivery Total Pressure	2 5-Point Radially Averaging Rakes (Ganged)	Bourdon Gauge	0 to 200 psig	1.0 psi
	H.P. Compressor Delivery Total Temperature	2 Single FE/CON Thermocouple Probes (at 1/3 and 2/3 Radii) Readout Separately	Bristol Pyrometer	0 to 450°C	1.0°C
5	L.P. Turbine Outlet Total Pressure	3 5-Point Radially Averaging Probes (Ganged)	Bourdon Gauge	0 to 200"Hg	0.1"Hg
	L.P. Turbine Outlet Total Temperature	a. 4 Single CR/AL Thermocouple Probes at Mid-Radius (Ganged)	Bristol Pyrometer	0 to 1200°C	2.0°C
		b. 3 5-Point Radially Averaging CR/AL Thermocouple Probes	Bristol Pyrometer	0 to 1200°C	2.0°C
		MISCELLANEOUS PERFORMANCE PARAMETERS			
	L.P. Spool Speed	Aircraft Tachometer Generator	Aircraft Dial Gauge	0 to 110%	0.1%
	H.P. Spool Speed	Aircraft Tachometer Generator	Aircraft Dial Gauge	0 to 100%	0.1%
3	Anti-Surge Bleed Total Pressure	2 20-Point Averaging Rakes Separate Readouts Port and Starboard	Manometers	0 to 80"M-3	0.05"M-3
	Anti-Surge Bleed Total Temperature	Single Point FE/CON Thermocouple Probe in Each of Two Bleed Pipes	Bristol Pyrometer	0 to 450°C	1.0°C
4	Fuel Flow Rate	Turbine Meter in L.P. Line	Frequency Converter and Self-Balancing Potentiometer, Direct Reading	0 to 20,000 lb/hr	10 lb/hr
5	Thrust	Hydraulic Load Cell at Forward End of Floating Test Bed	Bourdon Gauge	0 to 30,000 lb	10 lb
		MAIN BLEED EXTRACTION FLOW PARAMETERS			
4	Bleed Total Temperature	Single FE/CON Thermocouple Probe Upstream of Measuring Orifice in Main Bleed Pipe	Bristol Pyrometer	0 to 450°C	1.0°C
	Measuring Orifice Upstream Pressure	Single Wall Tap	Bourdon Gauge	0 to 147 psig	0.1 psig
	Measuring Orifice Differential Pressure	¼-Diameter Wall Taps	Manometer	0 to 80"M-3	.05"M-3
	Orifice Plate Metal Temperature	Single Buried FE/CON Thermocouple Probe	Bristol Pyrometer	0 to 450°C	1.0°C
	Bleed Total Pressure	Single Pitot at ⅔ Radius	Bourdon Gauge	0 to 200 psig	1.0 psig
		OPERATIONAL PARAMETERS			
	Fuel Inlet Pressure	Wall Tap at Entry to Engine Fuel System	Bourdon Gauge	0 to 100 psig	1.0 psi
	Oil Temperature	Thermocouple Probe in Accessory Gearbox	Galvanometer	0 to 250°C	1.0°C
	Oil Pressure	Oil Pump Delivery Line	Bourdon Gauge	0 to 100 psig	1.0 psi
	Oil Tank Breather Pressure	Oil Tank Vent Line	Manometer	0 to 40"M-3	0.05"M-3
	Vibration Intake, Interspool, H.P. Compressor Delivery, Turbine	Seismic Mass Accelerometers Mounted in the Horizontal Plane at all Four Stations	Integrating Meter with Direct Displacement Readout	0 to 5 thou	0.1 thou

for cabin pressurization and air conditioning. Two additional 1½-inch diameter ports were provided to supply anti-icing air for protecting the intake components of the engine. Only one of these latter two ports would normally be used, the other being provided for alternative accessory locations. To achieve the main bleed flow rates required for the companion investigation, all four ports were connected to a header plenum as shown in Figures 2 and 4. Part way through the program a fifth port, identical with the two cabin bleed offtakes, was added in an attempt to increase the main bleed flow rate further.

Main bleed air was discharged laterally through the two branches of the T-nozzle shown in Figures 3 and 4. This nozzle configuration was chosen to eliminate axial thrust generated by the main bleed efflux. Bleed flow rate was governed by the size of the two discharge orifices in the T-nozzle.

2.3 Instrumentation

Table I shows the instrumentation fitted to the engine for this test program. Station coding is defined in Sketch A. Figure 2 illustrates the anti-surge bleed extension pipe (port side) with the total pressure rake fitted. Figure 4 indicates the location of the main bleed flow measuring orifice and other bleed flow instrumentation points.

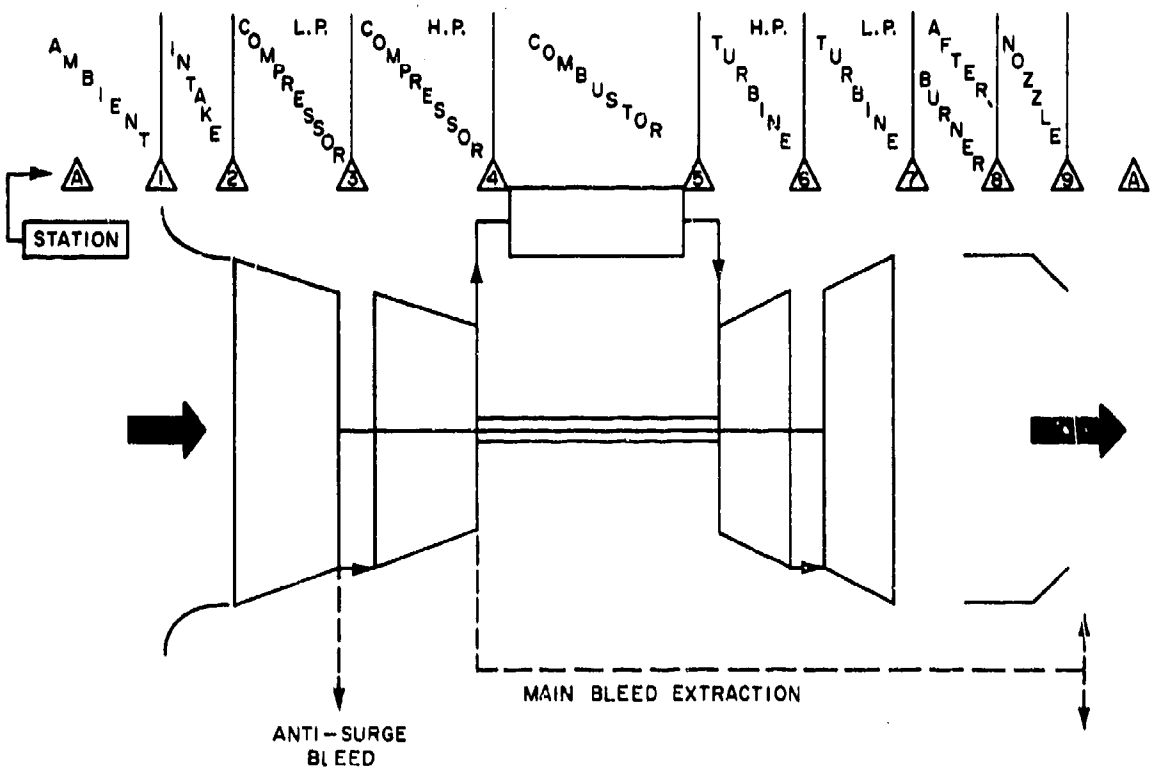

SKETCH A : THERMODYNAMIC CYCLE SHOWING BLEED EXTRACTION POINTS

2.4 Testing Technique

A Calibration Run was made from idle to Military power in steps of approximately 5% L.P. spool speed. Subsequent tests were then performed with successively increased bleed nozzle discharge orifices.

In all cases the limiting indicated turbine outlet temperature of 595°C was observed. Despite low ambient temperatures, this limit restricted the maximum operating speed whenever main bleed flow rates exceeded about 6% of the engine intake flow rate.

Later in the program, the engine propelling nozzle area was increased by adjusting the "closed position" stops (Fig. 3). This decreased the observed turbine outlet temperature and thus permitted operation to higher speeds and higher bleed flow rates.

A sample "Raw Data" log sheet is incorporated in Appendix A.

3.0 DATA REDUCTION PROCEDURE

The data reduction routine utilized the rigorous thermodynamic techniques outlined in Reference 2, as well as temperature and fuel-air-ratio dependent thermodynamic properties for the working fluid as outlined in Reference 5, to describe the processes within the various engine components. These techniques were used directly in evaluating parameters for which all required variables were measured, and indirectly, by trial and error, to establish values for variables that were not measured. All experimental data were corrected to standard-day inlet conditions of 15°C and 29.92" Hg.

The program was coded in Fortran IV for the NRC IBM System 360 TSS. Sample raw data and output sheets are included herein as Appendix A. Raw input data were tabulated together with the computed cycle parameters on a single output sheet for each test point. The output format was arranged in a style similar to that of the cycle analysis programs of References 1 and 2.

3.1 Intake Air Mass Flow Rate

Engine inlet air flow rate was calculated from total temperature and static pressure measurements taken near the exit from the entry bellmouth. Total pressure was determined from the local barometric pressure and the measured test cell depression. Inviscid one-dimensional flow assumptions were used initially. Later, a correlation was introduced to account for two-dimensional flow, based on an analysis of the flow in the bellmouth performed by Davis at Carleton University (Ref. 4).

3.2 Compressor Parameters

The L.P. and H.P. compressor pressure ratios and isentropic efficiencies were calculated directly from total pressure and total temperature measurements taken at inlet and exit from these components.

Anti-surge bleed flow rate was computed from total temperature and total pressure measurements made at the exit planes of the extension tubes fitted to the

bleed ports (see Fig. 2). Port and starboard flow rates were calculated separately and the sum was subtracted from the intake mass flow rate to give the H. P. compressor flow rate.

Work requirements for both compressor spools were determined from the appropriate temperature rise and mass flow rate data.

3.3 Main Bleed Flow Parameters

The main bleed flow rate was measured by a British Standard sharp-edged orifice situated between the prerequisite lengths of straight duct in the bleed discharge pipe (see Fig. 4). Total temperature and pressure were measured upstream of this orifice plate. A theoretical maximum available bleed horsepower was computed by assuming isentropic expansion from the bleed orifice inlet conditions to ambient total pressure. These data are grouped separately on the output sheet (see Appendix A).

3.4 Combustor and Turbine Inlet Conditions (A)

Combustor efflux conditions were predicted from H. P. compressor outlet measurements using the measured fuel flow rate (with an Effective Calorific Value in accordance with Ref. 5) and an assumed total pressure loss of 5%.

3.5 Turbine Parameters and Turbine Inlet Conditions (B)

Total temperature and total pressure were measured at the outlet of the L. P. turbine. The work requirements for the two compressor spools were used in conjunction with the turbine mass flow rate (adjusted from the H. P. compressor flow rate to account for main bleed extraction and fuel addition) to give a second estimate of the inlet temperature to the H. P. turbine. This value was printed below the value obtained from the combustor calculations of Section 3.4, and agreement to within about 3% was obtained in most cases.

The H. P. turbine inlet pressure was determined from the measured L. P. turbine outlet pressure by adjusting the assumed turbine efficiencies to give close agreement with the value derived from the combustor calculations of Section 3.4 (i.e. 95% of the H. P. compressor delivery pressure). No means were incorporated for changing turbine efficiencies in relation to engine speed and a constant value of 85% isentropic efficiency was found to give agreement to within about 5% over the useful operating range of the engine.

3.6 Propelling Nozzle Parameters and Overall Engine Performance

Calculated thrust was derived from measured values of L. P. turbine outlet temperature, nozzle mass flow rate, and (hot) final nozzle area, together with a thrust-multiplier type of nozzle 'efficiency' that accounted for real-flow deviations from the theoretical isentropic expansion process. An 'efficiency' value of 96% gave good agreement between calculated and measured thrust at all significant engine operating speeds. The nozzle-inlet total pressure determined during the thrust calculations was compared with the measured L. P. turbine outlet pressure to estimate the loss of total pressure in the afterburner tailpipe.

Specific thrust and specific fuel consumption completed the engine cycle printout, as shown in Appendix A.

4.0 THE OFF-DESIGN-POINT PERFORMANCE PREDICTION PROGRAM

The off-design-point (O.D.P.) cycle analysis program is one of the series of gas turbine cycle calculation routines generated at the Engine Laboratory. It predicts cycle parameters and engine performance for a range of decreasing engine speeds, both at sea level static and at altitude flight conditions. It is described fully in Reference 1 and hence only a brief outline will be presented herein.

The fundamental thermodynamic routines and the component subroutines are the same as used in the design point (D.P.) program of Reference 2. The O.D.P. program first calculates the 100% speed, sea level static case for the engine cycle specified by the input data (see Appendix B). The routine then resets the intake parameters to the altitude flight conditions specified in the input data and generates the 100% speed, altitude case. During this and all part-throttle cases, the turbine and propelling nozzle areas are fixed at the values established during the 100% speed, sea level static case. The program iterates throughout the entire cycle calculation until the areas are matched at each part-throttle speed. To aid convergence, the differential analysis technique of Reference 3 is used to predict the changes required in the major engine variables for each iteration.

The major assumptions incorporated within the O.D.P. program are:

(a) Component (compressor and turbine) efficiencies remain constant at the design point values

(b) Combustor efficiency, pressure losses, and nozzle thrust "efficiency" remain constant at the design point values

and (c) Corrected engine intake mass flow rate varies in direct proportion to the corrected L.P. compressor rotational speed.

Appendix B contains sample O.D.P. input and output sheets to illustrate their respective formats.

5.0 CORRELATION OF EXTERIMENTAL AND COMPUTED PERFORMANCE OF THE BASIC ENGINE

The term "Basic Engine" is used throughout this report to denote the geometric configuration of the J-75/P-3 engine as originally tested and matched to the computed cycle. Perturbations to the Basic Engine cycle were:

(a) Extraction of (massive) bleed air from the H.P. compressor outlet diffuser casing

(b) Increase of propelling nozzle area

and (c) Combinations of (a) and (b).

The thermodynamic cycle is depicted schematically in Sketch A, Section 2.3, including both anti-surge and main bleed extractions. It will be recalled that the anti-surge bleed from the L. P. compressor is required for normal engine operation at speeds below about 78%, irrespective of any additional main bleed air extraction from the H. P. compressor outlet diffuser.

5.1 Technique of Describing Anti-Surge Bleeds

The current version of the O. D. P. program has the capability of analysing an engine cycle in which different quantities of overboard bleed are extracted from the outlets of both compressor spools, at sea level static and at altitude flight conditions. The turbine and propelling nozzle areas are established for sea level static intake conditions with the bleed extraction quantities specified for the sea level static case. These areas remain fixed for all throttle settings at the altitude intake conditions and the altitude bleed quantity specified. This program feature provided simulation of the anti-surge bleeds on the J-75 engine, by processing two dual calculations (see below) both with the same (sea level static, no anti-surge bleed) base cycle. A negligible altitude of 15 feet was specified for the second part of each cycle in order to permit the incorporation of the interspool bleed at the lower speeds.

CYCLE I (a)	Sea Level	No A/S Bleeds	100% Speed
(b)	15 ft Altitude	No A/S Bleeds	100% Speed to 80% Speed
CYCLE II (a)	Sea Level	No A/S Bleeds	100% Speed
(b)	15 ft Altitude	6.1% A/S Bleed	100% Speed to 40% Speed (100% to 80% Discarded)

Cycles I(a) and II(a) are of course identical. Cycle I(b) describes engine performance at part-throttle speeds down to 80% where the anti-surge bleed ports are closed. Cycle II(b) describes engine performance at part-throttle speeds of 75% and below where approximately 6.1% anti-surge bleed is extracted from the L. P. compressor delivery plenum.

This technique was used to describe the extraction of anti-surge bleed air from the L. P. compressor in all J-75 cycles, both with and without main bleed extraction from the H. P. compressor.

5.2 Matching Computed Performance to Measured Data

Figures 6 to 17 show the comparison between the measured engine parameters and those predicted by the O. D. P. program for part-throttle settings down to 40% L. P. spool speed. The inputs for the Design Point cycle were selected to give reasonable agreement with the experimental data at the higher L. P. spool speeds (80% to 100% N_1). The thermodynamic parameters of the most representative Design Point cycle are listed, together with the comparable experimental values, in the following Table.

PARAMETER		EXPERIMENTAL	D.P. CYCLE
L.P. Compressor	PR	3.80	3.80
	η_{isent}	0.85 ave	0.85
	PL	(0.00)	0.00
Anti-Surge Bleed Flow		6.1% ave @ ≤ 78% N_1	6.10% @ ≤ 78% N_1
H.P. Compressor	PR	3.09	3.09
	η_{isent}	0.90 ave	0.91
	PL	(0.00)	0.00
Combustor	PL	(0.05)	0.05
	η_{cc}	(0.98)	0.98
Turbine Inlet Temperature		a 1187°K b 1201°K	1173°K
H.P. Turbine	η_{isent}	(0.85)	0.85
	η_{mech}	(1.00)	1.00
	PL	(0.00)	0.00
L.P. Turbine	η_{isent}	(0.85)	0.85
	η_{mech}	(1.00)	1.00
	PL	(0.06)	0.06
Propelling Nozzle	η_x	(0.96)	0.96
Performance at 100% N_1			
Specific Thrust		62.41 $lb_f/lb_m/sec$	64.08 $lb_f/lb_m/sec$
Specific Fuel Consumption		0.868 $lb_m/hr/lb_f$	0.852 $lb_m/hr/lb_f$

Experimental cycle values in parentheses were either inferred from measurements of other parameters or assumed.

No account was taken of accessory drive power extraction from either spool or for extraction and return of turbine disc cooling airflows.

It can be seen from Figures 6 to 17 that very close agreement was achieved between most measured and computed part-throttle data down to the speed at which the anti-surge bleed valves opened (about 78% N_1). The step-change in nearly all parameters

at the onset of anti-surge bleed flow was also accurately predicted by the O.D.P. program using the technique described in Section 5.1. The considerable scatter of compressor efficiencies, which were derived from measured engine data, is discussed in Section 5.4.

5.3 Implications of the Assumed Linear Relation Between Mass Flow and Low Pressure Spool Speed

Figure 7 shows the measured variation of intake air mass flow rate with L.P. spool speed compared with the O.D.P. program approximation of linear proportionality. One can see that, for this two-spool turbojet engine, the approximation underestimated the air mass flow rate by up to about 3% in the 100% to 75% speed range. Below 75% speed, the approximation continuously overestimated the intake flow rate, the discrepancy reaching a maximum of 7% at 40% L.P. spool speed.

The effect of this imperfect correlation on mass-flow-rate-dependent parameters such as fuel flow rate and thrust can be noted on Figures 11 and 15a respectively. Both parameters show increasing differences between experimental and computed values as engine speed decreases, the latter values being greater in both cases. However, the absolute magnitude of the error is not large, amounting to less than 3% at useful engine speeds of 75% and above.

Greater discrepancies in mass-flow-dependent performance parameters may be expected in high bypass ratio turbofan engine cycles where a significant proportion of the total engine performance is due to the unheated bypass stream.

5.4 Implications of Assumed Constant Compressor Efficiency

The experimentally determined values of L.P., H.P., and overall compressor efficiencies exhibited considerable scatter, as shown on Figures 8c, 9c, and 10c. An average isentropic efficiency, biased toward the higher operating speeds, was selected for the D.P. cycle. This value was converted to a polytropic efficiency for input into the O.D.P. program and the corresponding isentropic efficiencies were computed at each throttle setting (pressure ratio) for this fixed D.P. polytropic efficiency.

A strong decline in the measured efficiency of the L.P. compressor spool from 80% to 100% engine speed (Fig. 8c) was evident, and yet the part-throttle predictions of L.P. pressure ratio (Fig. 8a) and L.P. temperature rise (Fig. 8b) based on the constant polytropic efficiency are acceptably close to the measured values, even at engine speeds as low as 40%.

The measured values of the H.P. compressor efficiency do not show as strong a trend with engine speed (Fig. 9c) and hence the constant polytropic efficiency prediction more closely approximates the scattered experimental data. Moreover, excellent agreement between the measured and predicted values of pressure ratio and temperature rise across the H.P. compressor spool can be noted from Figures 9a and 9b at engine speeds down to about 70%. Below this speed, however, the H.P. compressor pressure ratio predicted by the O.D.P. program remains substantially constant

whereas the experimental values continue to fall significantly. This suggests that, in fact, the H.P. compressor efficiency drops more than the predicted data indicate in this low speed region. It will be noted also from Figure 6 that the O.D.P. program predicts considerably higher H.P. spool speeds than were measured at L.P. spool speeds of 70% and below.

The predicted overall compressor characteristics shown on Figures 10a, 10b, and 10c agree closely with the experimental values. Unlike the individual compressor characteristics, these overall experimental data are independent of measurements made at the interspool station (④) and the scatter is noted to be considerably less, even for the efficiency values shown on Figure 10c.

No experimental data were obtained to permit calculation of individual or overall turbine efficiencies. As detailed in Section 3, the assumed values of turbine efficiencies used in the experimental data reduction program were adjusted to give a reasonable match between turbine inlet pressures determined from upstream and downstream measuring stations. The same turbine efficiency values were used in the O.D.P. program simulation of the engine cycle.

6.0 COMPUTED AND MEASURED EFFECTS OF BLEED EXTRACTION FROM THE BASIC ENGINE

The major engine parameters affected by the extraction of main bleed air from the H.P. compressor delivery plenum are:

1. L.P. and H.P. compressor operating lines
2. Turbine inlet and turbine outlet temperatures
3. Thrust
4. Specific fuel consumption.

In general terms, main bleed extraction will: increase the surge margin of both L.P. and H.P. compressors; increase both turbine inlet and turbine outlet temperatures (and the turbine temperature drop); decrease specific thrust based on the inlet air mass flow rate; and increase the specific fuel consumption.

Two experimental runs were made with main bleed air extraction from the H.P. compressor delivery plenum of the Basic Engine. Total geometric areas for the two T-nozzle orifices (recall Section 2.2) were 6.28 sq. in. and 14.14 sq. in. yielding average bleed mass flow rates of 3.6% and 5.9% of engine intake mass flow respectively (see Fig. 18). Data from these two tests were reduced by the Data Reduction Routine described in Section 3.0, and were compared with experimental data from the calibration runs of the Basic Engine to obtain the measured effects of main bleed extraction on various engine parameters.

Predicted effects of main bleed extraction were obtained by comparing the O.D.P. program ouputs for the basic engine and for the engine with various fixed percentages of main bleed air. The same technique of manipulating the O.D.P. program was used to describe main bleed extraction from the H.P. compressor as was used to describe the anti-surge bleed extraction from the L.P. compressor (Section 5.1). Four sets of dual cycles were processed to yield values for 3.7%, 5.0%, 6.0%, and 10.0% main bleed flow rate.

		ALTITUDE	A/S BLEED	MAIN BLEED	L.P. SPOOL SPEED RANGE
CYCLE A	1)	Sea Level	NIL	NIL	100%
	2)	15'	NIL	MB%	100% to 80%
CYCLE B	1)	Sea Level	NIL	NIL	100%
	2)	15'	6.1%	MB%	100% to 40% (100% to 80% discarded)

where MB% = 3.7%, 5.0%, 6.0%, 10.0%

As explained in Section 5.1, this technique maintained the basic engine values for turbine and propelling nozzle areas during the part-throttle cycles with dual bleeds.

Comparisons of the predicted and measured effects of main bleed extraction were made for the engine parameters listed at the beginning of this Section. Both dimensional and non-dimensional data were compared. The latter are presented in terms of 'Influence Coefficients' (ξ's), which were defined as follows:

$$\xi_A \equiv \left\{ \frac{\left[\frac{A_{\substack{MB\% \\ BLEED}} - A_{\substack{BASIC\ ENGINE \\ NO\ BLEED}}}{A_{\substack{BASIC\ ENGINE \\ NO\ BLEED}}} \right]}{MB\%_{\ MAIN\ BLEED}} \right\} \text{----- (1)}$$

where: A represents any engine parameter

and $MB\%$ is the percentage of main bleed

The influence coefficient describes the percentage change in the engine parameter A for one percent main bleed extracted from the H.P. compressor delivery plenum. At very small bleed flow rates these influence coefficients would be constant regardless of the percentage bleed. However, calculations for bleed flow rates of interest showed this not to be the case for some parameters, particularly turbine inlet and turbine outlet temperatures and specific fuel consumption (Fig. 19). Hence it was necessary to compare predicted and experimental values using the influence coefficients for the correct (experimentally determined) percentage main bleed. To facilitate this approach, influence coefficients for the relevant engine parameters were determined from the O.D.P. outputs for 3.7%, 5.0%, 6.0%, and 10.0% main bleed flow rates using the general form of equation (1) above for various engine speeds. These values were plotted as shown in Figure 20 (using the specific fuel consumption influence coefficients as an example). Individual values were then read off for the speed and main bleed flow rate conditions measured during the experimental tests (e.g. Fig. 18).

The calculation procedure was tabulated as indicated in the following example (for the specific fuel consumption response):

J-75: COMPARISON OF MEASURED AND PREDICTED RESPONSE TO MAIN BLEED EXTRACTION

(Specific Fuel Consumption)

A/S BLEED	① % N_1	② % BLEED (EXP.)	③ PREDICTED ξ_A	④ Δ BASIC ENG. EXP.	⑤ Δ MEASURED BLEED	⑥ PREDICTED $\Delta\Delta$	⑦ MEASURED $\Delta\Delta$	⑧ MEASURED ξ_A
OPEN	40	3.02	2.900	1.4880	1.3867	+0.1313	-0.1013	-2.254
	50	3.10	2.760	1.0585	N/R	0.0906	-	-
	60	3.25	2.592	0.9020	0.9663	0.0760	0.0643	2.193
	70	3.47	2.375	0.8375	N/R	0.0690	-	-
	75	3.58	2.265	0.8235	0.8923	0.0668	0.0688	2.334
CLOSED	80	3.64	1.980	0.7740	0.8356	0.0558	0.0616	2.186
	85	3.70	1.840	0.7880	0.8483	0.0536	0.0603	2.068
	90	3.76	1.740	0.8090	0.8689	0.0529	0.0599	1.969
	95	3.80	1.655	0.8350	0.8320 Rdg. Error	0.0525	-	-
	100	3.83	1.590	0.8660	0.9294	0.0527	0.0634	1.911
							RUN NO. 21	$\Delta \equiv$ SCF

COLUMN ② Experimental percentage bleed read from Figure 18 for the appropriate $\%N_1$ and Run No.

COLUMN ③ Predicted influence coefficient read from Figure 20 for the speed and percentage bleed of Columns ① and ② .

COLUMN ④ Specific fuel consumption of the basic engine without main bleed at the appropriate speed read from calibration plot (Fig. 16).

COLUMN ⑤ Specific fuel consumption of the engine with percentage bleed per Column ② read from the Data Reduction Routine output sheets for the appropriate Run No. and speed.

COLUMN ⑥ Predicted change in spedific fuel consumption obtained from the product of Columns ②, ③ , and ④ .

COLUMN ⑦ Measured change in specific fuel consumption obtained from the difference of Column ⑤ - Column ④ .

COLUMN ⑧ Measured influence coefficient obtained from $\dfrac{\text{Column ⑦}}{\text{Column ④} \times \text{Column ②}}$

Dimensional values from Columns (6) and (7), and influence coefficients from Columns (5) and (8) were plotted against L.P. spool speed from Column (1) as shown in Figure 28. Figures 21 to 28 illustrate the comparison between measured and predicted response of other salient engine parameters in the same format.

Both dimensional changes and influence coefficients related to the L.P. compressor pressure ratio show good agreement with predicted values at all useful engine speeds (see Fig. 21). Although analytical and experimental H.P. compressor pressure ratio responses show a common trend (see Fig. 22) the absolute values are in reasonable agreement only at higher engine speeds. Under throttled-back conditions, predictions and experimental data deviate considerably, and actually become of opposite sign at the lower engine speeds.

Fuel flow rate, turbine inlet temperature, and turbine outlet temperature all increased by considerably greater amounts than were predicted by the O.D.P. program (see Figs. 23, 24, and 25). Nevertheless, the experimental influence coefficients confirm the linearity of these responses with small changes in main bleed rate. The similarity in discrepancy between predicted and experimental results for the fuel flow rate and the turbine temperatures suggests the effect is real, as compatibility of errors in two separate measuring systems is unlikely. From an operational viewpoint, the results indicate that the increase in limiting (turbine inlet) temperature caused by main bleed air extraction is likely to be more severe than the O.D.P. program predicts, and hence some conservatism is justified when predicting the maximum permissible main bleed extraction rate.

The higher-than-predicted fuel flow and turbine temperature responses are reflected in lower-than-predicted (negative) thrust and specific thrust responses (see Figs. 26 and 27); i.e., the higher temperatures prevented the thrust from decreasing as much as the O.D.P. program predicted. These two effects counteract one another to some extent and yield closer agreement between the experimental and predicted values of the specific fuel consumption response as illustrated in Figure 28.

No definitive explanation can be offered for these discrepancies between analytical and experimental response; however, the approximations of constant component efficiencies and constant pressure losses incorporated in the O.D.P. program were undoubtedly contributing factors.

7.0 COMPUTED AND MEASURED EFFECTS OF INCREASED PROPELLING NOZZLE AREA WITHOUT MAIN BLEED EXTRACTION

As pointed out in Section 6.0, one of the effects of compressor main bleed extraction was an increase in turbine inlet temperature - a major limiting operating parameter. Reduction of turbine back pressure, achieved by increasing the area of the propelling nozzle, reduces this temperature. In order to establish the effects of a change in nozzle area on the major cycle parameters, one test run was conducted with this area increased by 7.52%, without any main bleed extraction.

The analytical prediction of these effects was obtained from the O.D.P. program, which computes the propelling nozzle area from the continuity relation, by inputting a multiplier to modify the area generated during the calculation of the standard

sea level design speed cycle. By iterative calculation, the cycle was forced to adjust to this enlarged area for all subsequent full speed and part-throttle conditions. Analytically derived influence coefficients for area increases of 5% and 10% are plotted on Figure 29 to show the slight nonlinearity with nozzle area increase. The measured and predicted changes in engine parameters and the corresponding influence coefficients (as defined in Section 6.0) are plotted on Figures 30 to 37.

Very good agreement was found between measured and predicted values of L.P. compressor pressure ratio (Fig. 30) and specific fuel consumption (Fig. 37) over the useful engine operating range. With all other parameters, the O.D.P. program greatly overpredicted changes caused by the increased propelling nozzle area, especially above 77% L.P. compressor speed where the anti-surge bleeds are closed. Surprisingly, the computer program produced step changes opposite to those measured on the engine at the point where the anti-surge bleed valves closed. Because of this peculiarity, better agreement between experimental and analytical results can be observed at the lower end of the engine speed range. It is interesting to note that in all cases where discrepancies exist between measured and computed values, the O.D.P. program predicted changes greater by a factor of 1.5 to 2.0. Proportionate overestimation of fuel flow rate change (Fig. 32) and thrust change (Fig. 35) again yielded close agreement between the measured and predicted specific fuel consumption responses (Fig. 37), a case of "two wrongs making a right".

8.0 COMPUTED AND MEASURED EFFECTS OF INCREASED PROPELLING NOZZLE AREA WITH BLEED EXTRACTION

To establish the effects of combined bleed extraction and nozzle area change, one test was run in which the maximum amount of H.P. bleed air was extracted, with the propelling nozzle area increased by 7.52% relative to the Basic Engine. The bleed flow rate varied from 8.4% to 9.8%, generally increasing with engine speed as shown in Figure 18. This increased flow rate was achieved by further increasing the T-nozzle area to 20.00 sq. in.

Opening the final nozzle kept the turbine inlet temperature increase within 50°C at the higher engine speeds. Changes in the major cycle parameters as functions of L.P. compressor speed have been plotted on Figures 38 to 45. With two interacting disturbances to the Basic Engine cycle, viz., main bleed extraction and change in propelling nozzle area, unique influence coefficients were unobtainable as can readily be noted from the definition of these coefficients in Section 6.0. In addition to reduced experimental data and the O.D.P. program predictions, a second prediction has been displayed in the above Figures. This estimated change comprised the algebraic sum of the single-variable influence coefficients for main bleed extraction and propelling nozzle area change, viz.

$$\Delta A = \left\{ \xi_A \times \%MB + \psi_A \times \%\Delta A_{NOZ} \right\} \times A$$

where ξ_A and ψ_A are influence coefficients relating to compressor main bleed and propelling nozzle area increase respectively. "A" represents any engine parameter and ΔA its change.

Considering the rather unsuccessful attempts at predicting cycle parameter responses to main bleed extraction and nozzle area change individually, the relatively poor agreement between measured and predicted parameter changes in the case of combined disturbances to the Basic Engine cycle was anticipated. As one would expect, the two analytical curves (O.D.P. program and summation of individual influence coefficients) are quite similar in all plots. Although the relative agreement, or lack of it, between experimental results and analytical predictions varies for different parameters, none is good enough to justify quantitative use of the O.D.P. program predictions.

The best agreement occurred with the L.P. compressor pressure ratio (at L.P. spool speeds above 77%) and the specific fuel consumption, (see Figs. 38 and 45). The latter agreement again resulted from fortuitous combinations of individual discrepancies in fuel flow rate and thrust changes (see also Sections 6.0 and 7.0). The measured changes in H.P. compressor pressure ratio, thrust, and specific thrust were less than the predicted changes by a factor of approximately 2/3, as can be seen on Figures 39, 43, and 44. Responses of the other parameters, fuel flow rate and turbine temperatures, bore little resemblance to the predicted values. As can be noted from Figures 40, 41, and 42, all three of these variables increased significantly under the combined effects of bleed extraction and increased nozzle area, whereas the O.D.P. program forecast slight decreases at high engine speeds and only moderate increases at low engine speeds. This inability of the O.D.P. program to forecast accurately changes in turbine temperatures detracts seriously from its usefulness as a tool for assessing permissible maximum bleed extraction rates.

9.0 CONCLUSIONS

Comparisons between actual test results and values predicted by the current version of the O.D.P. program led to the following conclusions:

i) The Off-Design-Point program provided very good predictions of major cycle parameter changes of the Basic Engine under part-throttle operating conditions.

ii) The approximation of linear proportionality between corrected L.P. compressor speed and corrected air mass flow rate (used in the O.D.P.) underestimated the flow rate by as much as 3% in the 75% to 100% engine speed range. Below 75% engine speed, the approximation continuously overestimated the air mass flow rate.

iii) In general, the computer program with its simplifying approximations was capable of predicting only within a factor of two, responses of major cycle parameters to H.P. compressor bleed extraction, changes in propelling nozzle area, and combinations of both perturbations.

iv) In particular, the current version of the O.D.P. calculation routine underestimated the turbine inlet (and turbine outlet) temperature responses by a factor of two. This imprecision seriously detracts from its usefulness as a tool for assessing permissible maximum bleed extraction rates, and will be the subject of further analysis.

10.0 REFERENCES

1. Cockshutt, E.P. — Gas Turbine Cycle Calculations: A General Method for the Computation of Off-Design Performance. (To be published).

2. Chappell, M.S., Cockshutt, E.P., Sharp, C.R. — Gas Turbine Cycle Calculations: Design-Point Performance of Turbojet and Turbofan Engines. NRC, DME Aero. Report LR-407, National Research Council of Canada, October 1964.

3. Cockshutt, E.P. — Gas Turbine Cycle Calculations: Differential Methods in the Analysis of Equilibrium Operation. NRC, DME Aero. Report LR-481, National Research Council of Canada, March 1967.

4. Davis, W.R. — A Computer Program for the Analysis and Design of the Flow in Turbomachinery. Carleton University, Faculty of Engineering, Division of Aerothermodynamics Report No. ME/A 69-1, December 1969.

5. Chappell, M.S., Cockshutt, E.P. — Gas Turbine Cycle Calculations: Thermodynamic Data Tables for Air and Combustion Products. NRC, DME Aero. Report LR-517, National Research Council of Canada, January 1969.

6. Chappell, M.S., Grabe, W., Prince, E.J — J-75 Engine Compressor Bleed Air as a Source of Rig Turbine Drive Power. NRC, DME Lab. Tech. Report LTR-ENG-12, National Research Council of Canada, April 1971.

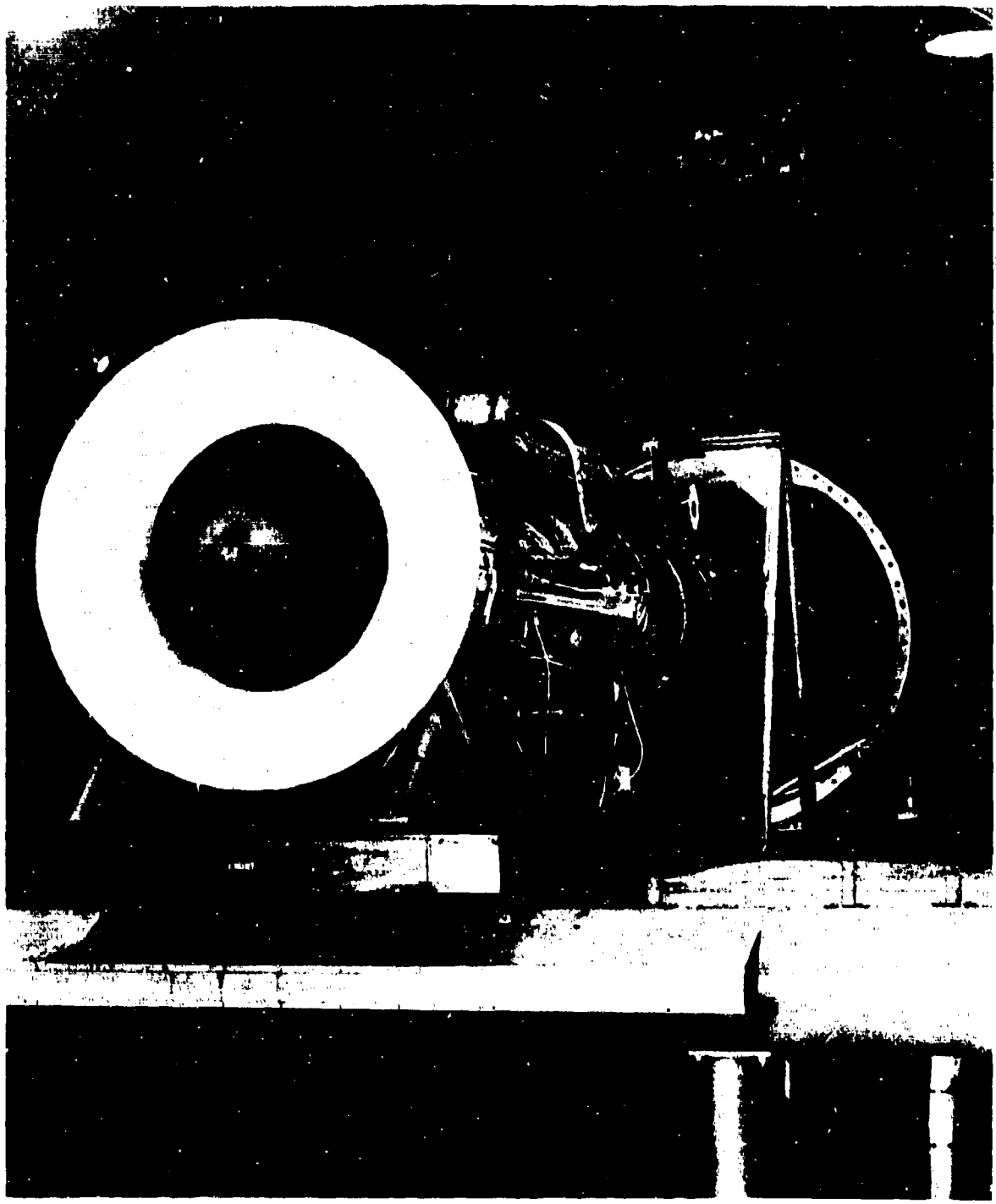

FIG. 1 : J-75 TURBOJET IN No.4 TEST CELL

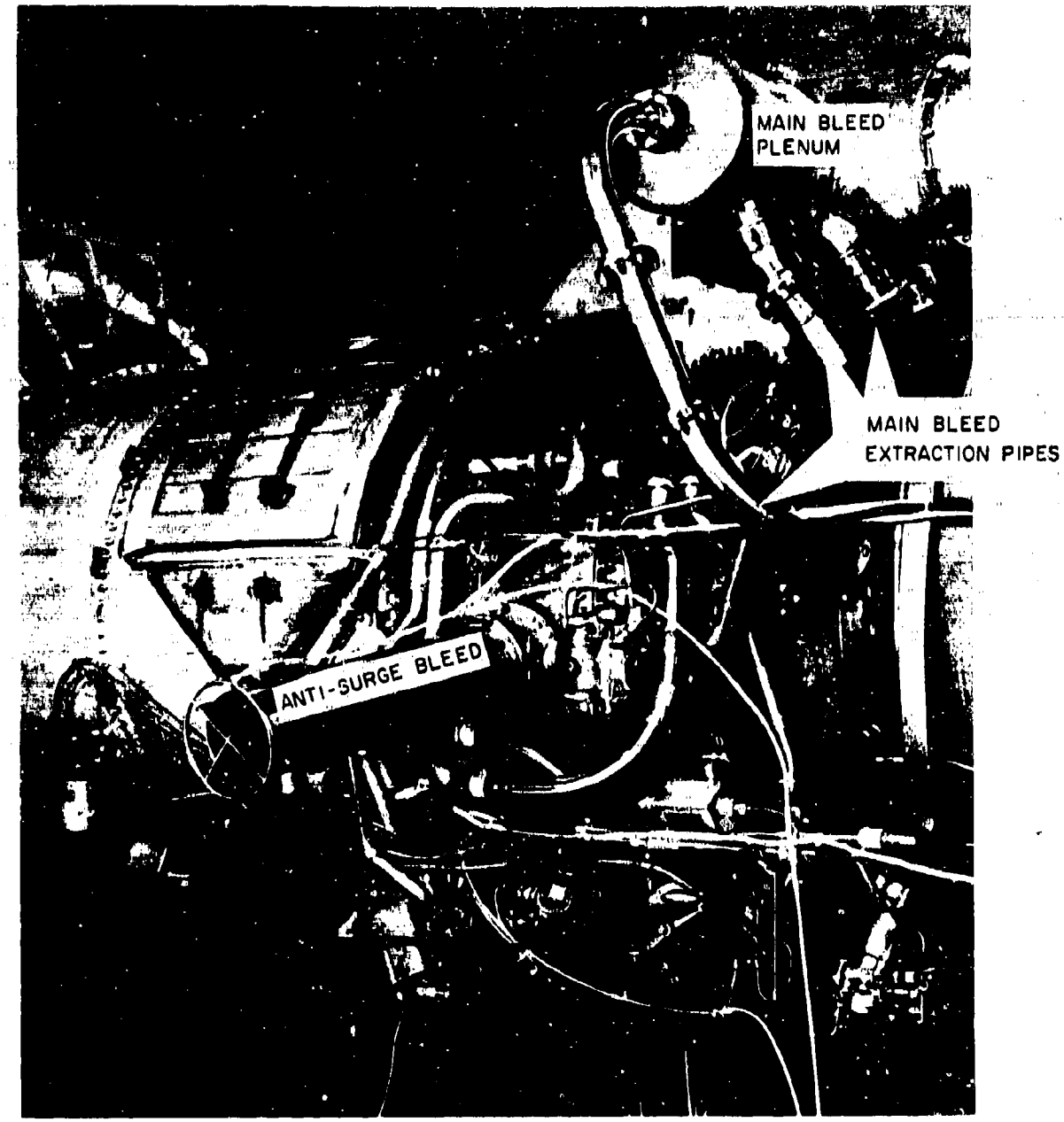

FIG. 2 : ANTI-SURGE AND MAIN BLEED EXTRACTION
PIPING CONFIGURATION

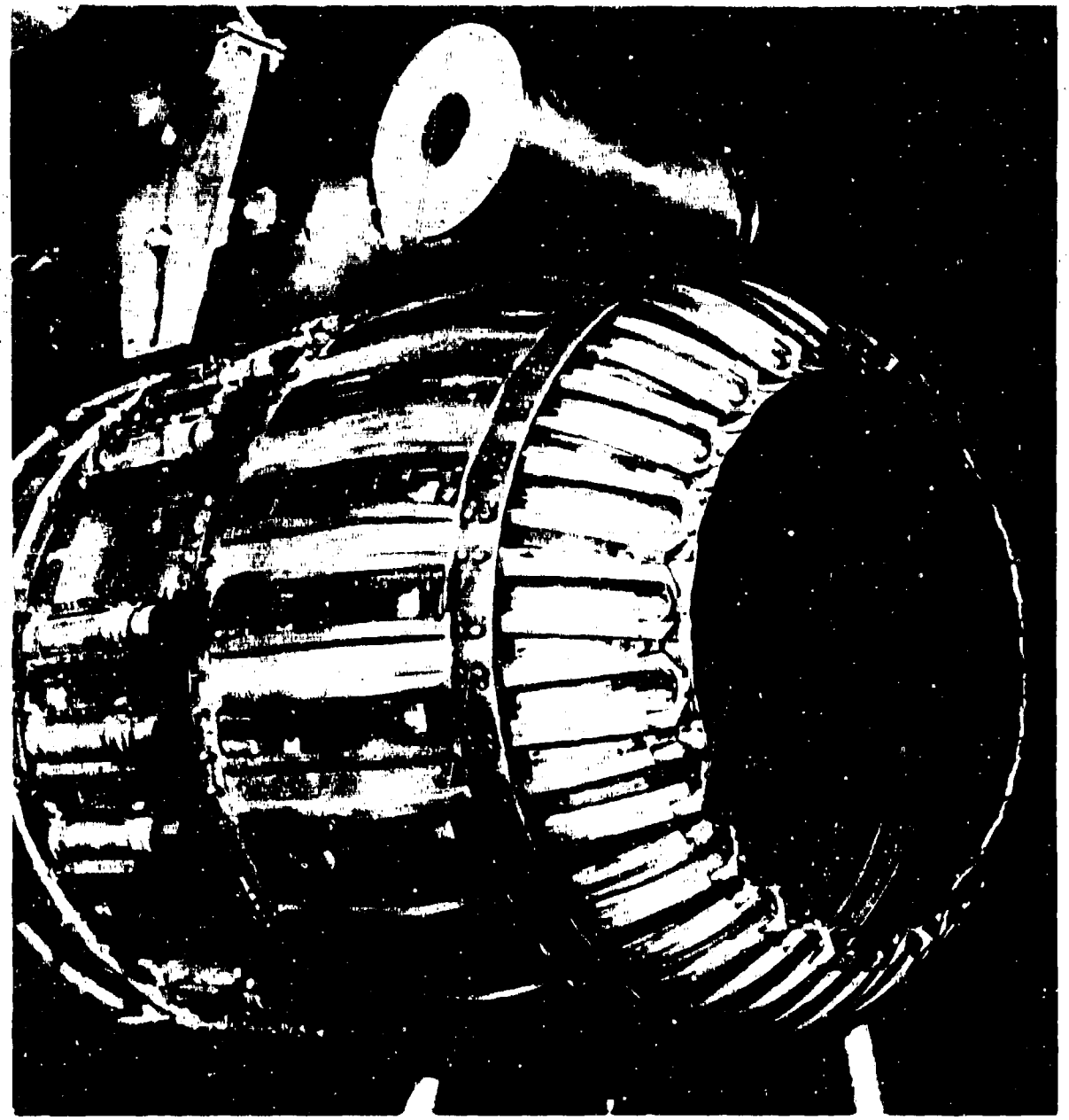

FIG. 3 : PROPELLING NOZZLE AND BLEED AIR T-NOZZLE

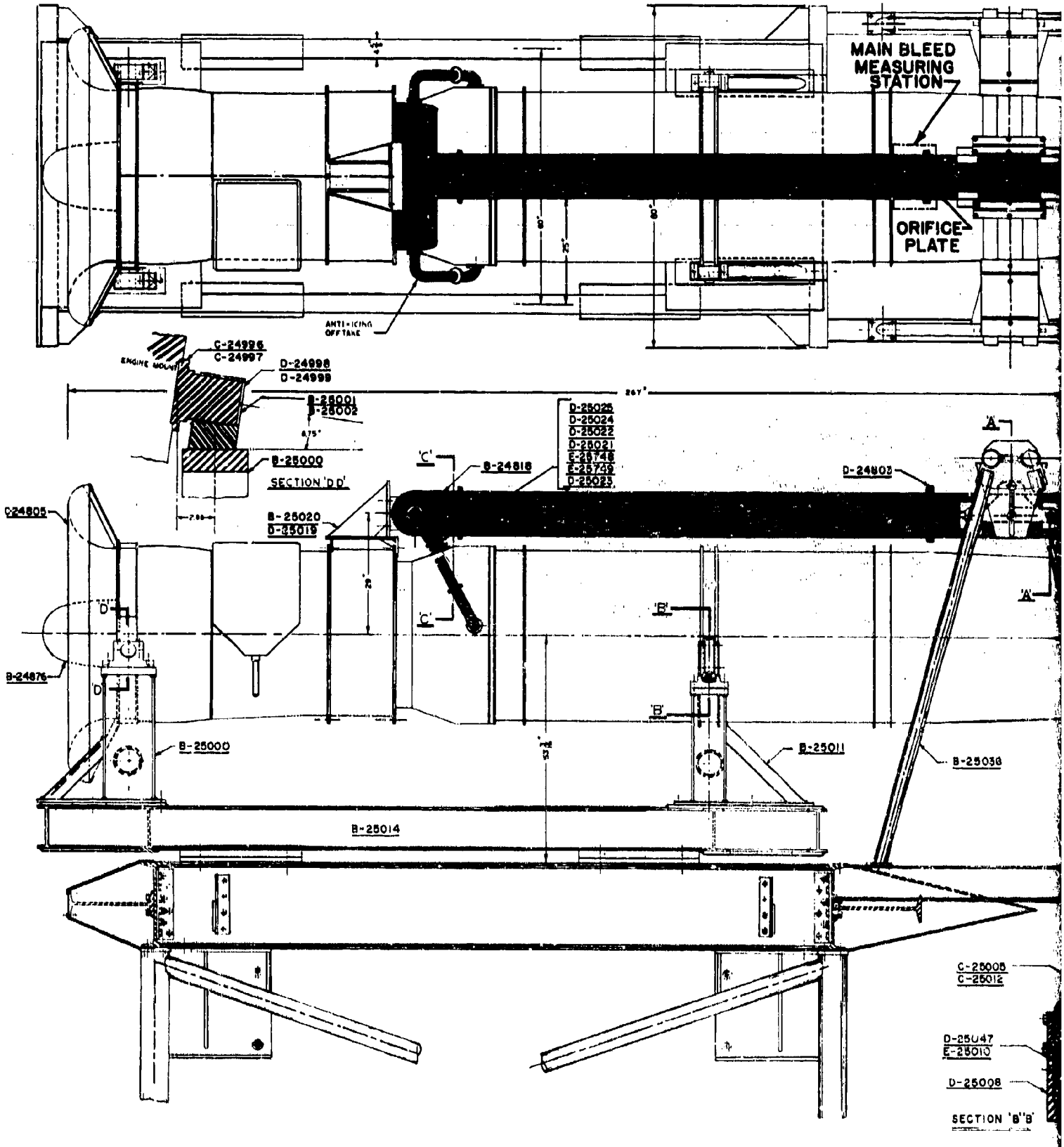
MAIN BLEED MEASURING STATION
ORIFICE PLATE
ANTI-ICING OFF TAKE
C-24996
C-24997
D-24998
D-24999
B-25001
B-25002
B-25000
SECTION 'D-D'
D-25025
D-25024
D-25022
D-25021
E-25748
E-25749
D-25023
B-24818
D-24803
B-24805
B-25020
D-25019
B-24876
B-25000
B-25011
B-25038
B-25014
C-25005
C-25012
D-25047
E-25010
D-25008
SECTION 'B''B'

B

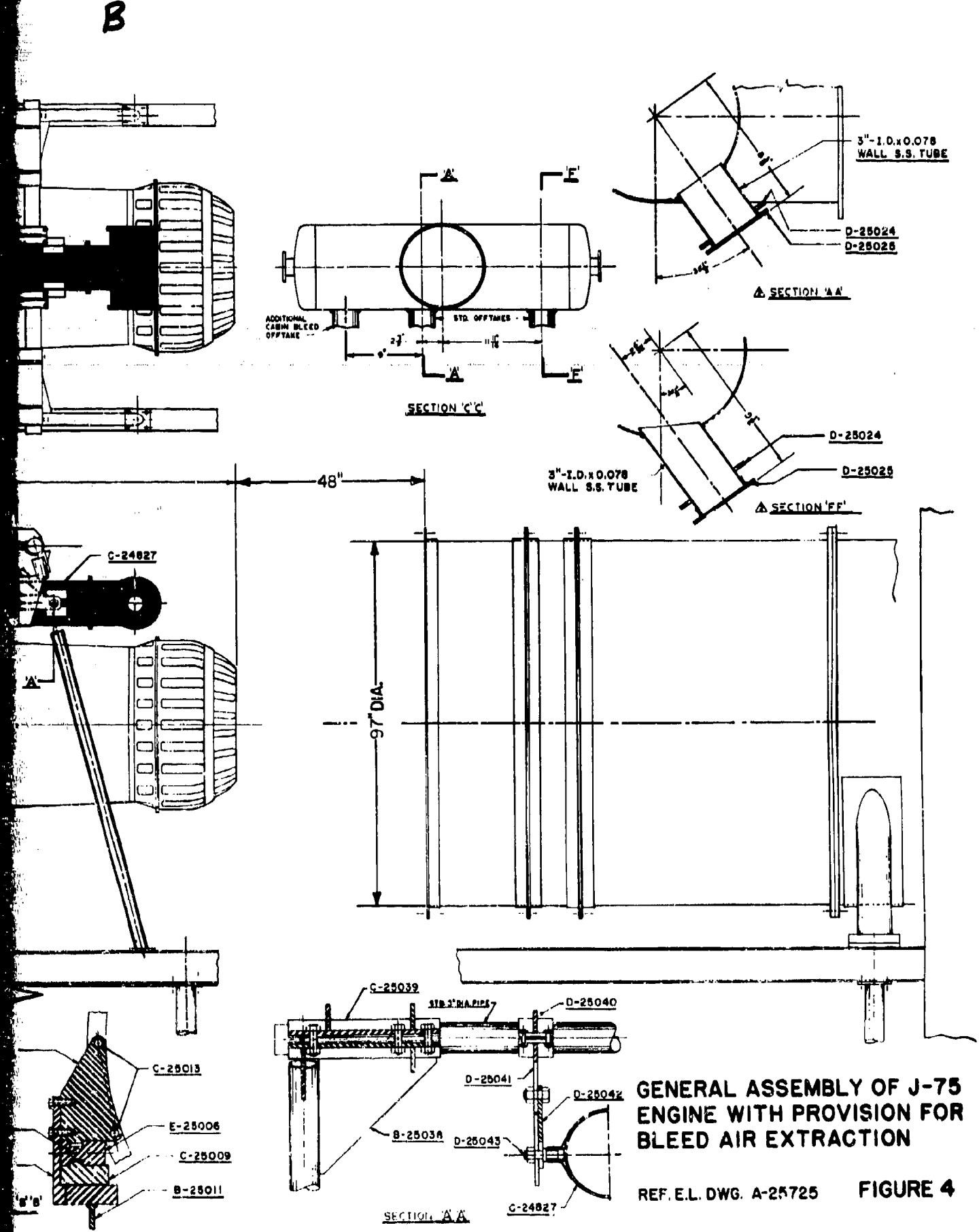

GENERAL ASSEMBLY OF J-75 ENGINE WITH PROVISION FOR BLEED AIR EXTRACTION

REF. E.L. DWG. A-25725

FIGURE 4

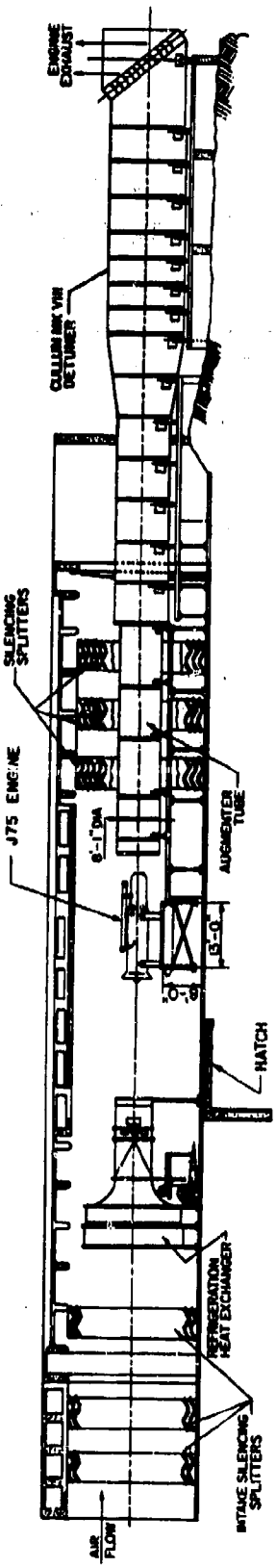

FIG. 5: SECTIONAL ELEVATION OF NO.4 TEST CELL SHOWING J-75 ENGINE INSTALLATION

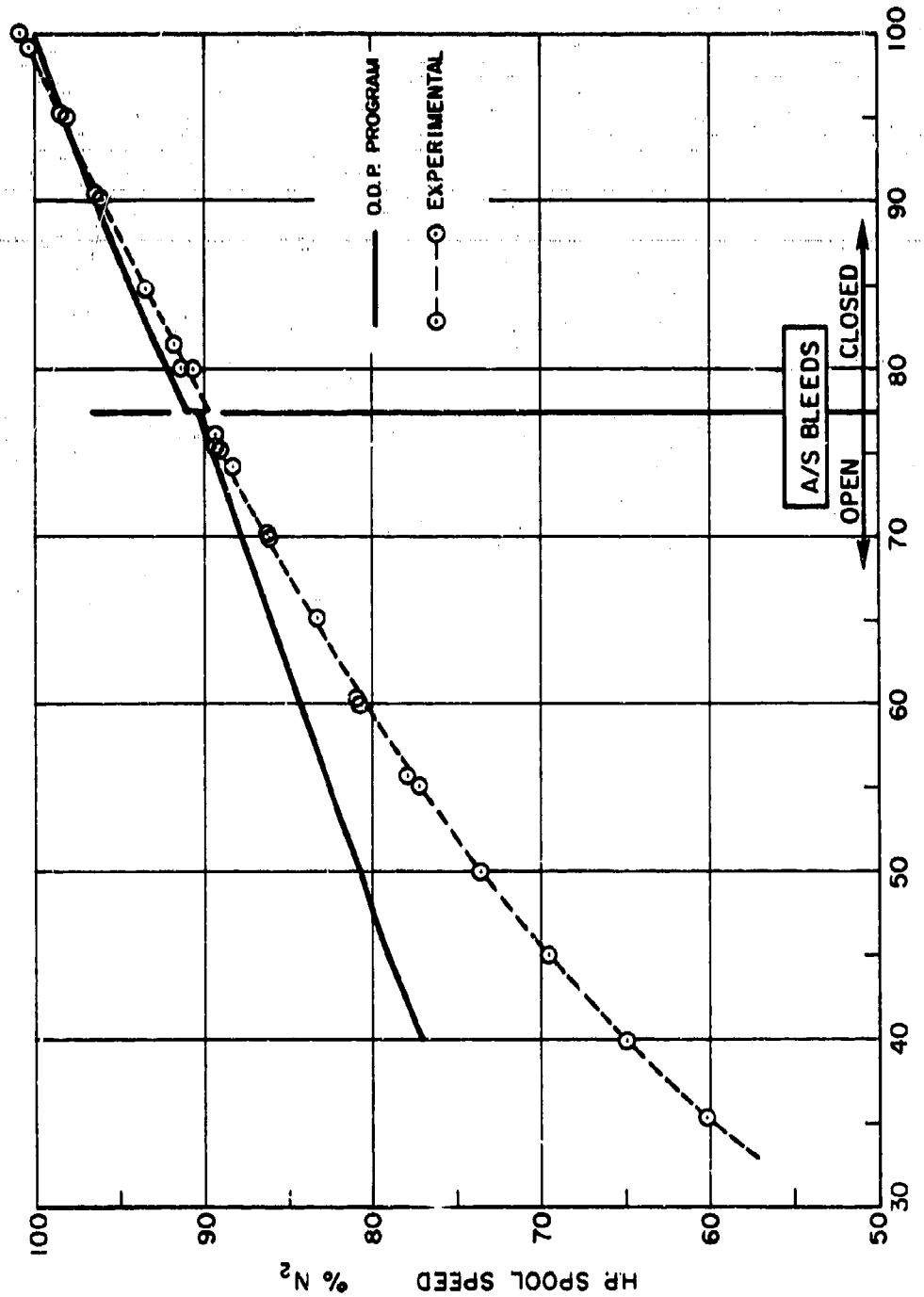

FIG. 6 : PERFORMANCE OF THE BASIC J-75 ENGINE

H.P. vs L.P. COMPRESSOR SPEED

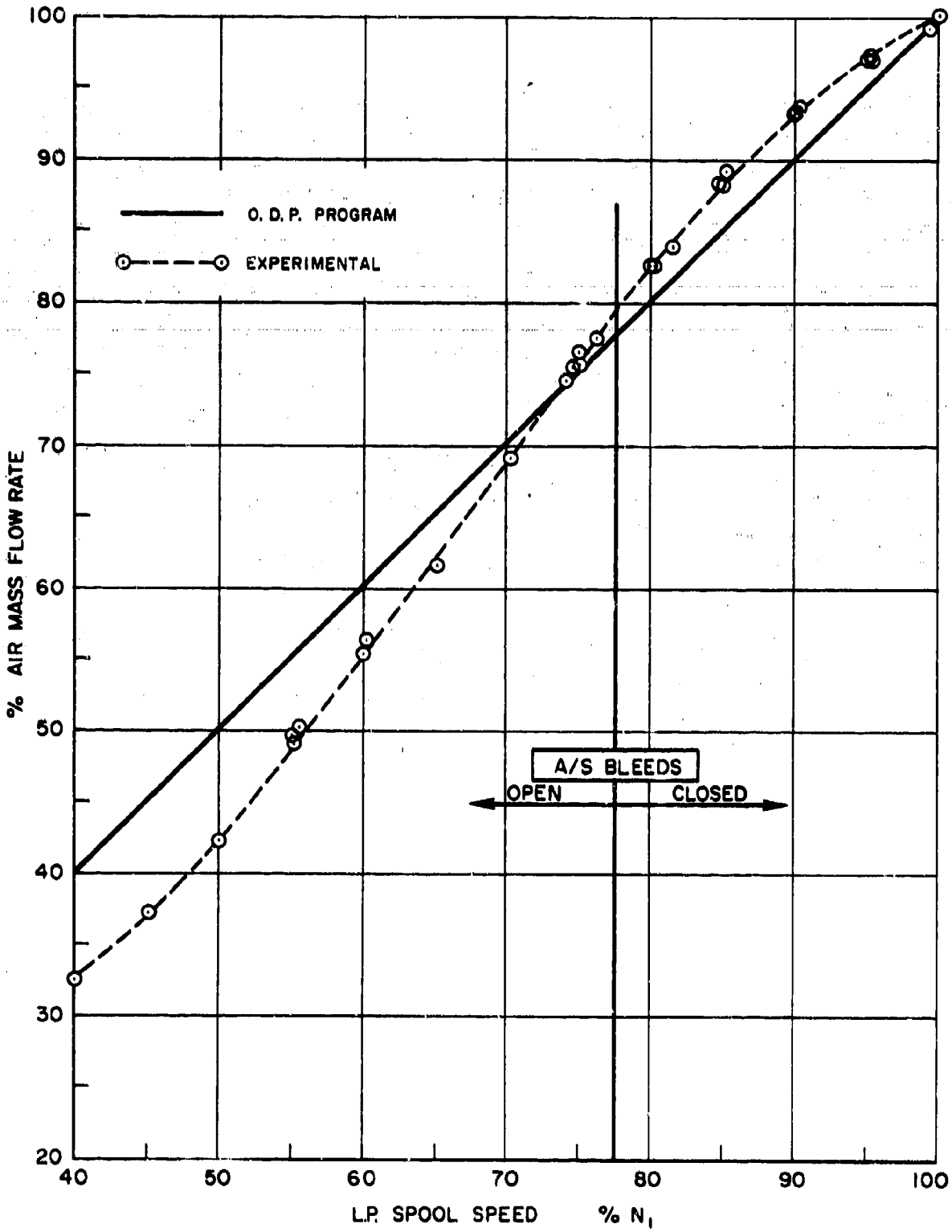

FIG. 7 : PERFORMANCE OF THE BASIC J-75 ENGINE
AIR MASS FLOW RATE vs L.P. SPOOL SPEED

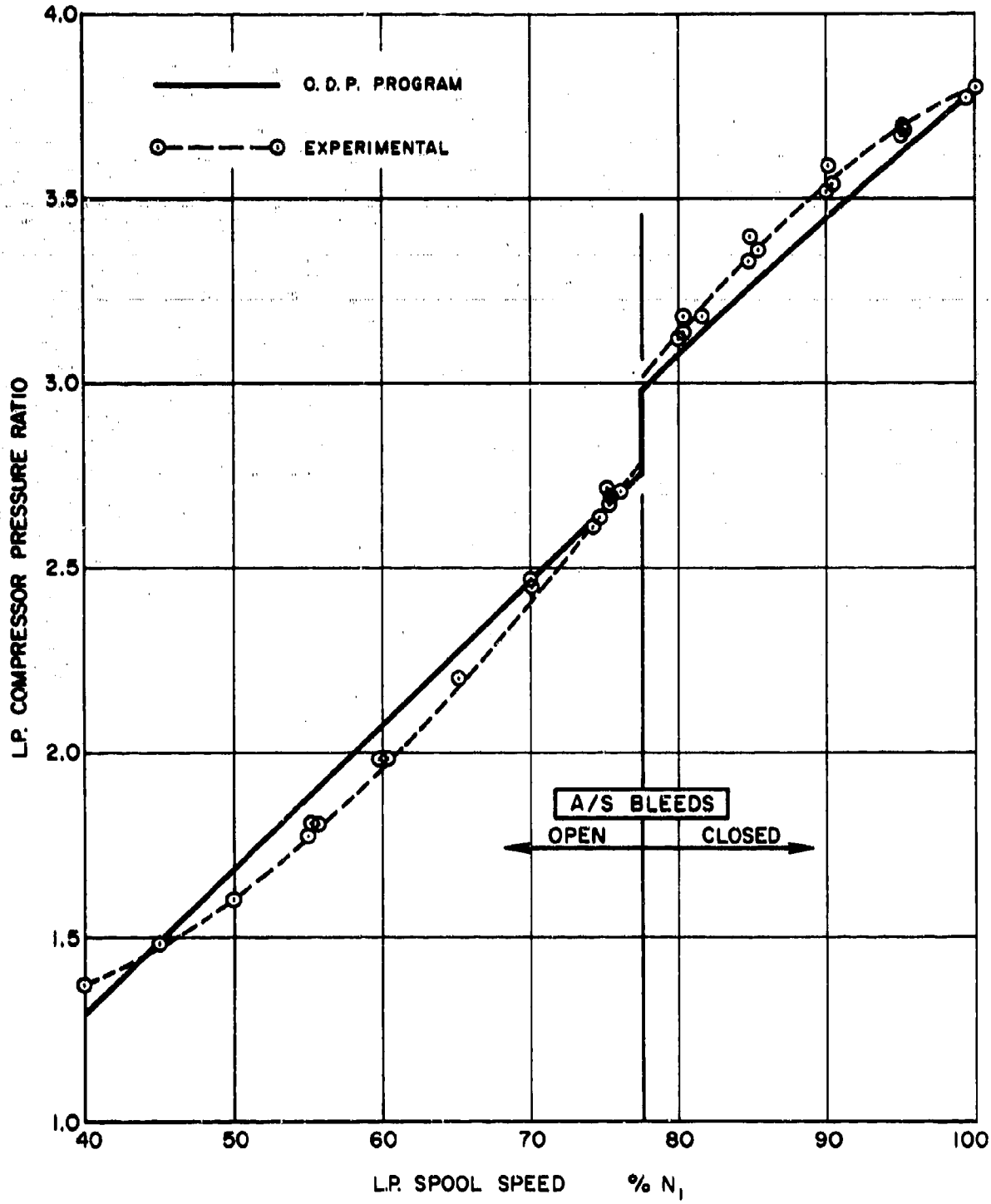

FIG. 8a : PERFORMANCE OF THE BASIC J-75 ENGINE
L.P. COMPRESSOR PRESSURE RATIO vs L.P. SPOOL SPEED

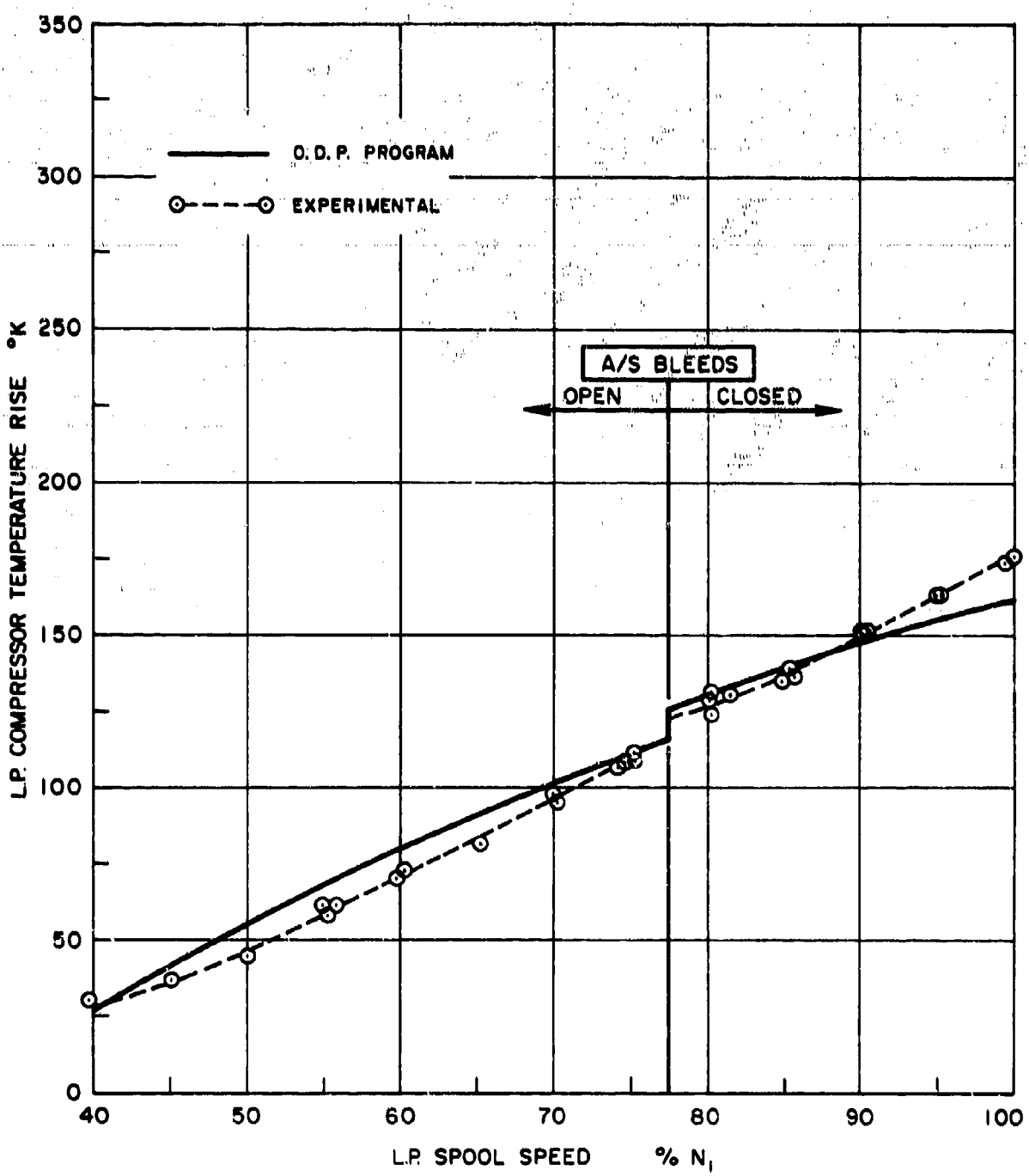

FIG. 8b : PERFORMANCE OF THE BASIC J-75 ENGINE
L.P. COMPRESSOR TEMPERATURE RISE vs L.P. SPOOL SPEED

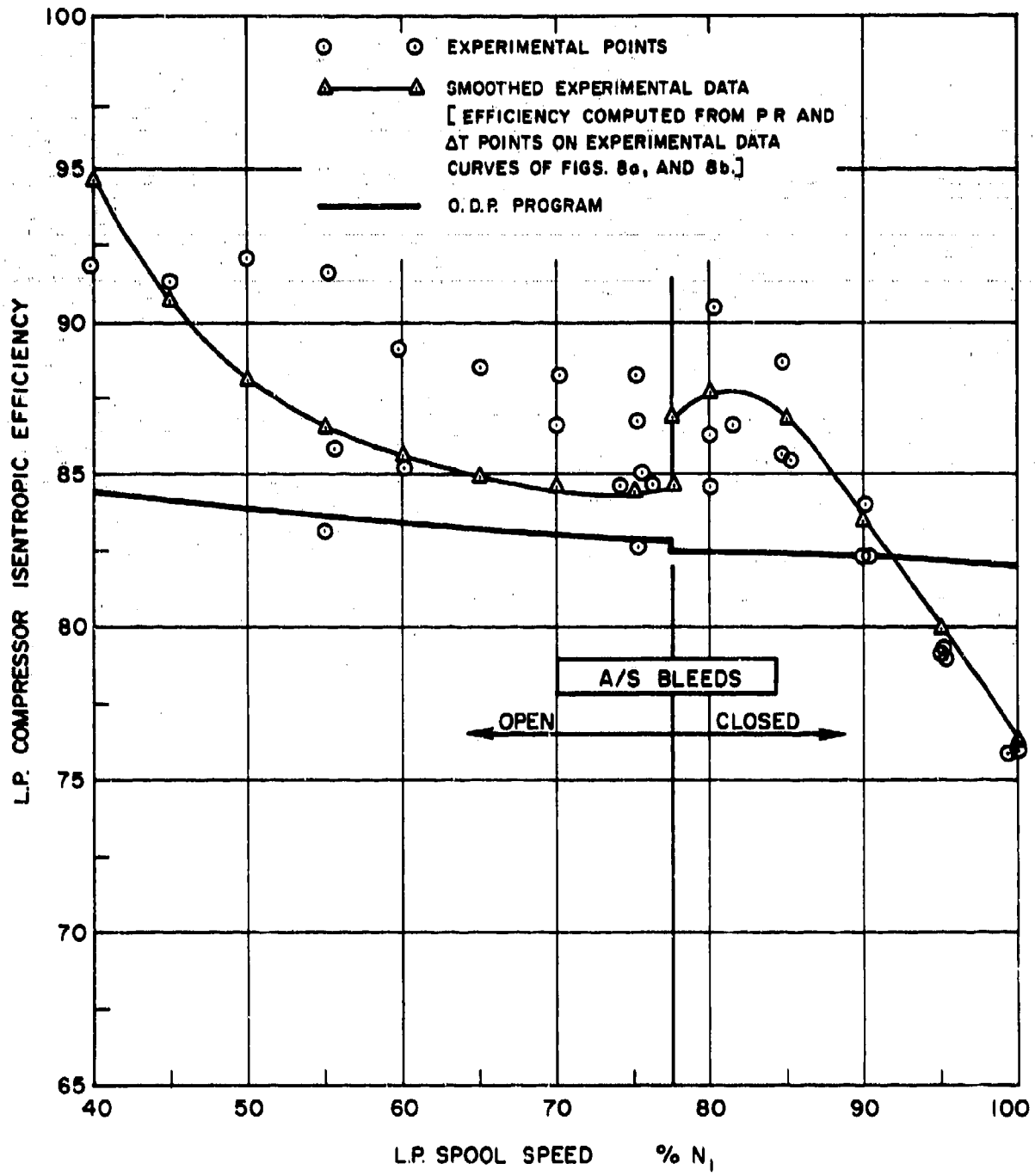

FIG. 8c : PERFORMANCE OF THE BASIC J-75 ENGINE
L.P. COMPRESSOR ISENTROPIC EFFICIENCY vs L.P. SPOOL SPEED

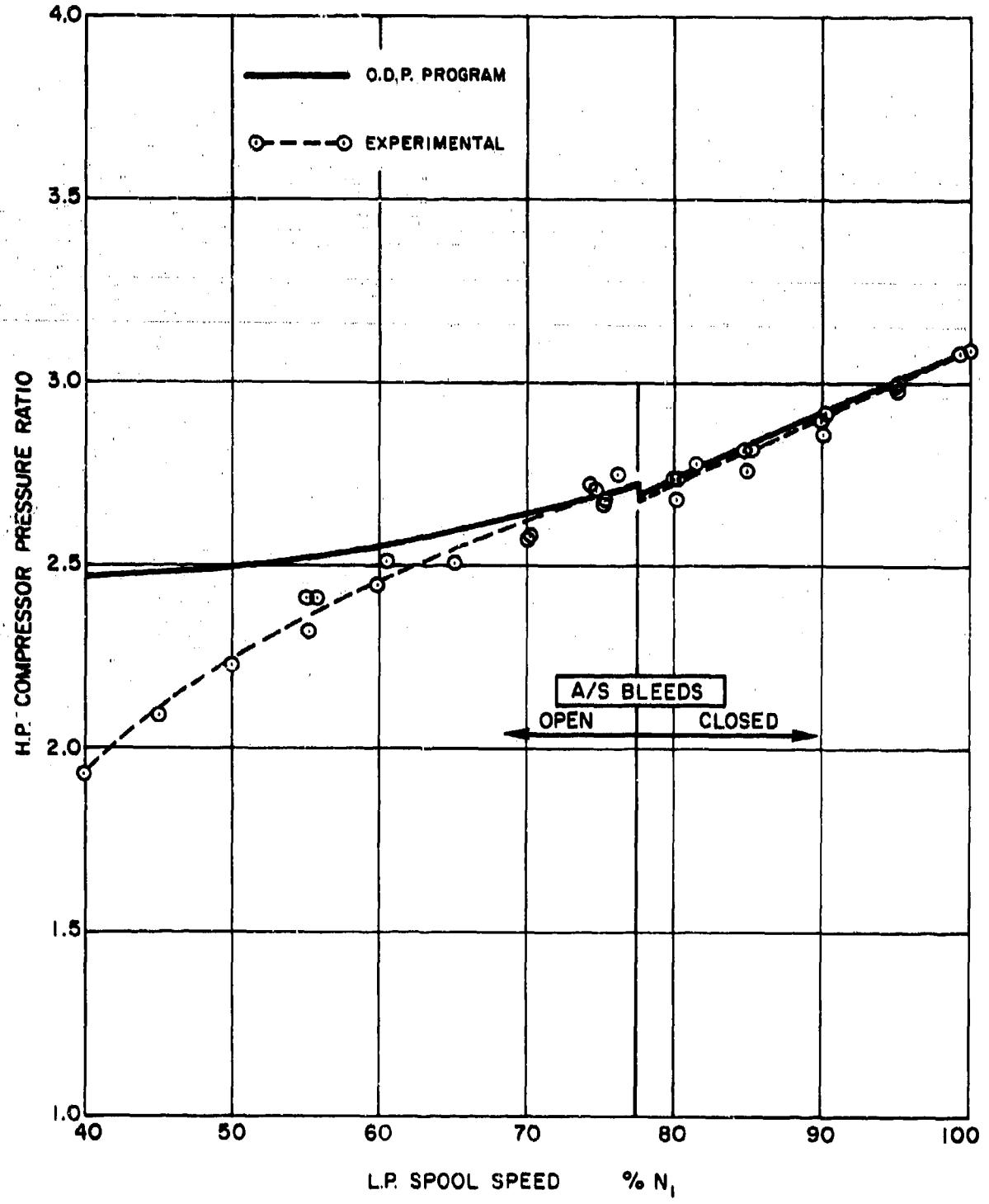

FIG.9a : PERFORMANCE OF THE BASIC J-75 ENGINE

H.P. COMPRESSOR PRESSURE RATIO vs L.P. SPOOL SPEED

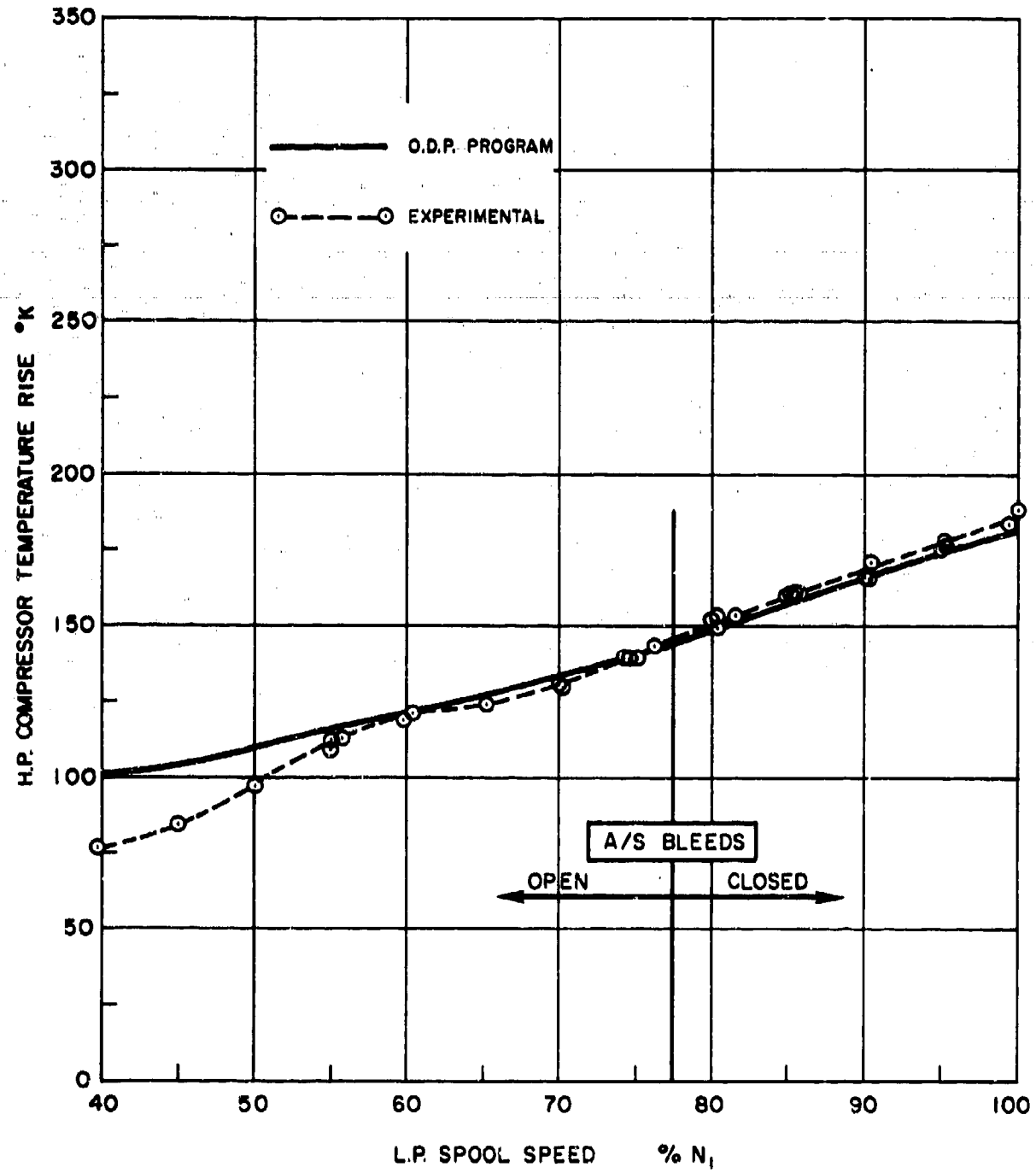

FIG.9b : PERFORMANCE OF THE BASIC J-75 ENGINE

H.P. COMPRESSOR TEMPERATURE RISE vs L.P. SPOOL SPEED

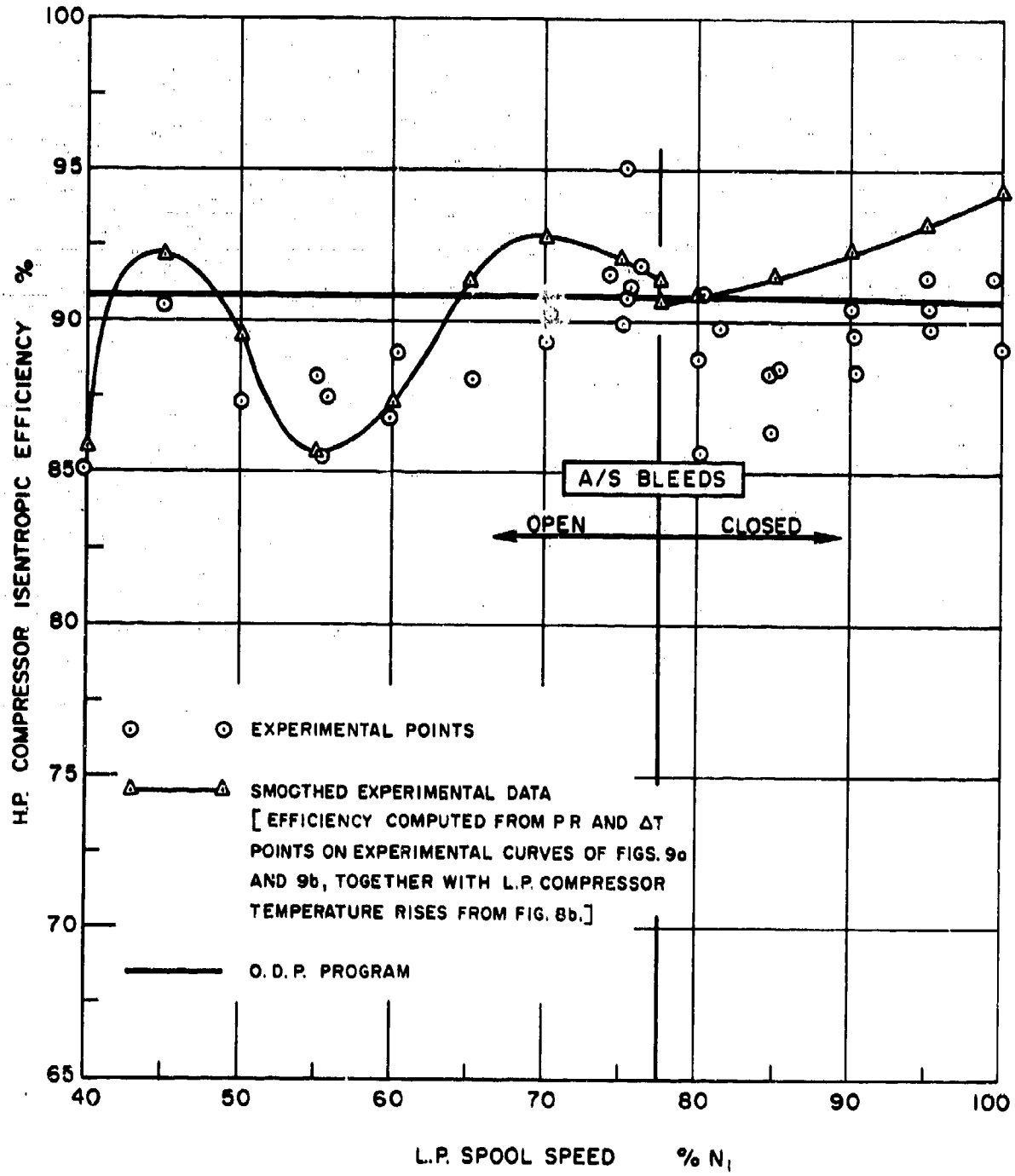

FIG. 9c : PERFORMANCE OF THE BASIC J-75 ENGINE

H.P. COMPRESSOR ISENTROPIC EFFICIENCY vs L.P. SPOOL SPEED

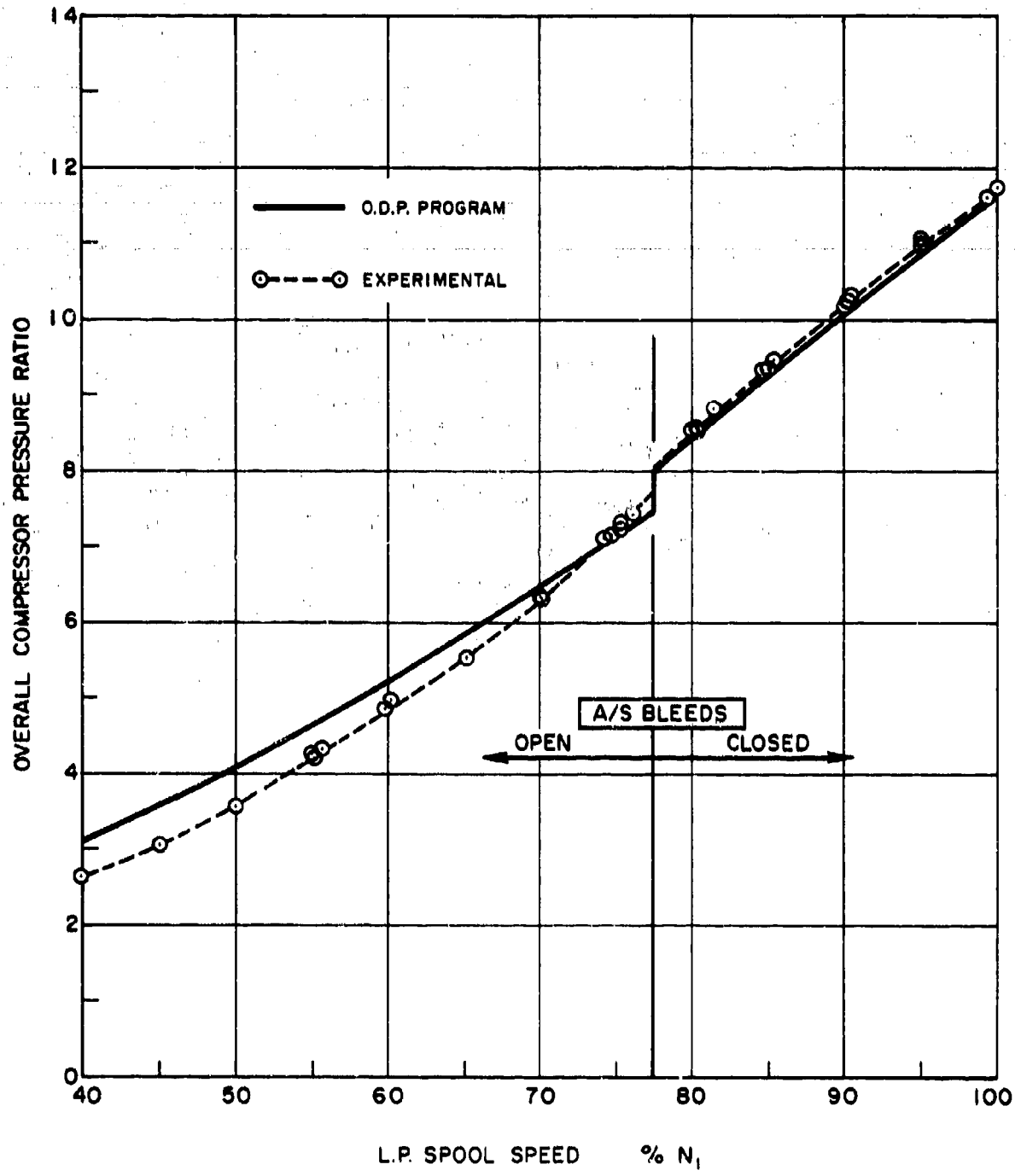

FIG. 10a : PERFORMANCE OF THE BASIC J-75 ENGINE
OVERALL COMPRESSOR PRESSURE RATIO vs L.P. SPOOL SPEED

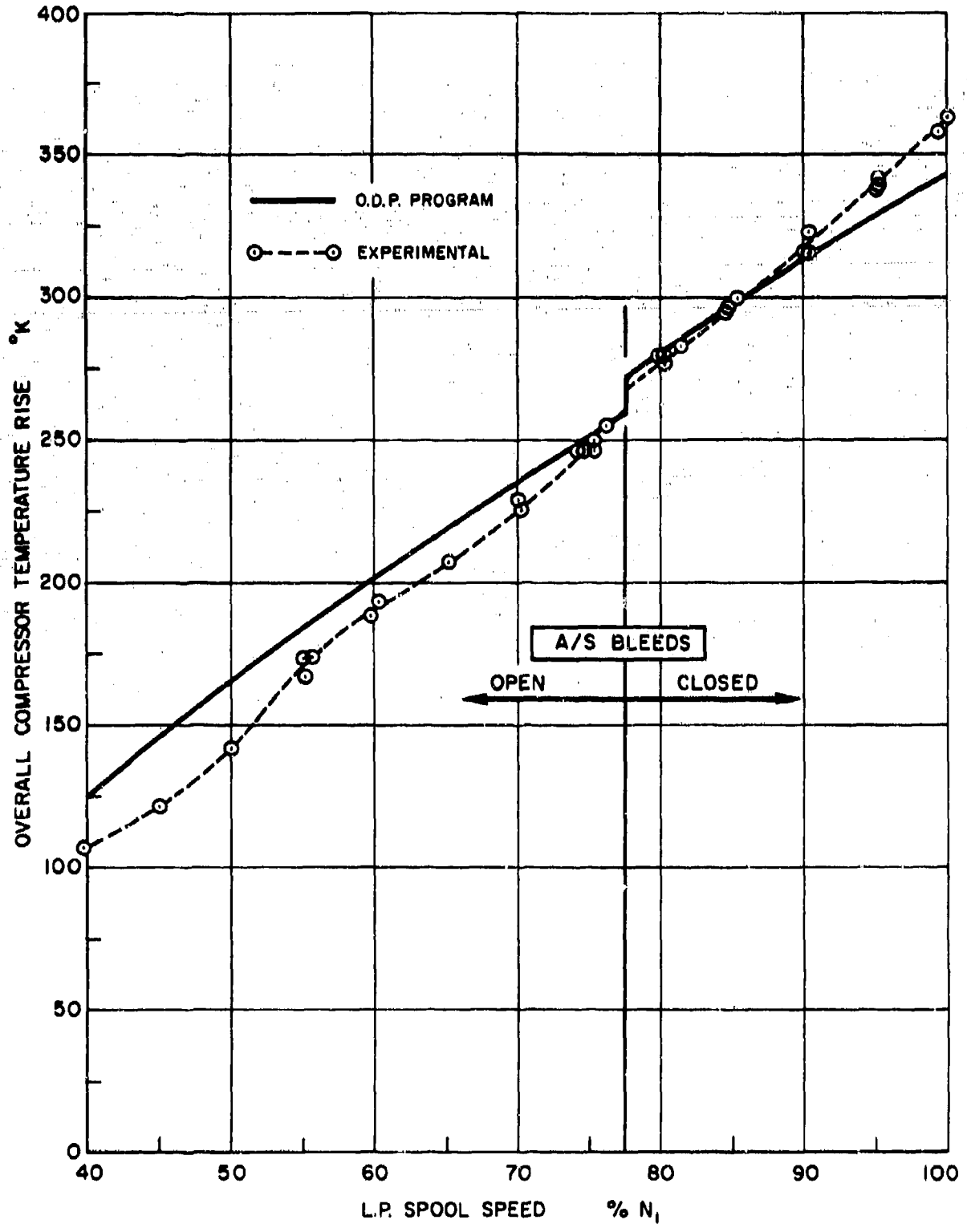

FIG. 10b : PERFORMANCE OF THE BASIC J-75 ENGINE
OVERALL COMPRESSOR TEMPERATURE RISE vs L.P. SPOOL SPEED

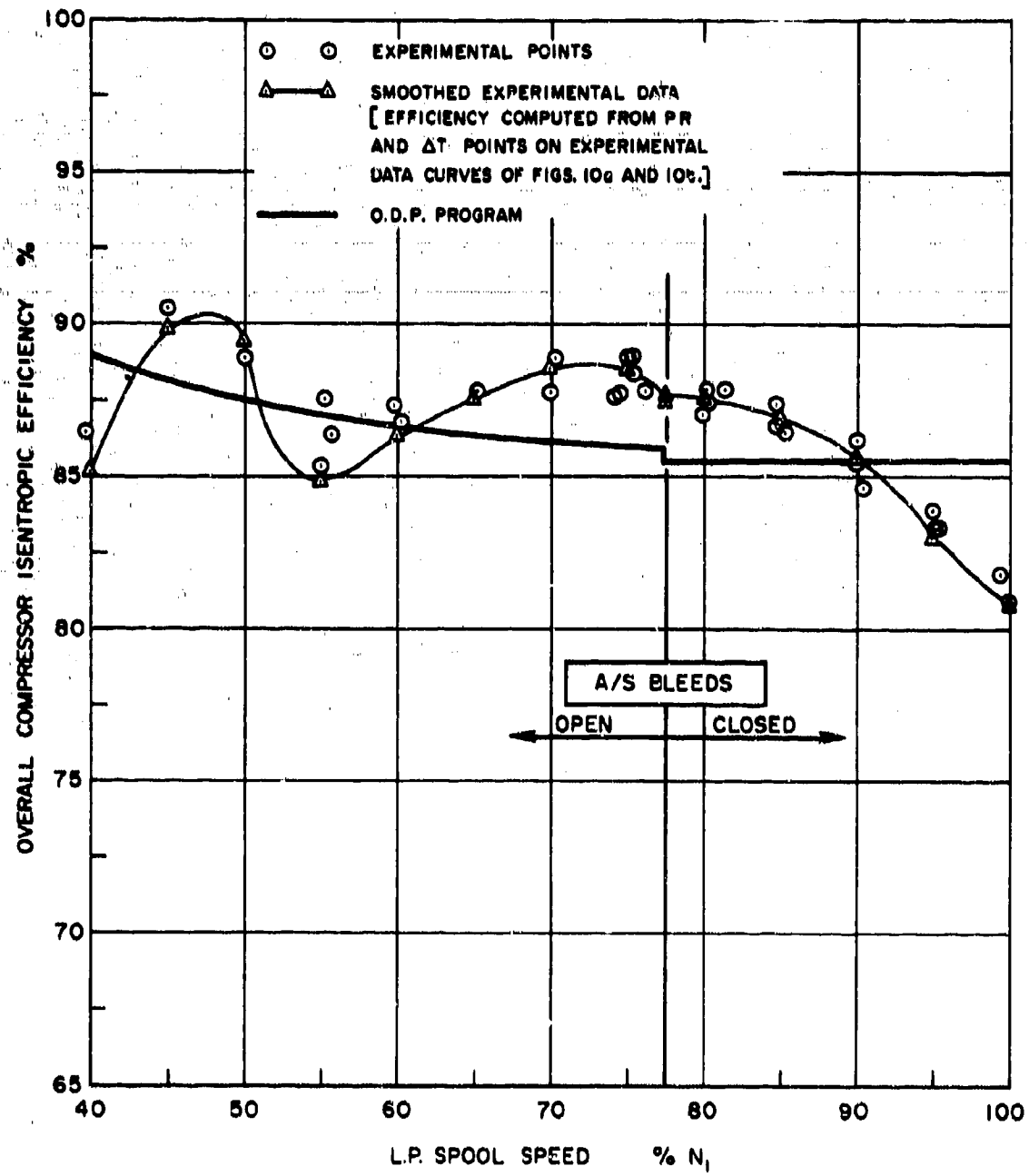

FIG.10c : PERFORMANCE OF THE BASIC J-75 ENGINE
OVERALL COMPRESSOR ISENTROPIC EFFICIENCY vs L.P. SPOOL SPEED

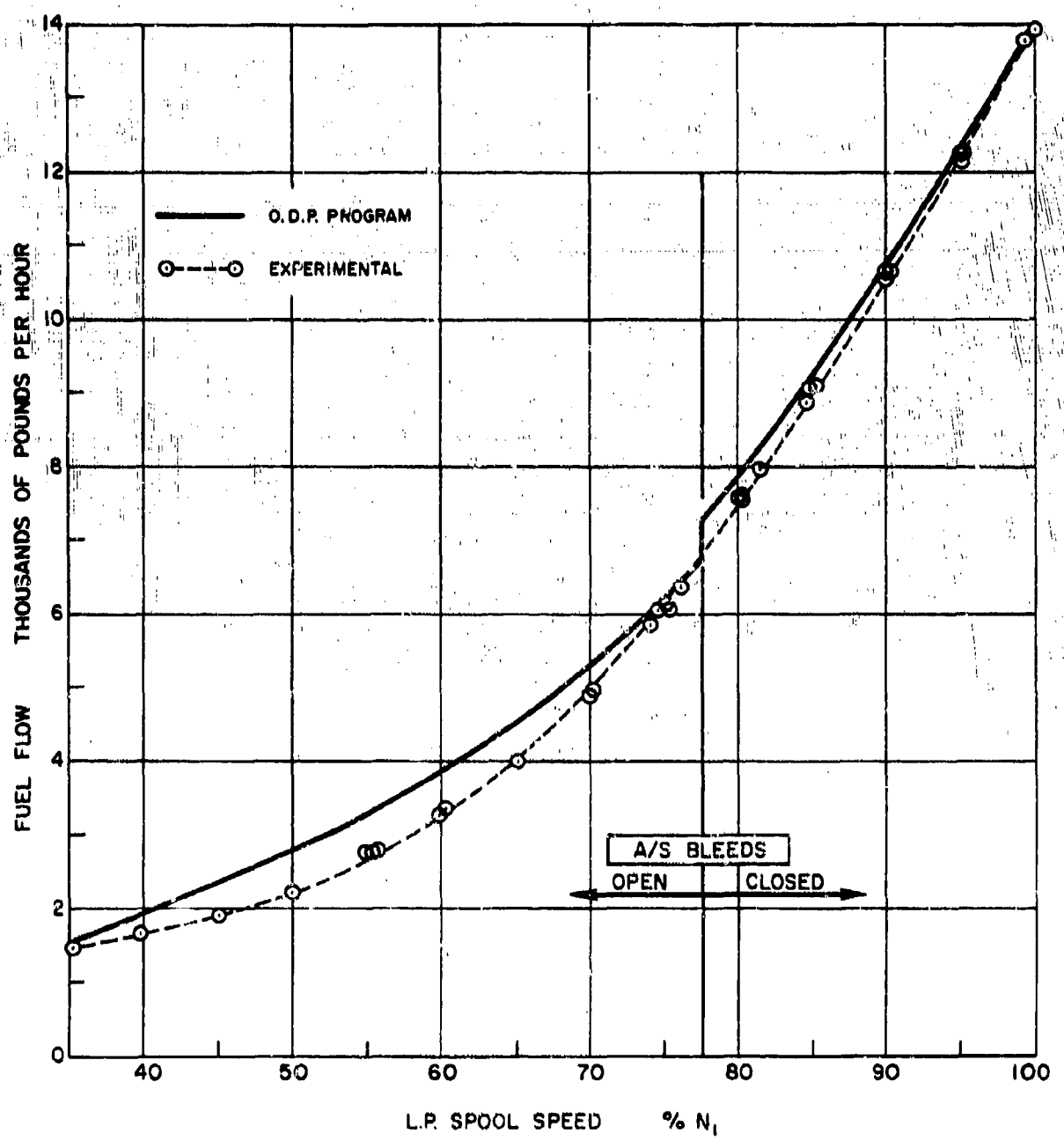

FIG.11 : PERFORMANCE OF THE BASIC J-75 ENGINE

FUEL FLOW vs L.P. SPOOL SPEED

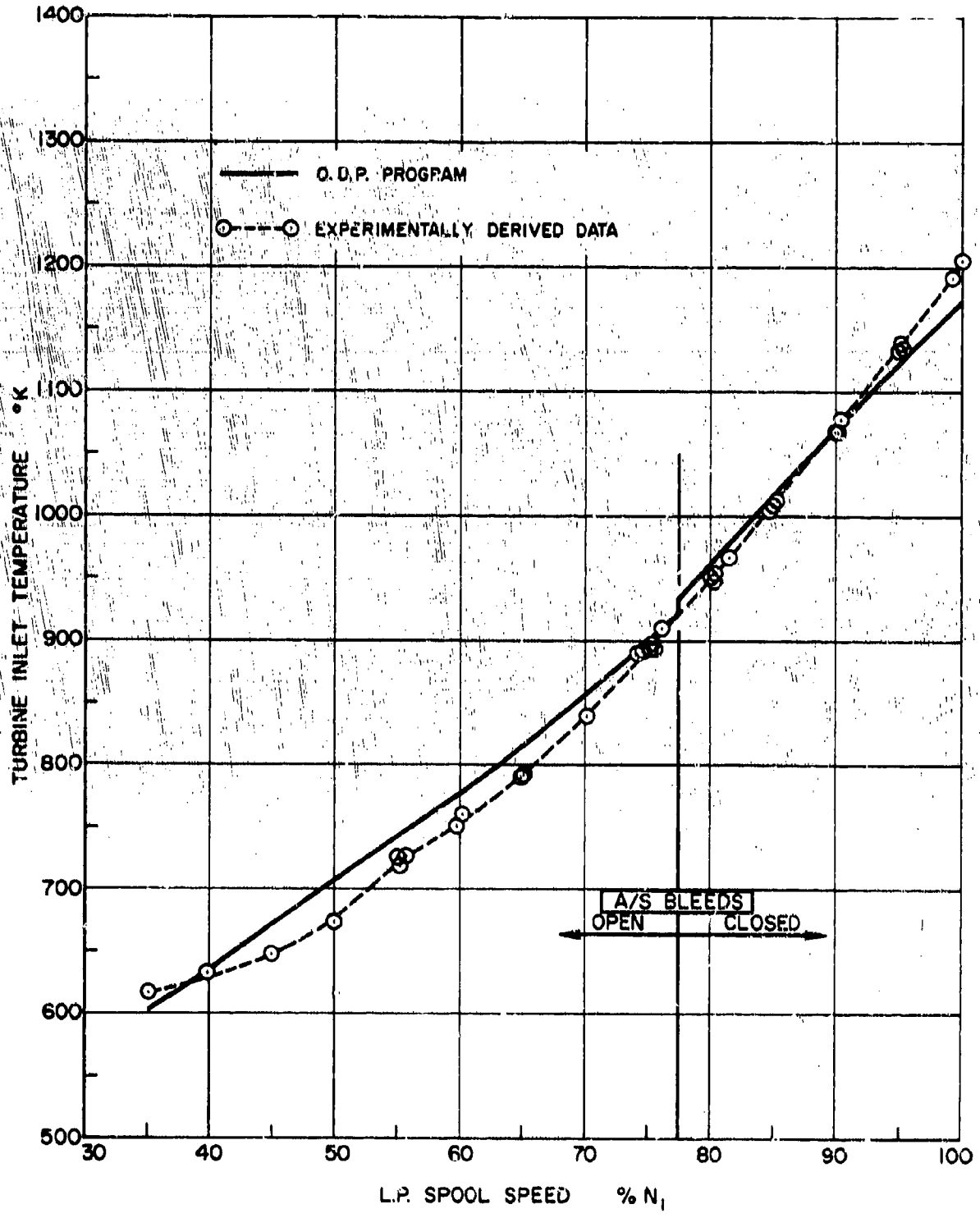

FIG. 12 : PERFORMANCE OF THE BASIC J-75 ENGINE
TURBINE INLET TEMPERATURE vs L.P. SPOOL SPEED

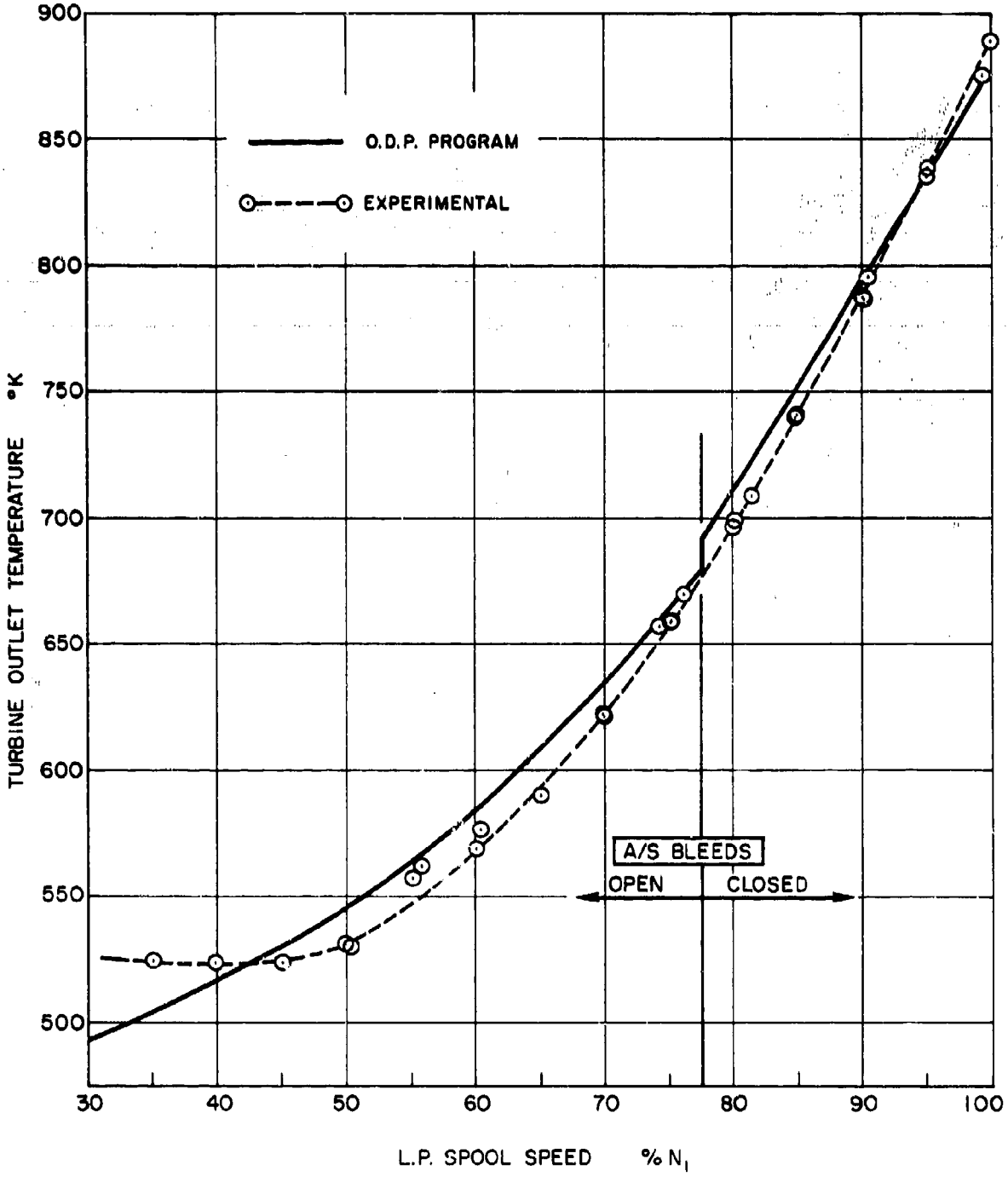

FIG. 13 : PERFORMANCE OF THE BASIC J-75 ENGINE
TURBINE OUTLET TEMPERATURE vs L.P. SPOOL SPEED

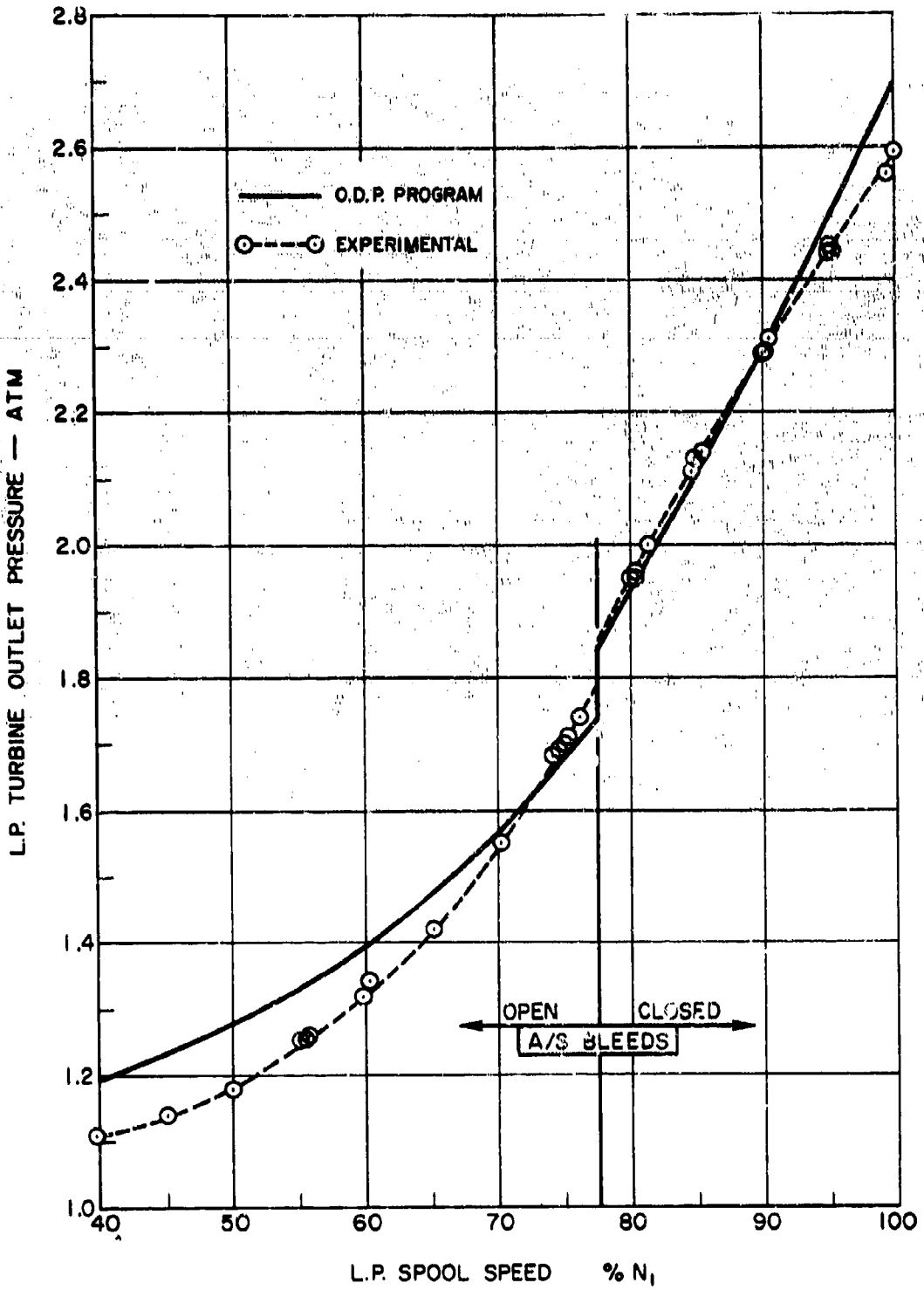

FIG. 14 : PERFORMANCE OF THE BASIC J-75 ENGINE
L.P. TURBINE OUTLET PRESSURE [E.P.R.] vs L.P. SPOOL SPEED

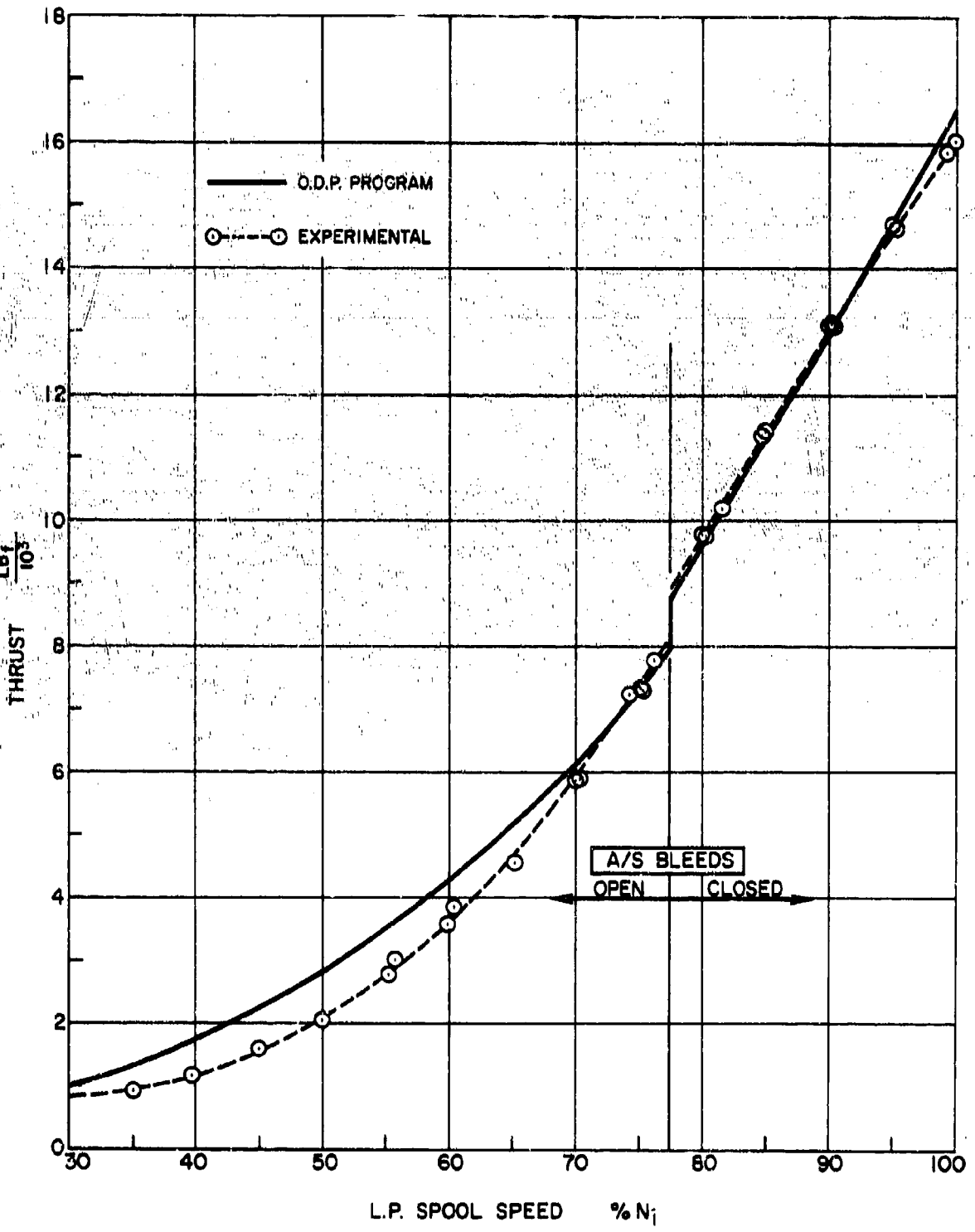

FIG. 15a : PERFORMANCE OF THE BASIC J-75 ENGINE
THRUST vs L.P. SPOOL SPEED

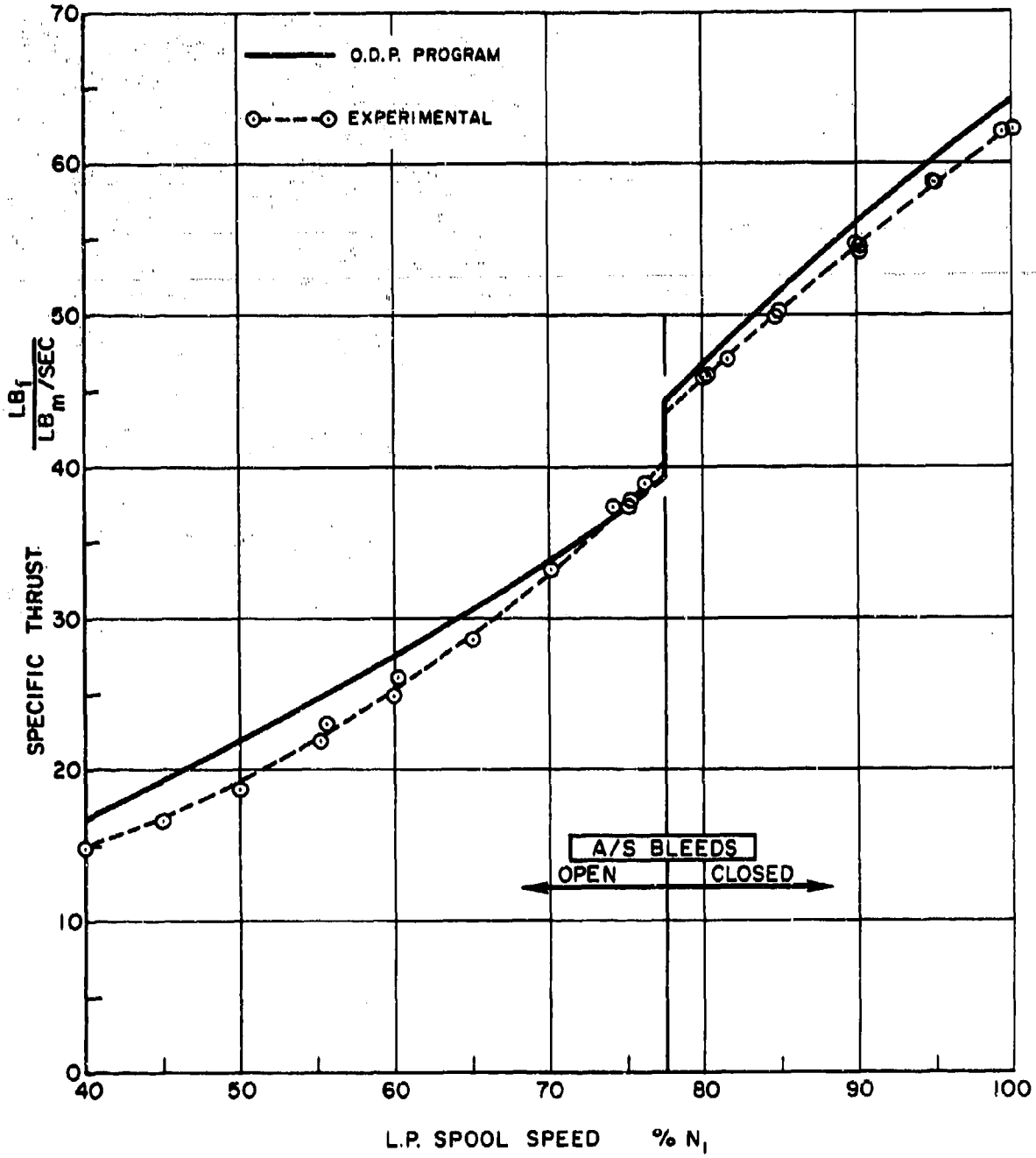

FIG.15b : PERFORMANCE OF THE BASIC J-75 ENGINE
SPECIFIC THRUST vs L.P. SPOOL SPEED

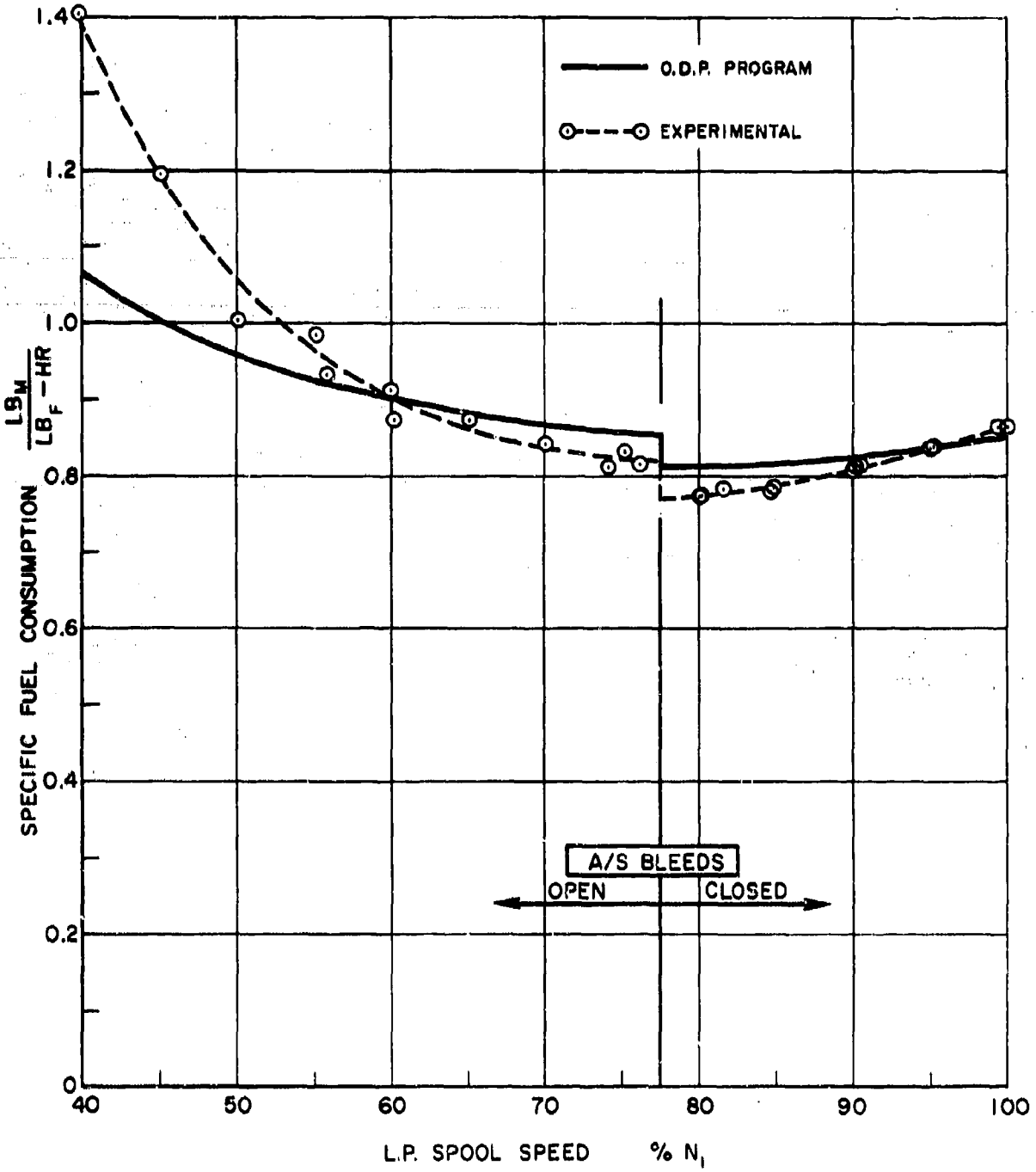

FIG. 16 : PERFORMANCE OF THE BASIC J-75 ENGINE
SPECIFIC FUEL CONSUMPTION vs L.P. SPOOL SPEED

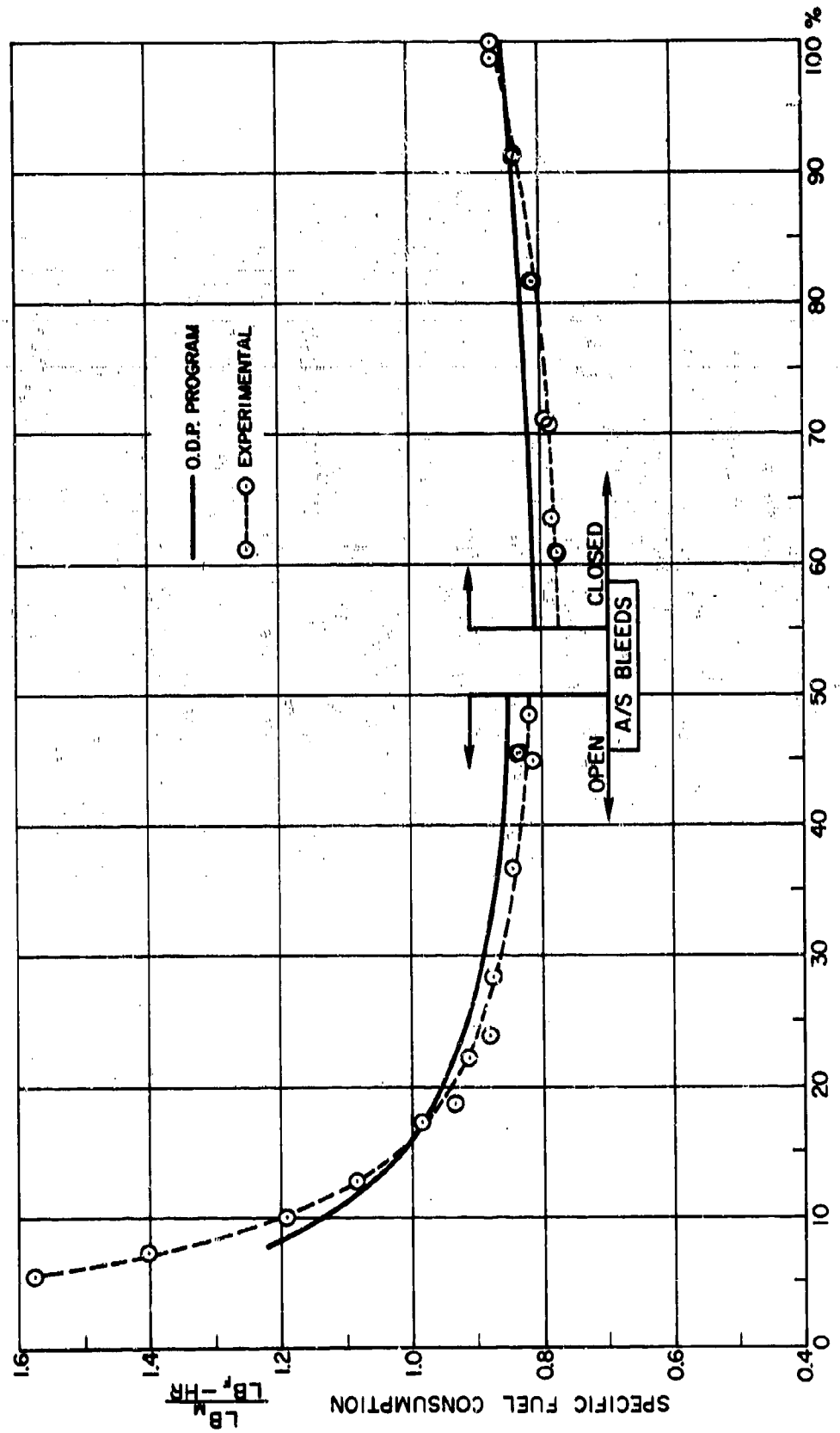

FIG. 17 : PERFORMANCE OF THE BASIC J-75 ENGINE
SPECIFIC FUEL CONSUMPTION vs PERCENT MAXIMUM THRUST

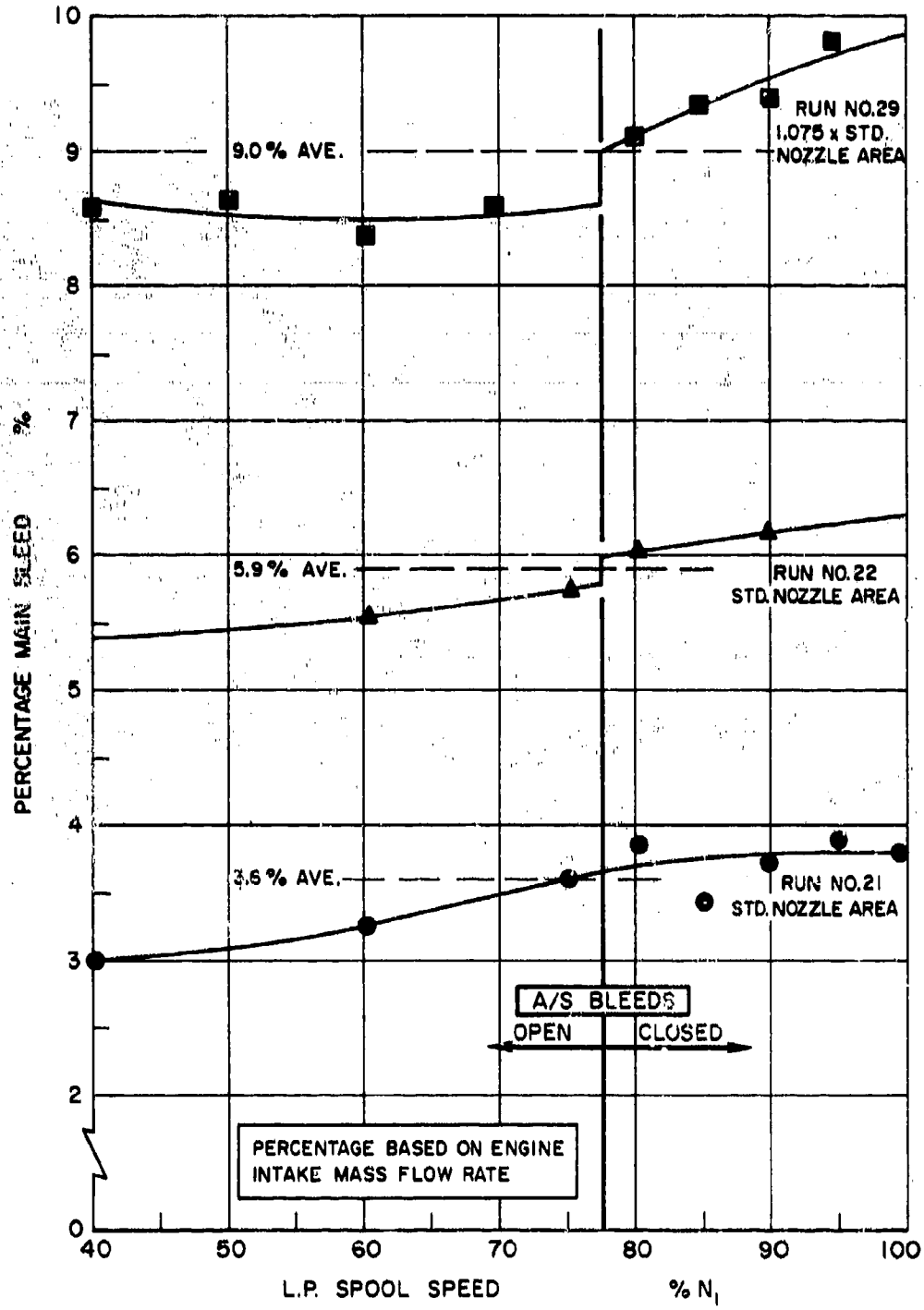

FIG. 18 : BLEED EXTRACTION

MEASURED MAIN BLEED FLOW RATE vs L.P. SPOOL SPEED

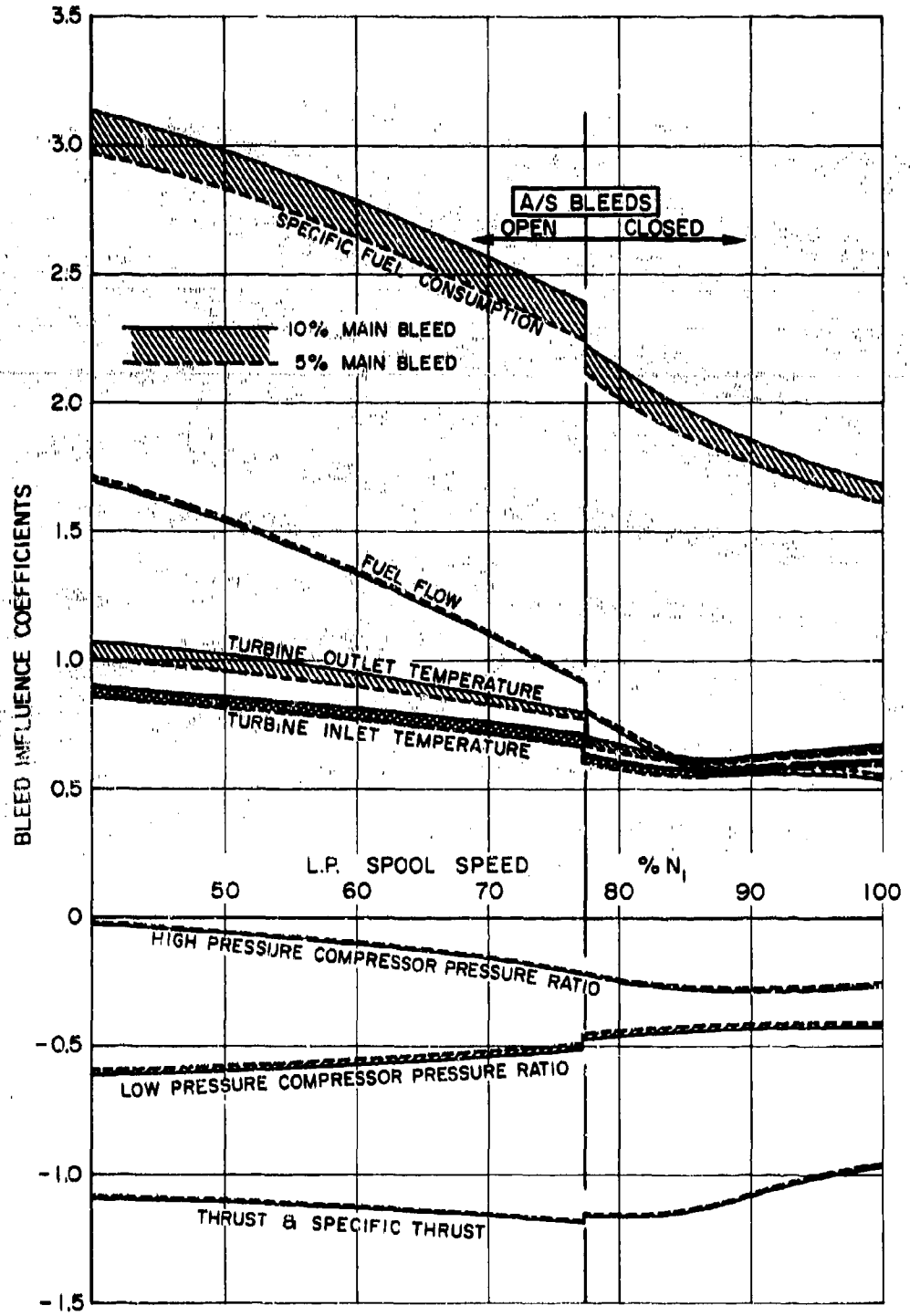

FIG. 19 : BLEED EXTRACTION

BLEED INFLUENCE COEFFICIENTS vs L.P. SPOOL SPEED

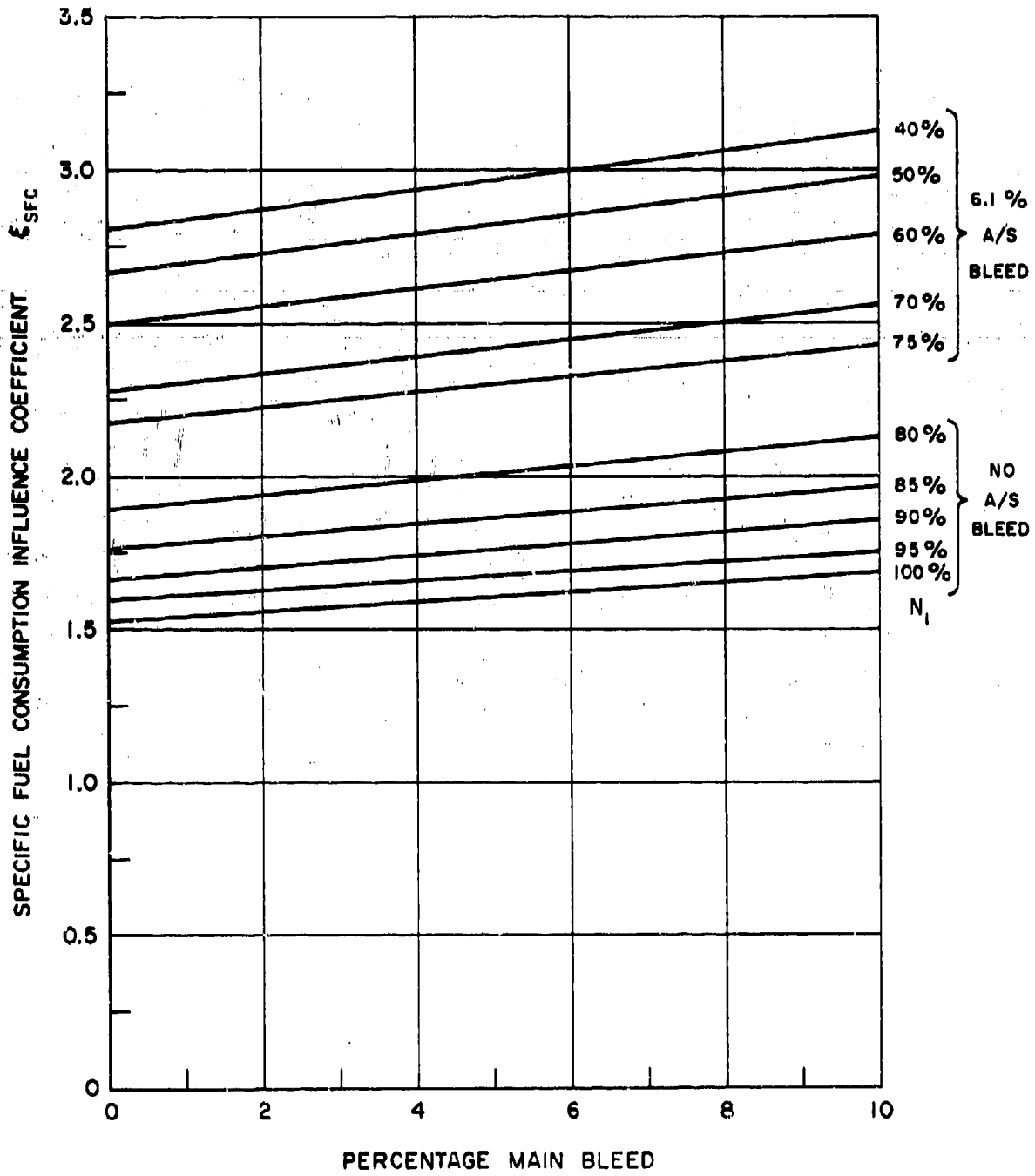

FIG. 20 : BLEED EXTRACTION

SPECIFIC FUEL CONSUMPTION INFLUENCE COEFFICIENT
VS
PERCENTAGE MAIN BLEED FOR VARIOUS ENGINE SPEEDS

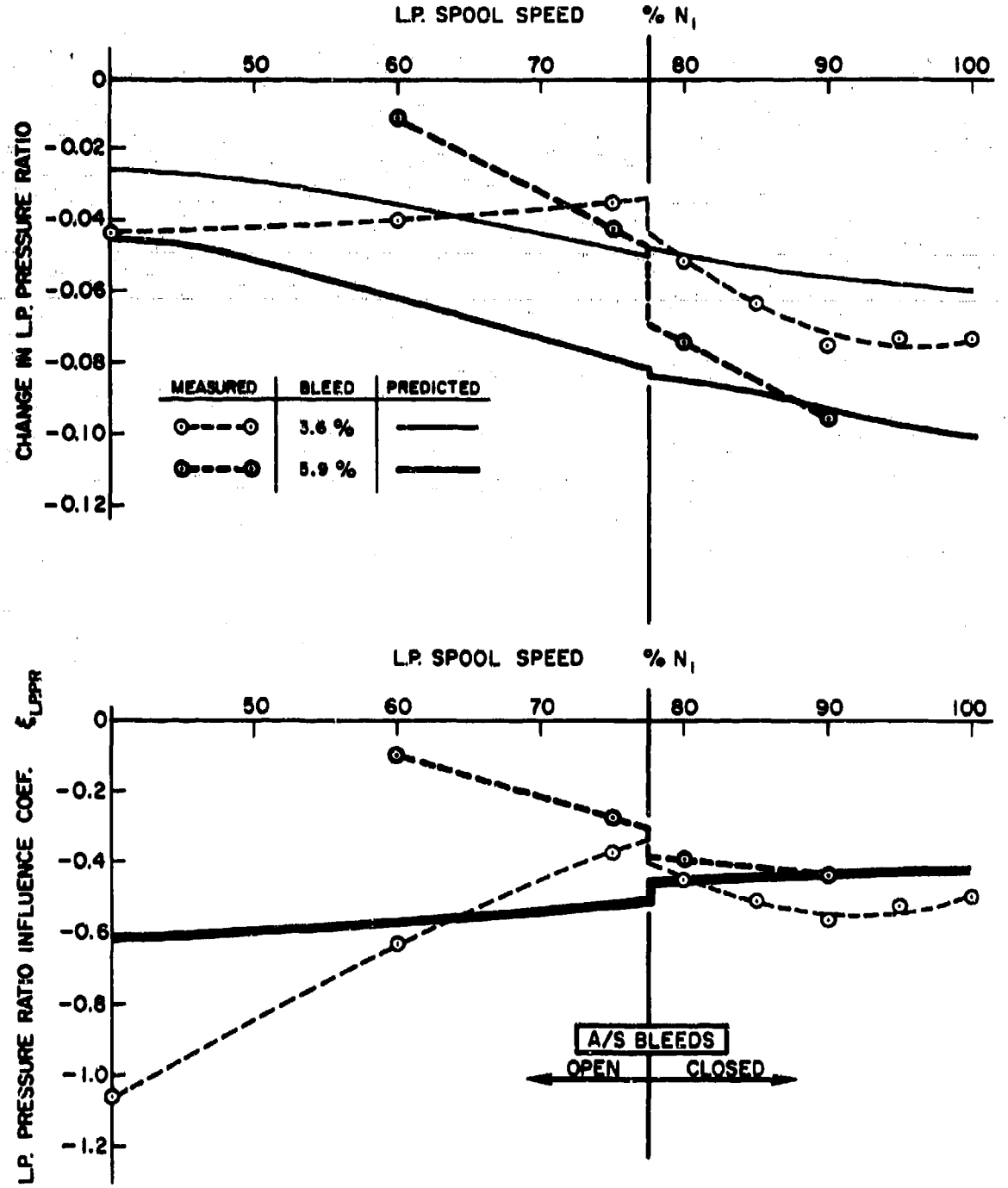

FIG. 21 : COMPARISON OF MEASURED AND PREDICTED EFFECTS OF MAIN BLEED EXTRACTION

L.P. COMPRESSOR PRESSURE RATIO vs L.P. SPOOL SPEED

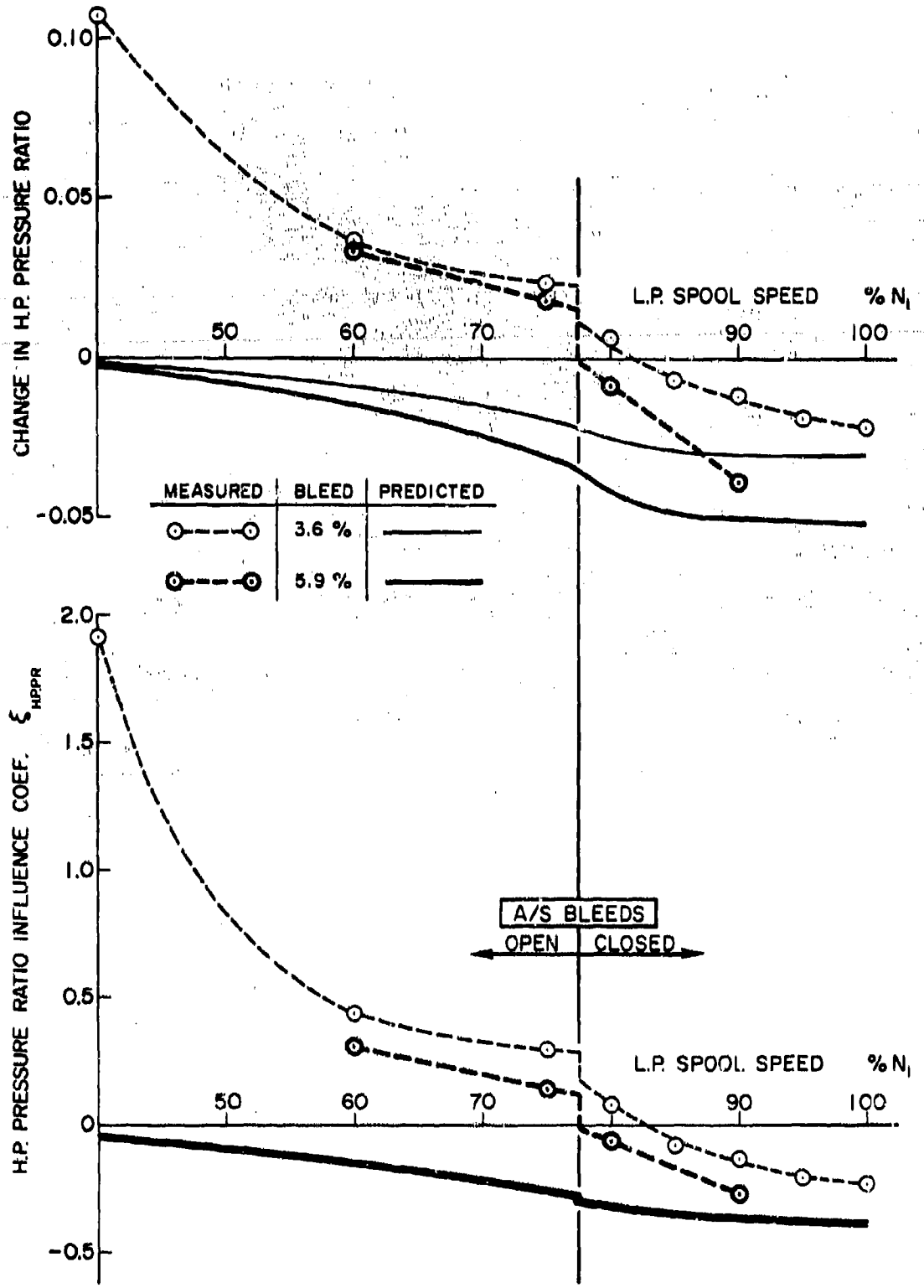

FIG. 22 : COMPARISON OF MEASURED AND PREDICTED EFFECTS OF MAIN BLEED EXTRACTION

H.P. COMPRESSOR PRESSURE RATIO vs L.P. SPOOL SPEED

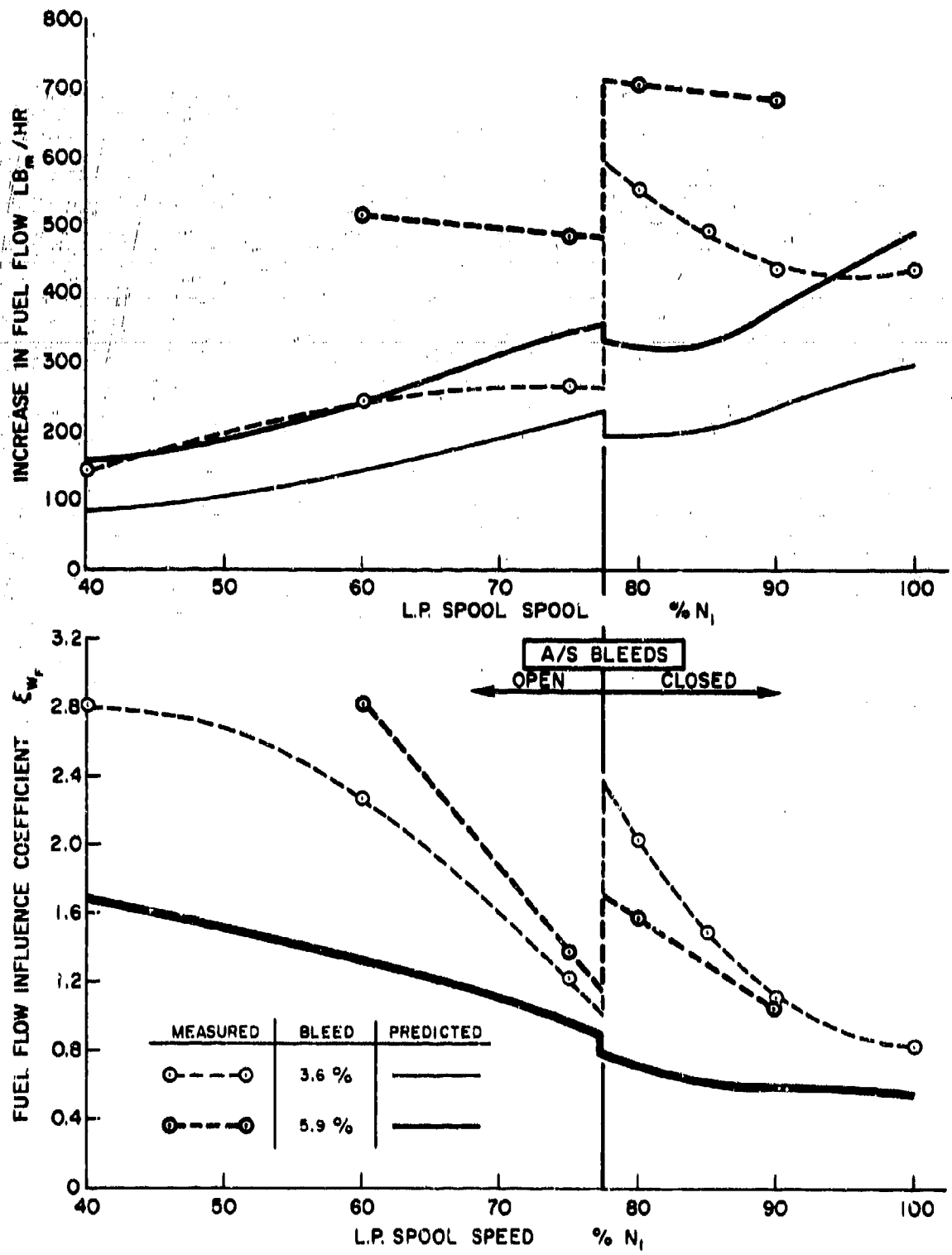

FIG.23 : COMPARISON OF MEASURED AND PREDICTED EFFECTS OF MAIN BLEED EXTRACTION

FUEL FLOW RATE vs L.P. SPOOL SPEED

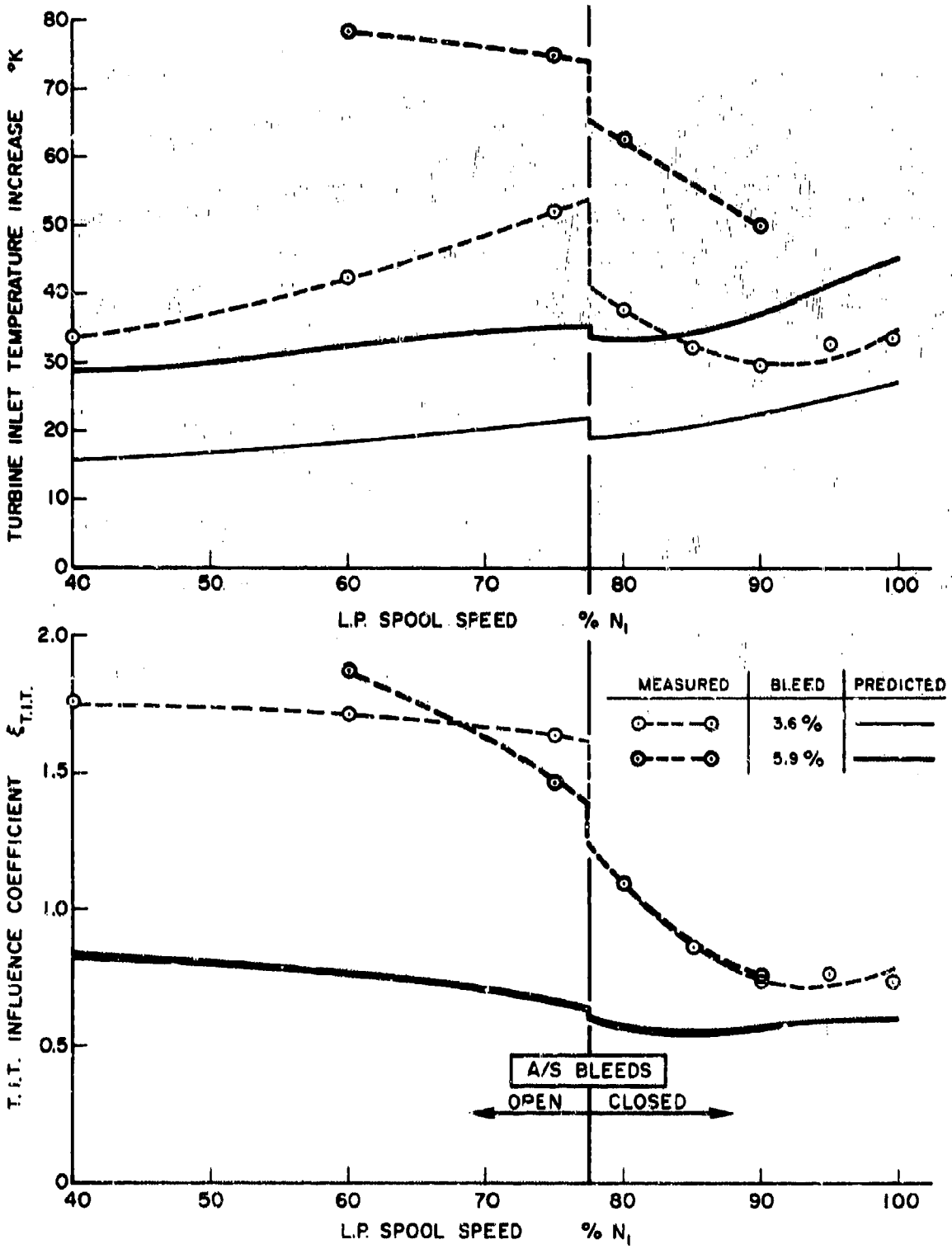

FIG.24 : COMPARISON OF MEASURED AND PREDICTED EFFECTS OF MAIN BLEED EXTRACTION

TURBINE INLET TEMPERATURE vs L.P. SPOOL SPEED

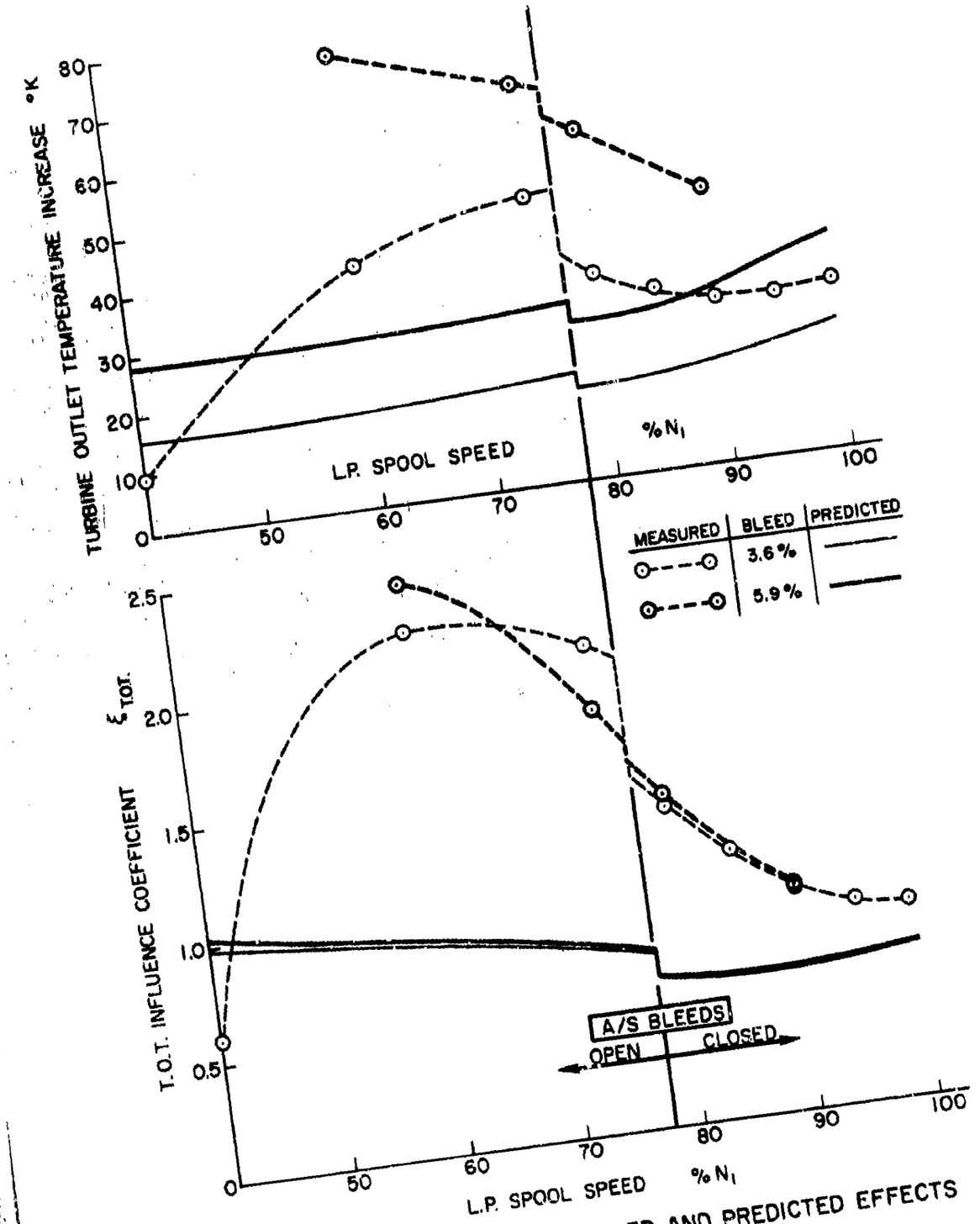

FIG. 25 : COMPARISON OF MEASURED AND PREDICTED EFFECTS OF MAIN BLEED EXTRACTION

TURBINE OUTLET TEMPERATURE vs L.P. SPOOL SPEED

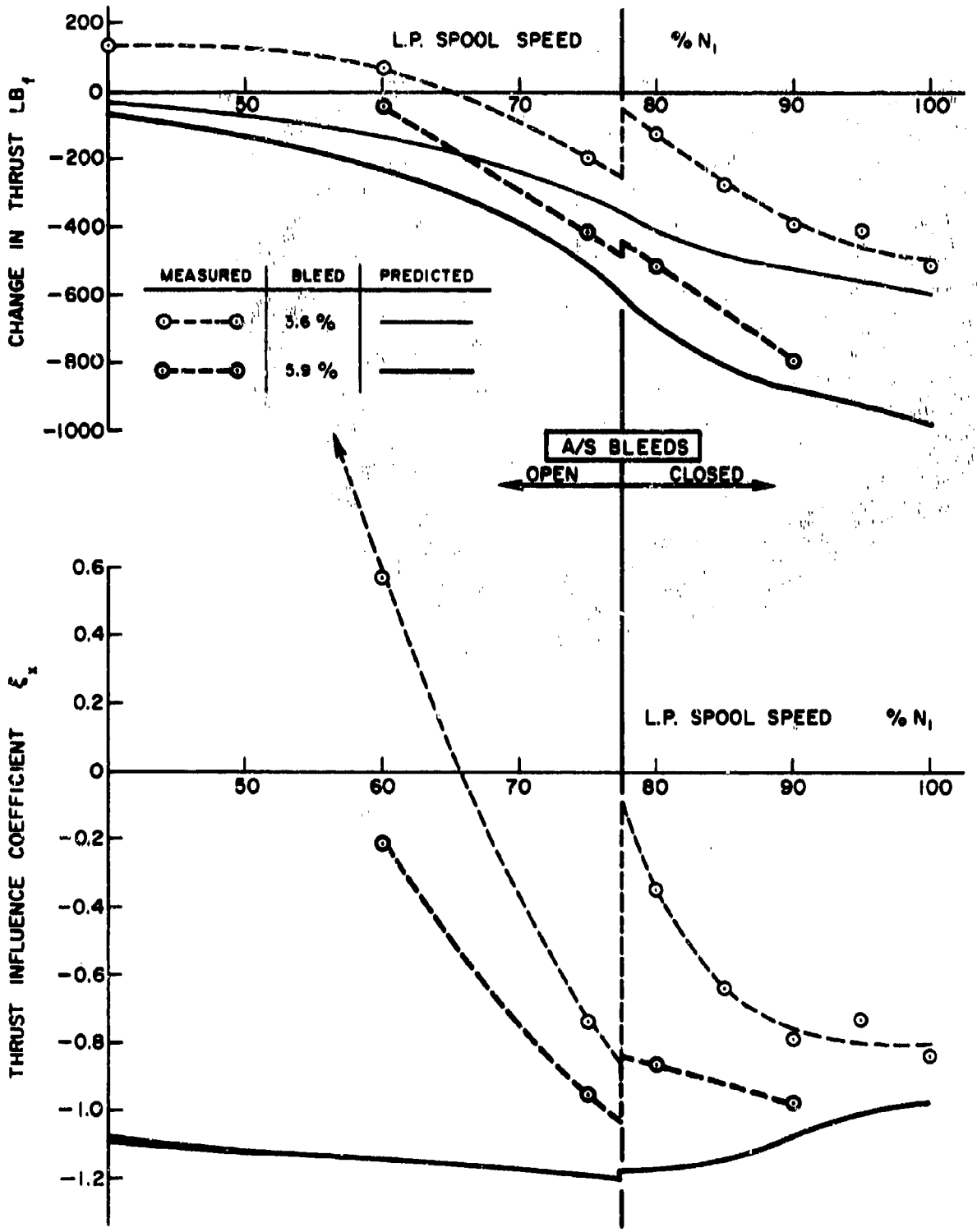

FIG. 26: COMPARISON OF MEASURED AND PREDICTED EFFECTS OF MAIN BLEED EXTRACTION

THRUST vs L.P. SPOOL SPEED

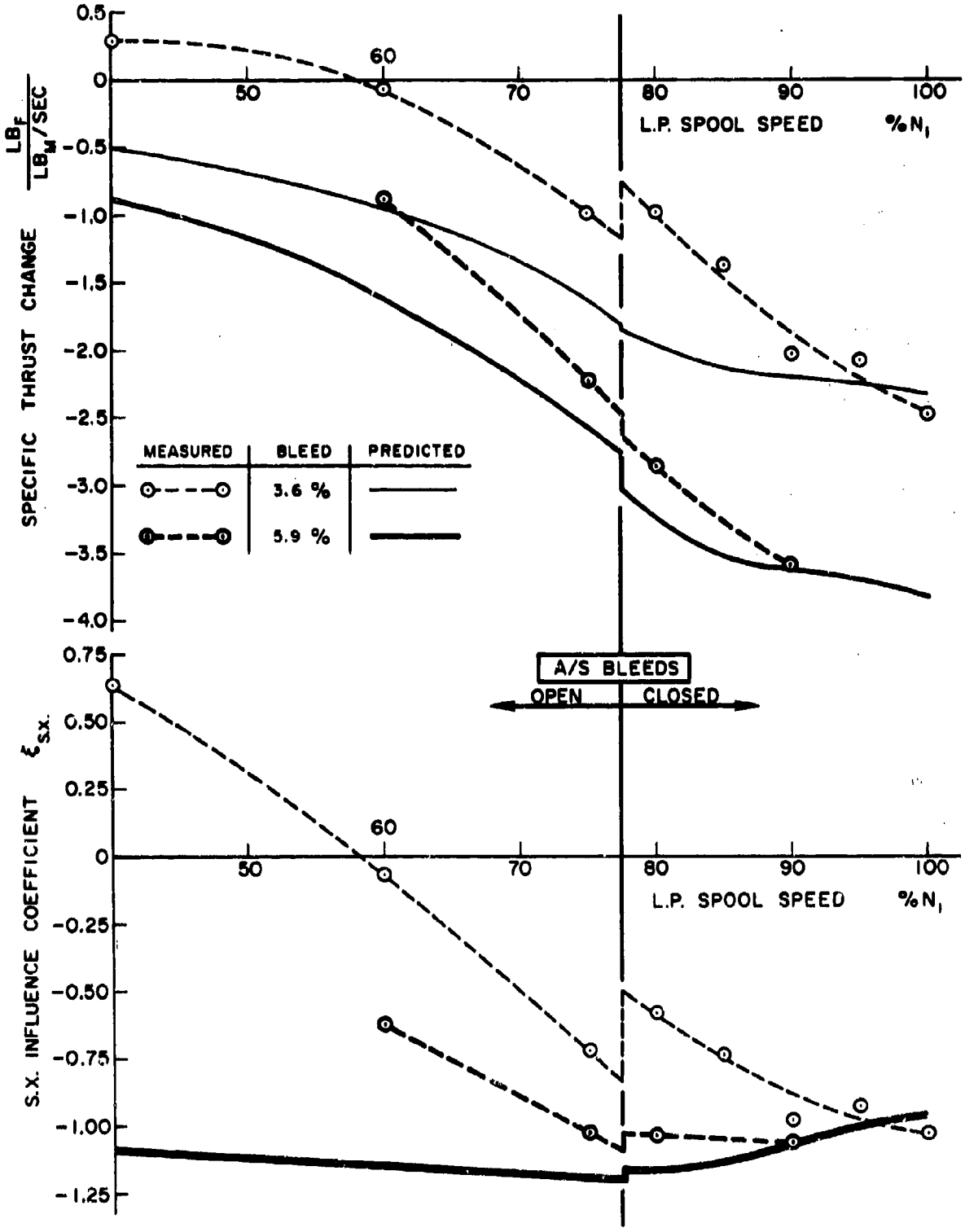

FIG. 27 : COMPARISON OF MEASURED AND PREDICTED EFFECTS OF MAIN BLEED EXTRACTION

SPECIFIC THRUST vs L.P. SPOOL SPEED

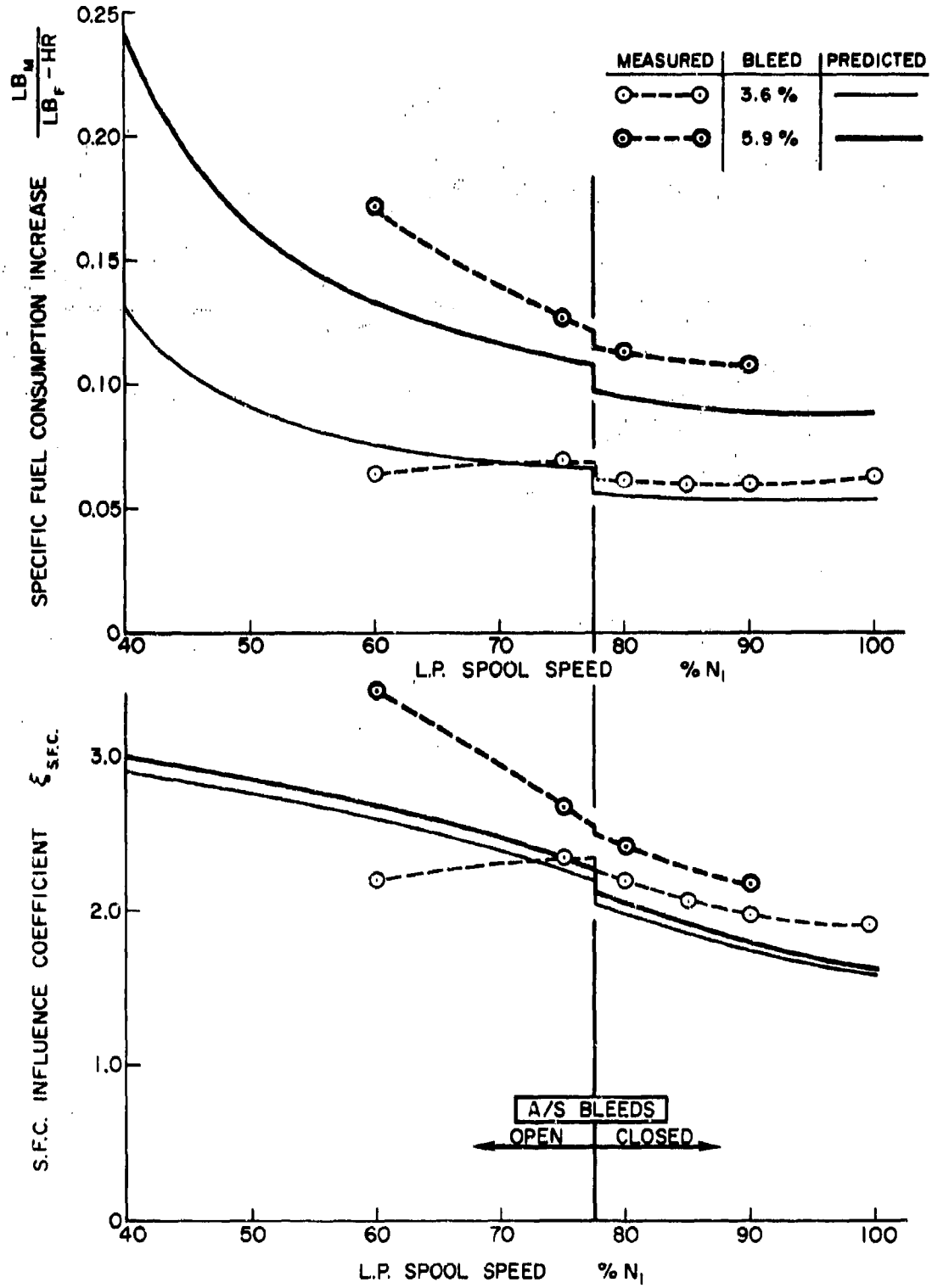

FIG. 28 : COMPARISON OF MEASURED AND PREDICTED EFFECTS OF MAIN BLEED EXTRACTION

SPECIFIC FUEL CONSUMPTION vs L.P. SPOOL SPEED

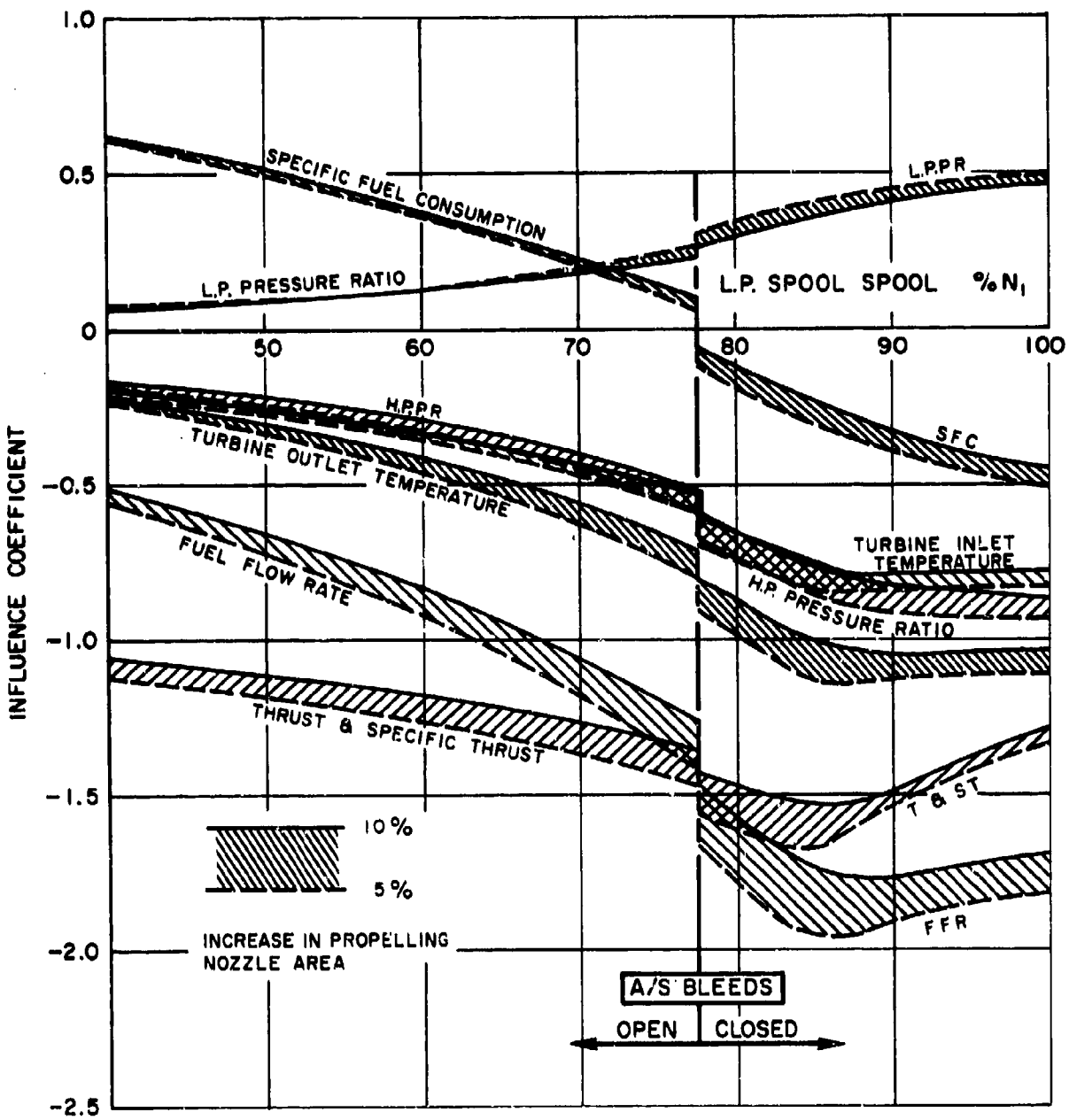

FIG. 29 : PROPELLING NOZZLE AREA CHANGE

INFLUENCE COEFFICIENTS RESULTING FROM CHANGE IN PROPELLING NOZZLE AREA vs L.P. SPOOL SPEED

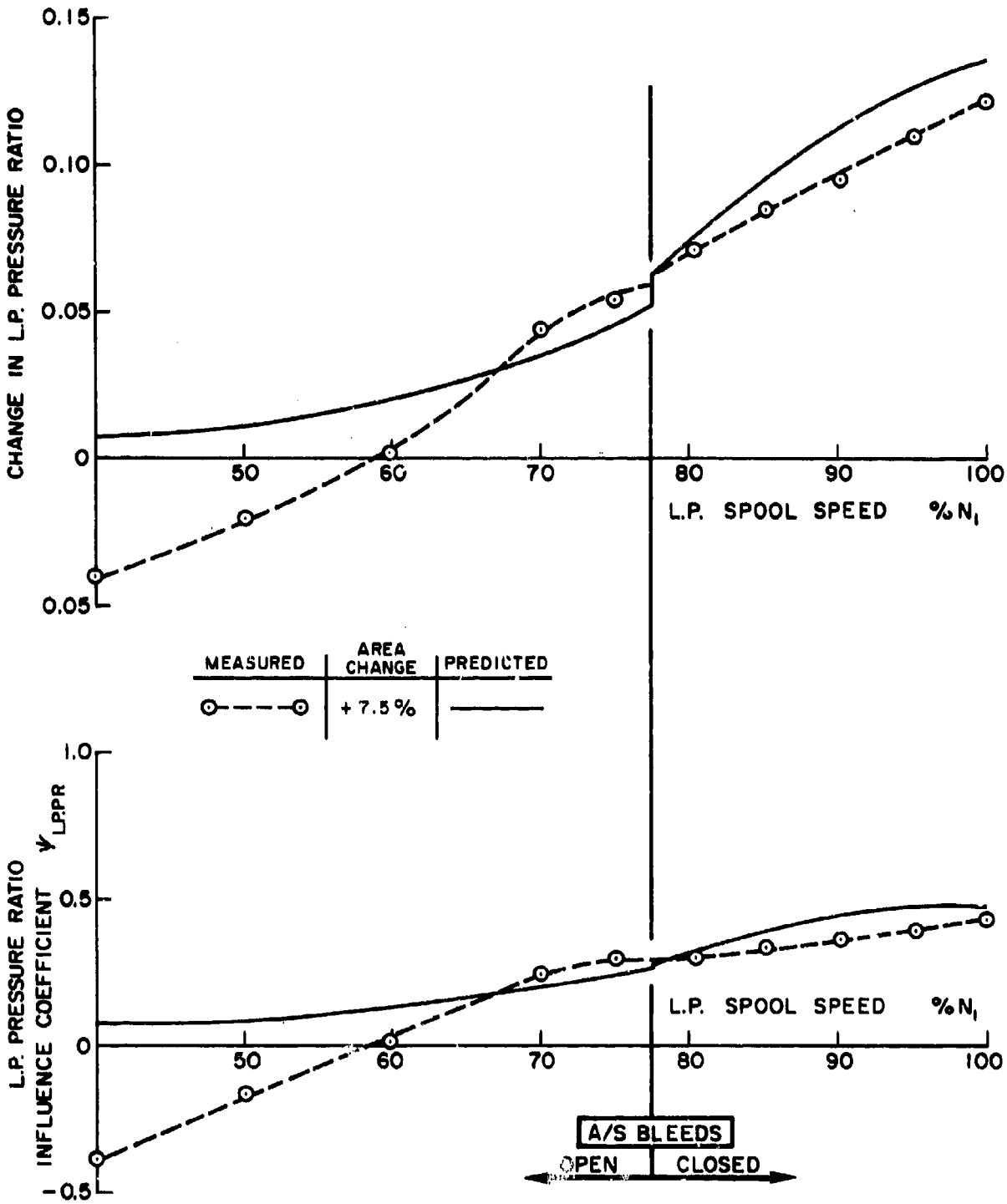

FIG. 30 : COMPARISON OF MEASURED AND PREDICTED EFFECTS OF CHANGE IN PROPELLING NOZZLE AREA

L.P. COMPRESSOR PRESSURE RATIO vs L.P. SPOOL SPEED

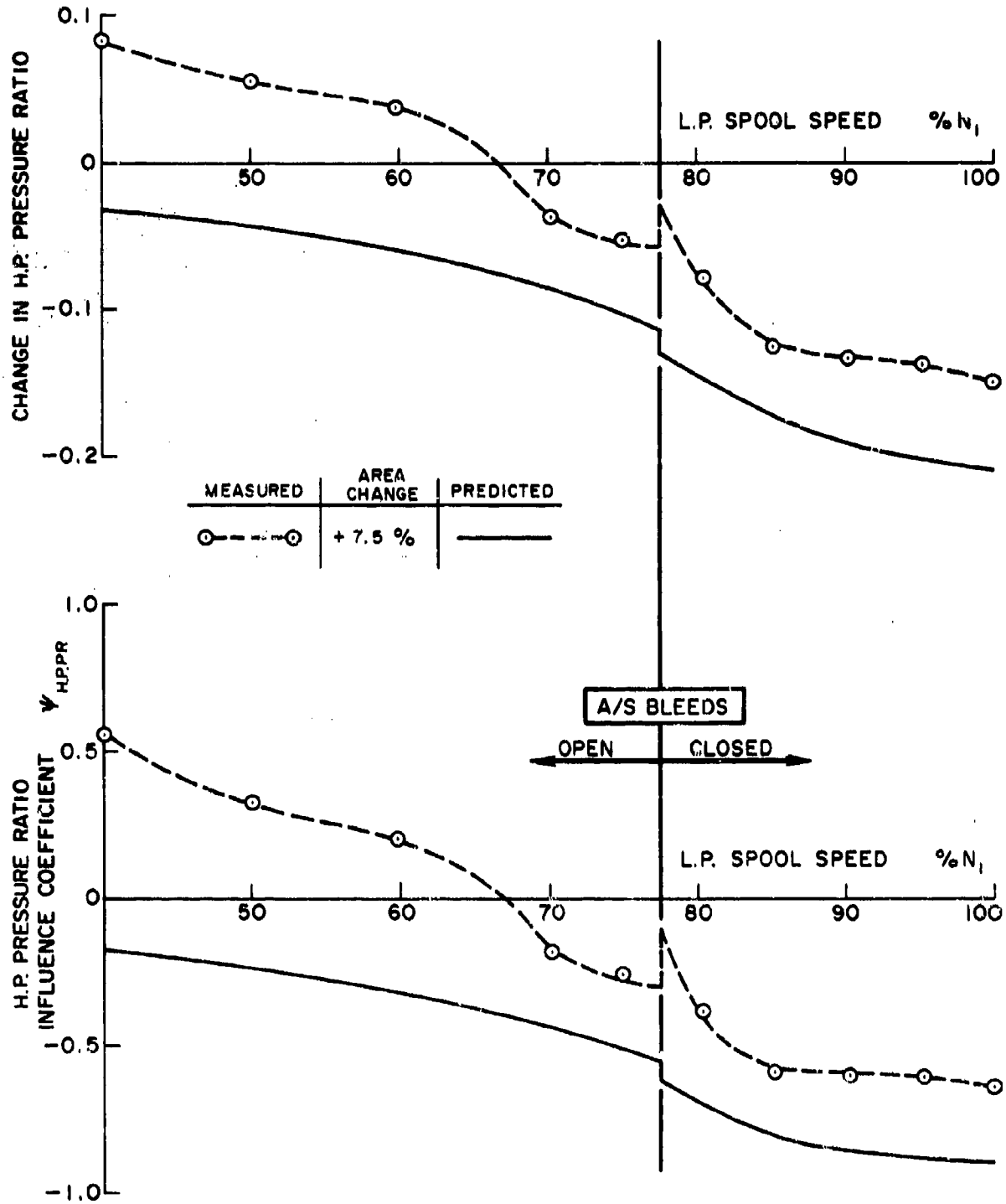

FIG. 31 : COMPARISON OF MEASURED AND PREDICTED EFFECTS OF CHANGE IN PROPELLING NOZZLE AREA

H.P. COMPRESSOR PRESSURE RATIO vs L.P. SPOOL SPEED

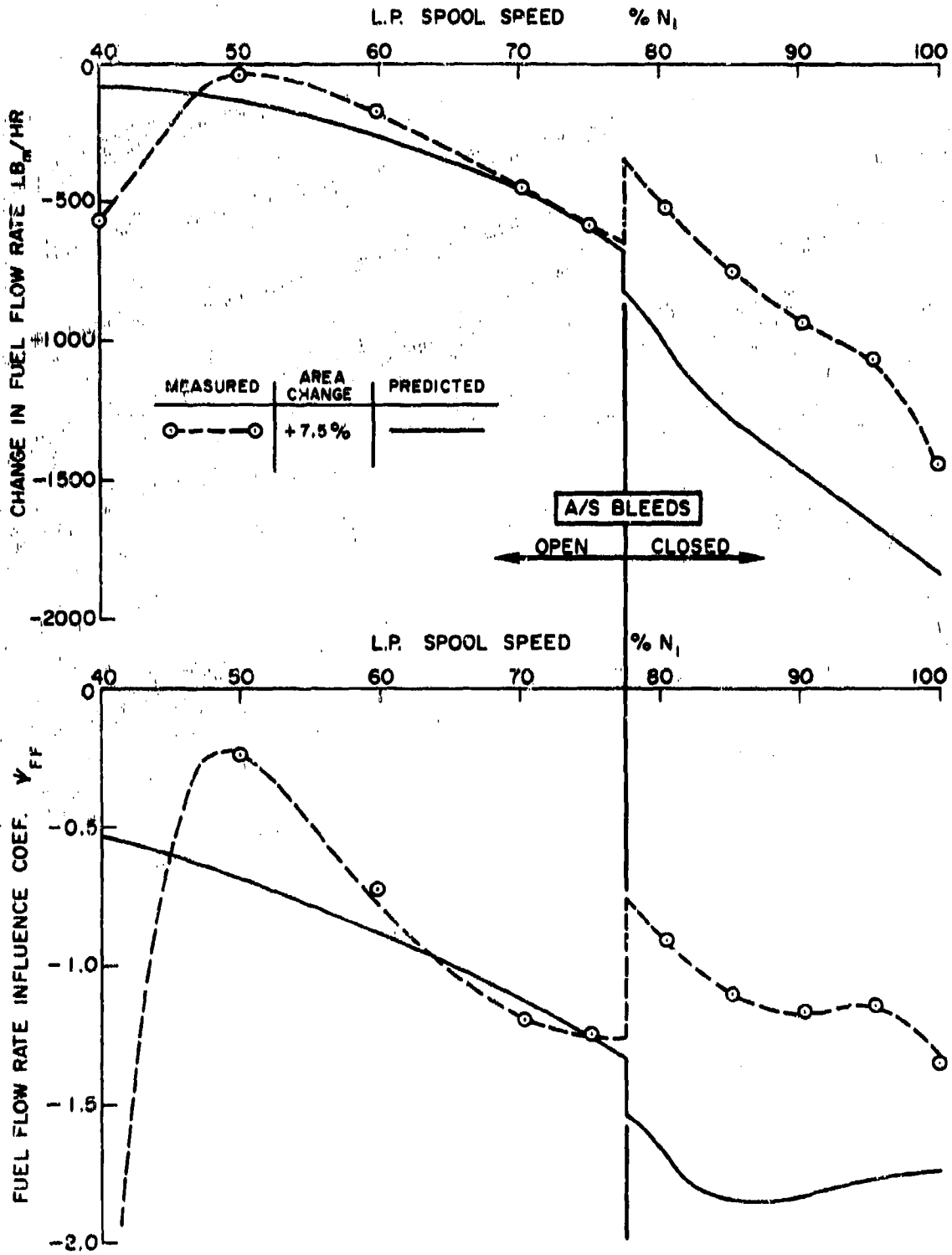

FIG.32 : COMPARISON OF MEASURED AND PREDICTED EFFECTS OF CHANGE IN PROPELLING NOZZLE AREA

FUEL FLOW RATE vs L.P. SPOOL SPEED

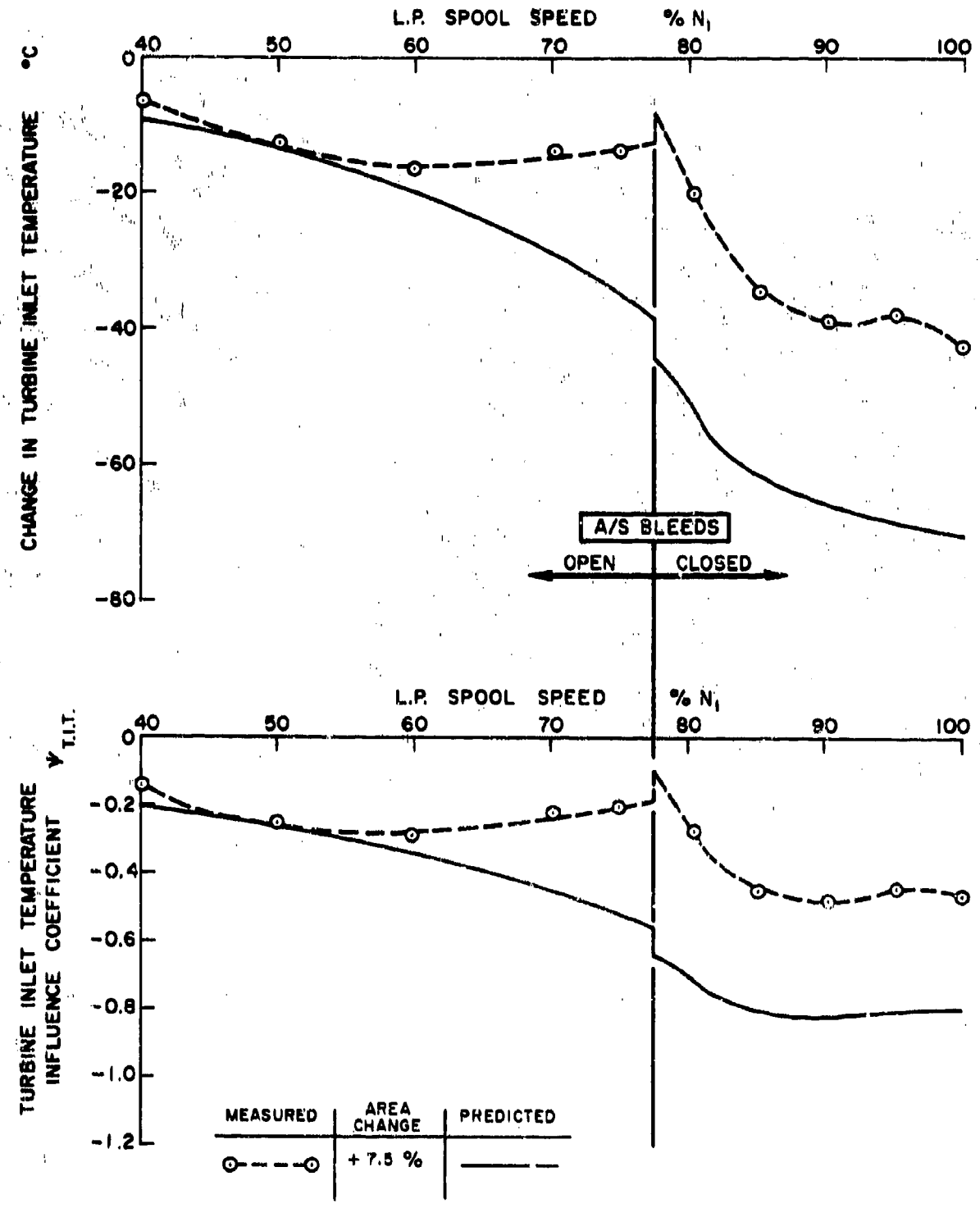

FIG. 33 : COMPARISON OF MEASURED AND PREDICTED EFFECTS OF CHANGE IN PROPELLING NOZZLE AREA

TURBINE INLET TEMPERATURE vs L.P. SPOOL SPEED

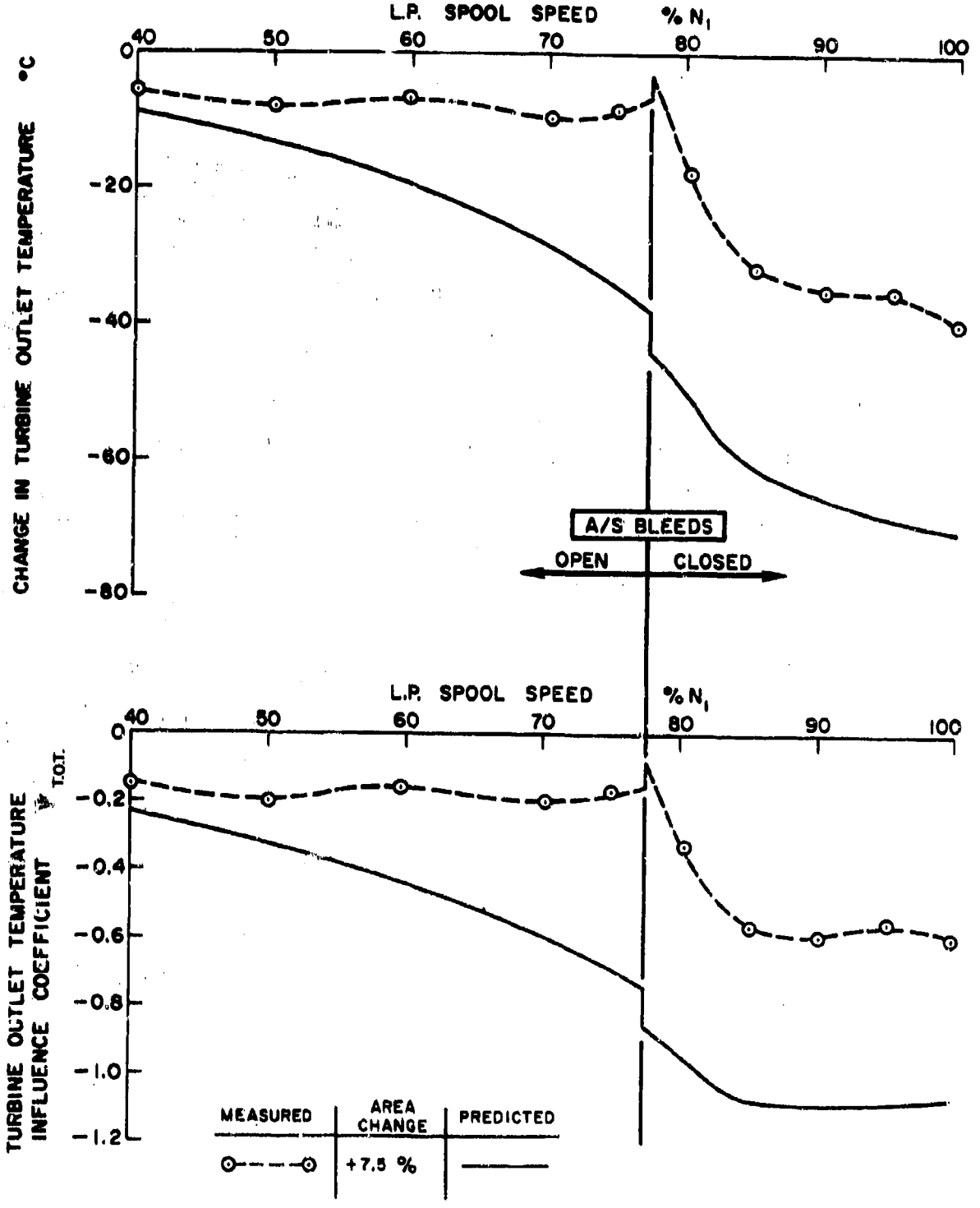

FIG. 34 : COMPARISON OF MEASURED AND PREDICTED EFFECTS OF CHANGE IN PROPELLING NOZZLE AREA

TURBINE OUTLET TEMPERATURE vs L.P. SPOOL SPEED

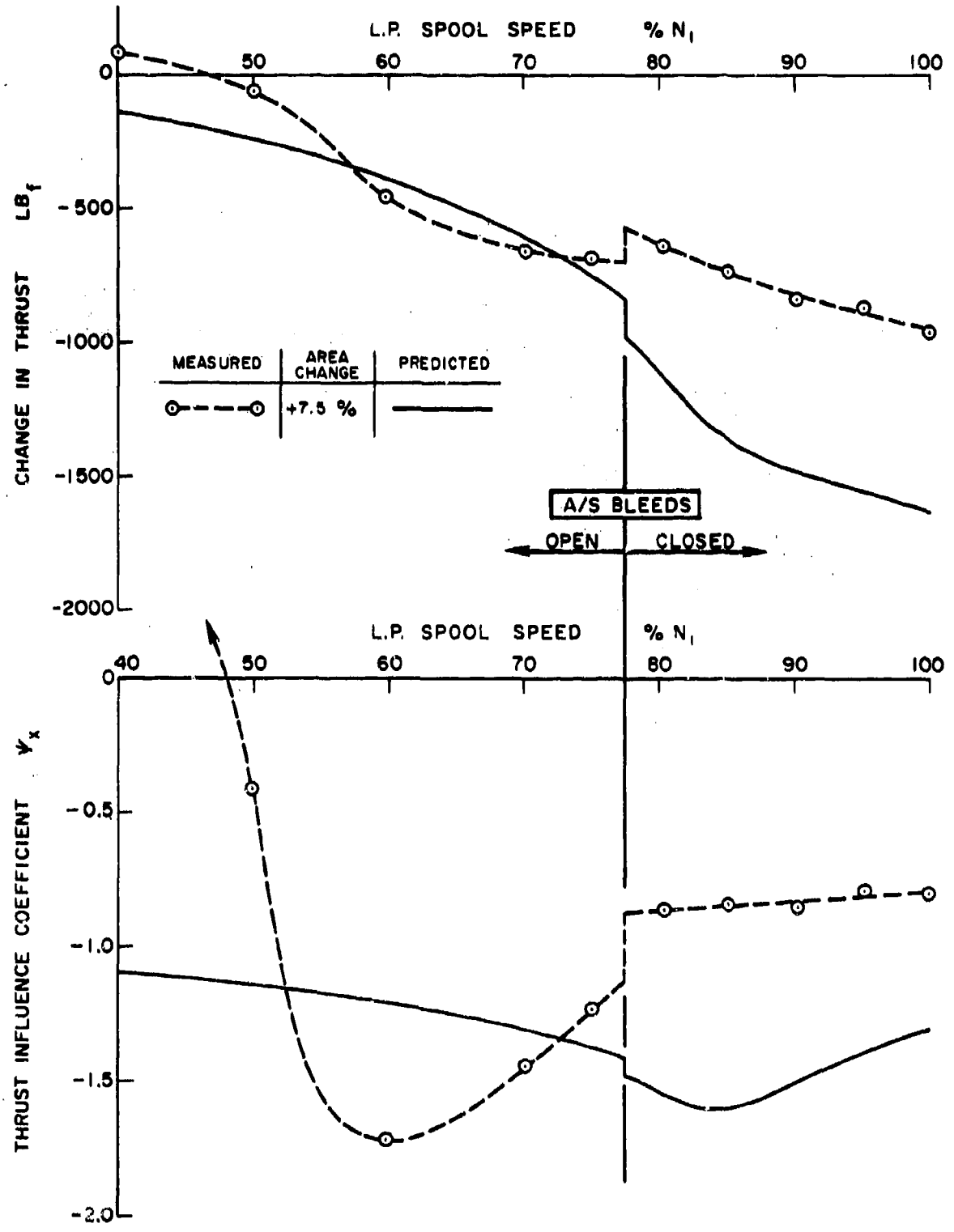

FIG. 35 : COMPARISON OF MEASURED AND PREDICTED EFFECTS OF CHANGE IN PROPELLING NOZZLE AREA

THRUST vs L.P. SPOOL SPEED

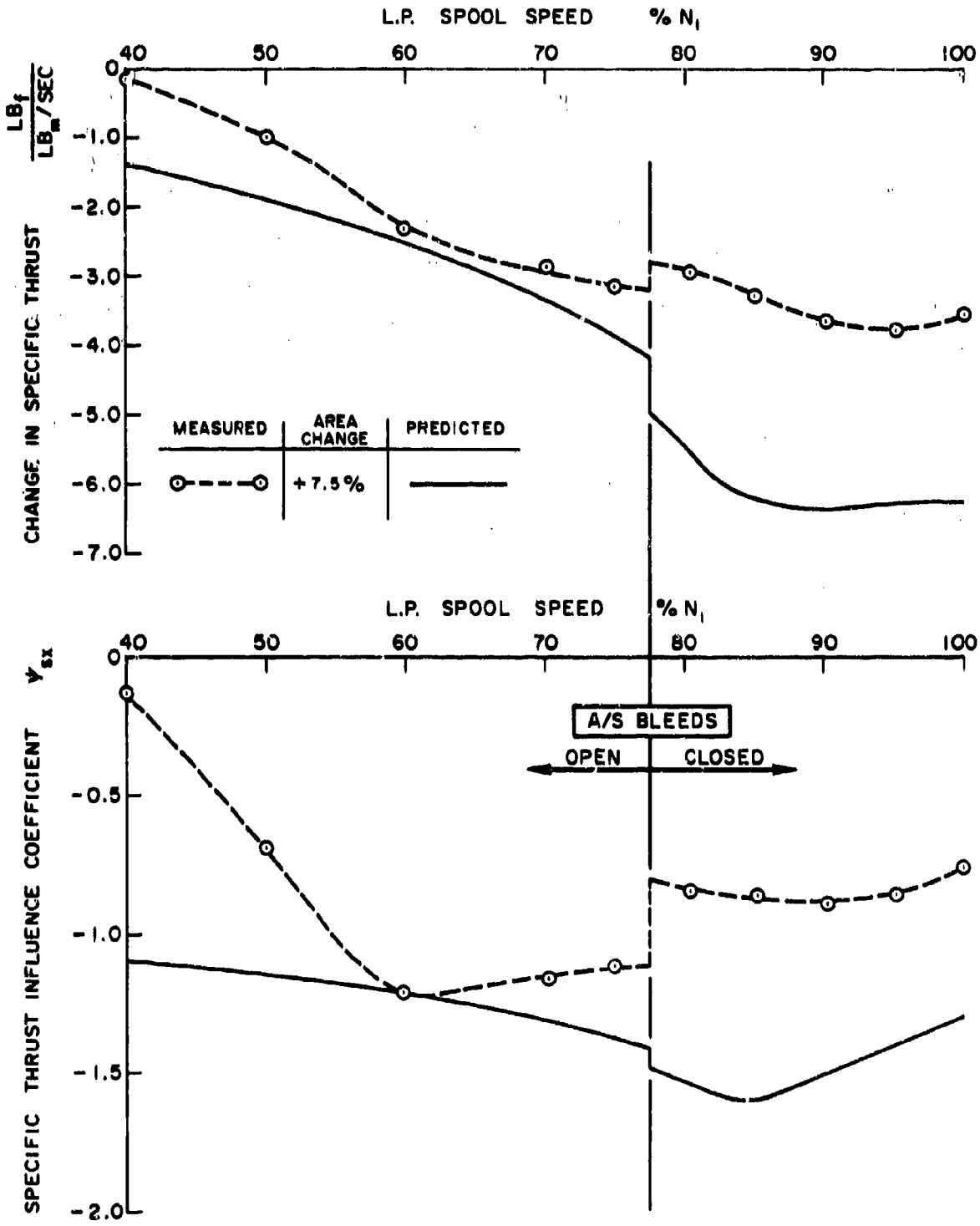

FIG. 36 : COMPARISON OF MEASURED AND PREDICTED EFFECTS OF CHANGE IN PROPELLING NOZZLE AREA

SPECIFIC THRUST vs L.P. SPOOL SPEED

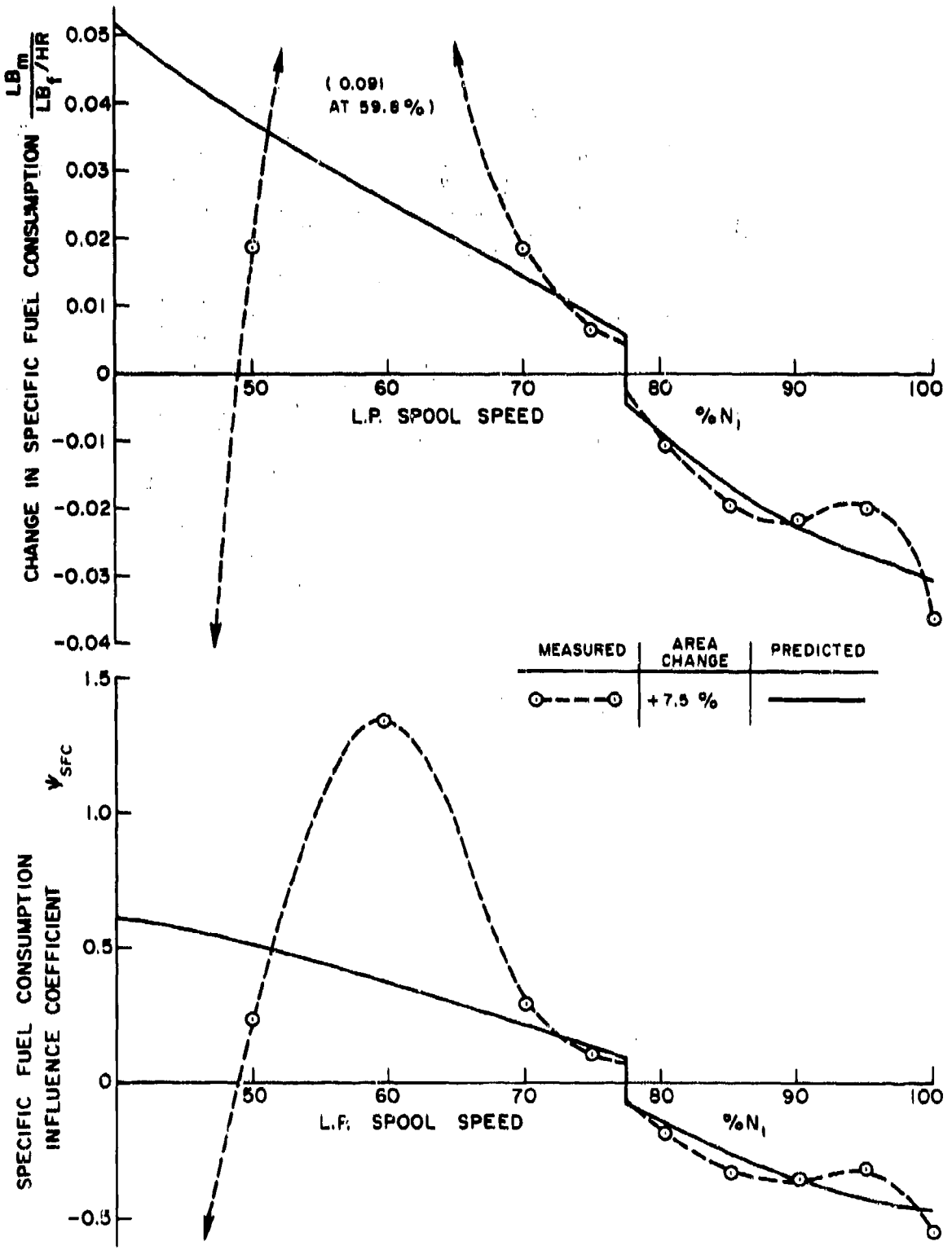

FIG.37 : COMPARISON OF MEASURED AND PREDICTED EFFECTS OF CHANGE IN PROPELLING NOZZLE AREA

SPECIFIC FUEL CONSUMPTION vs L.P. SPOOL SPEED

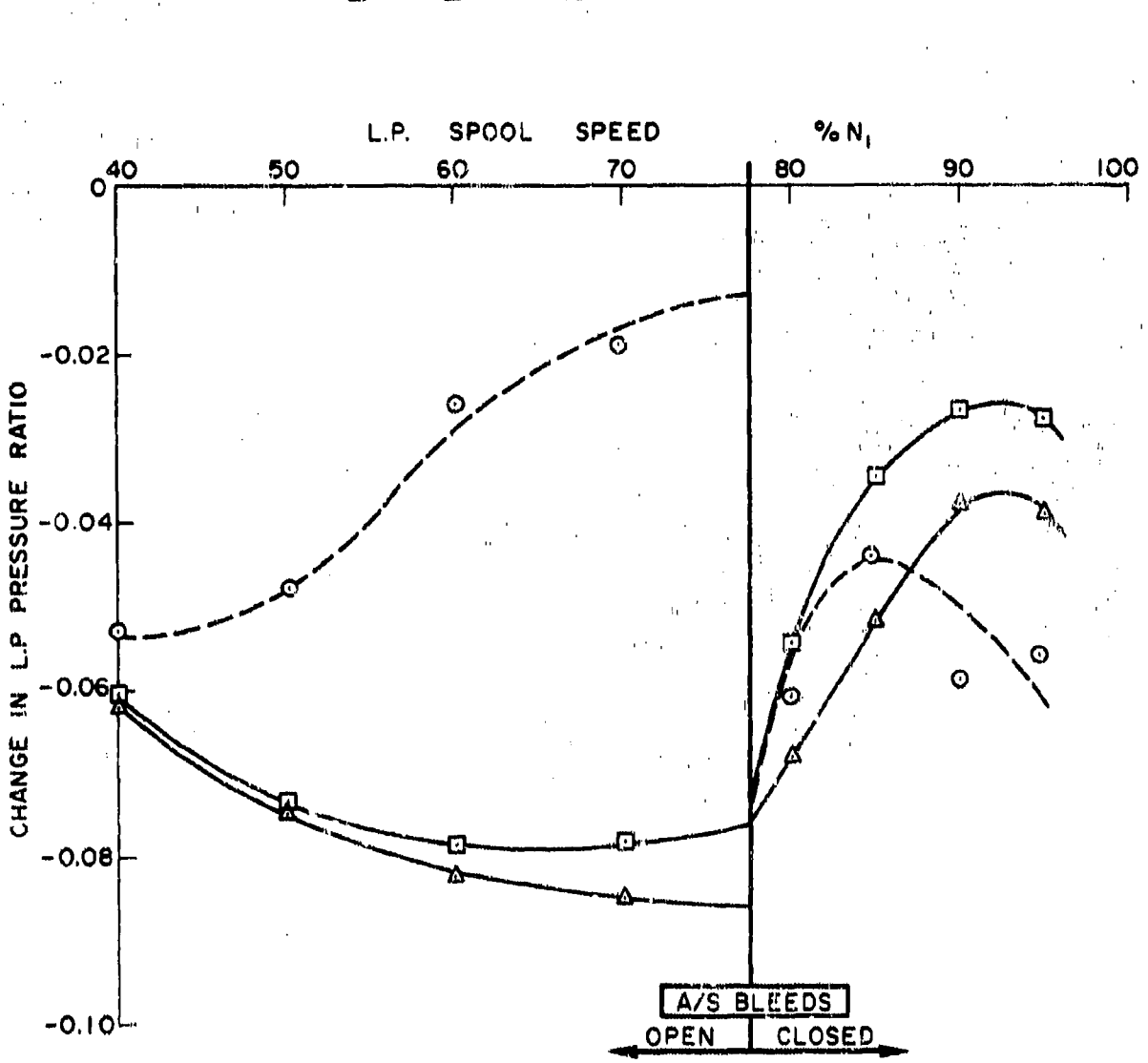

FIG. 38 : COMPARISON OF MEASURED AND PREDICTED EFFECTS OF MAIN BLEED AND PROPELLING NOZZLE AREA INCREASE

L.P. COMPRESSOR PRESSURE RATIO vs L.P. SPOOL SPEED

MB : 8.4 – 9.8 %, ΔA_N : 7.5 %

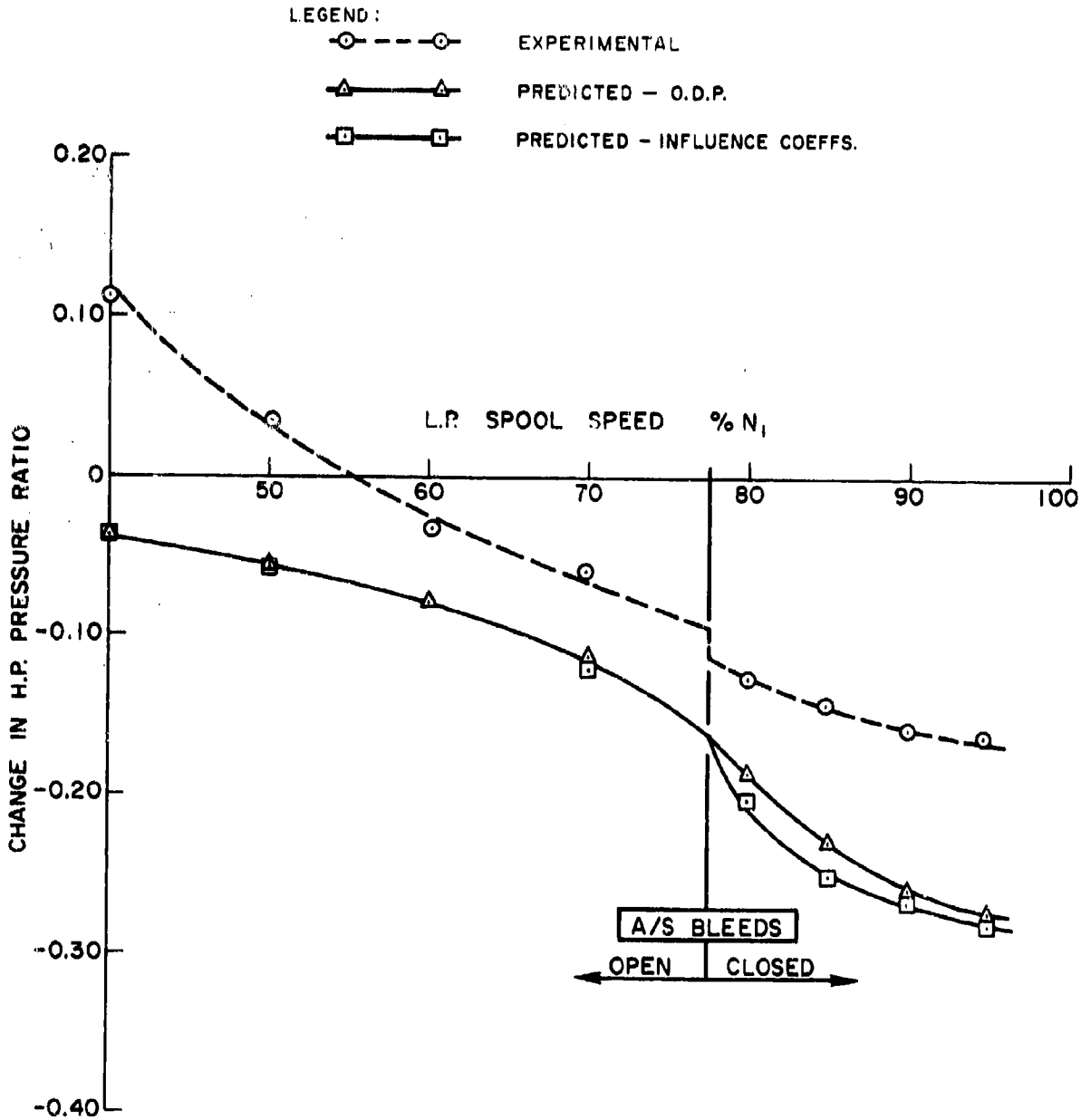

FIG. 39 : COMPARISON OF MEASURED AND PREDICTED EFFECTS OF MAIN BLEED AND PROPELLING NOZZLE AREA INCREASE

H.P. COMPRESSOR PRESSURE RATIO vs L.P. SPOOL SPEED

MB : 8.4 – 9.8 %, ΔA_N : 7.5 %

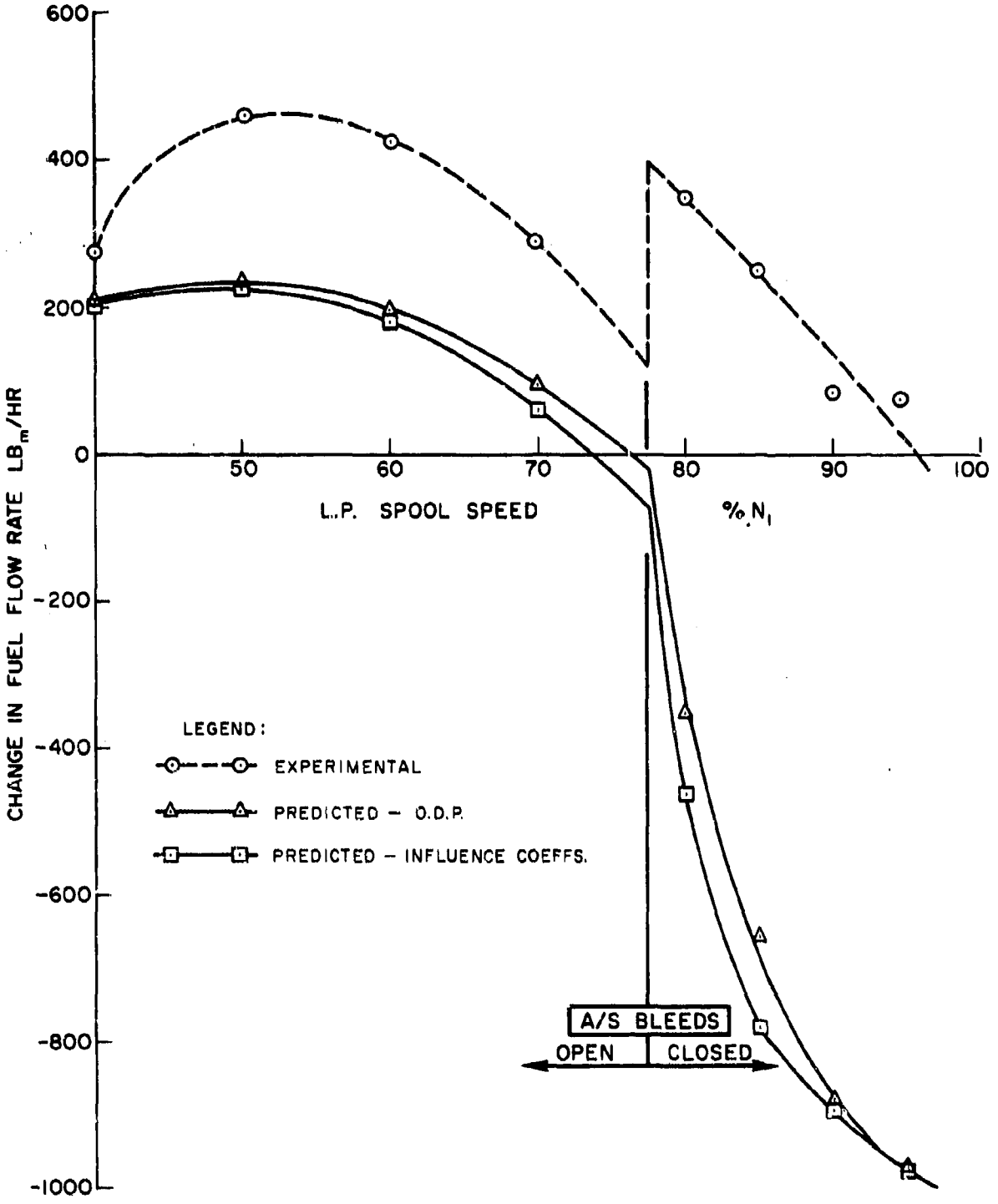

FIG. 40 : COMPARISON OF MEASURED AND PREDICTED EFFECTS OF MAIN BLEED AND PROPELLING NOZZLE AREA INCREASE

FUEL FLOW RATE vs L.P. SPOOL SPEED

MB : 8.4 – 9.8 %, ΔA_N : 7.5 %

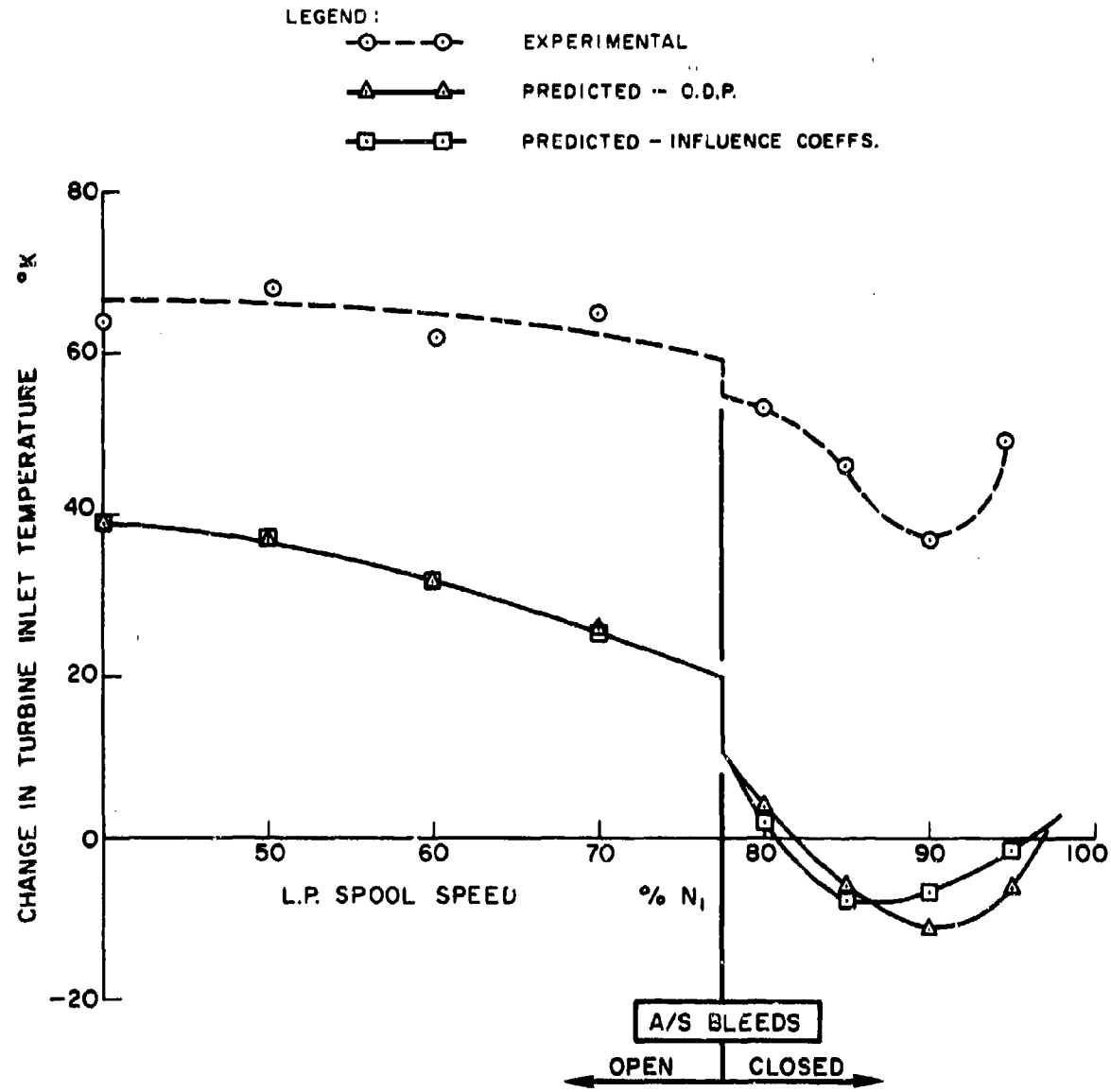

FIG. 41 : COMPARISON OF MEASURED AND PREDICTED EFFECTS OF MAIN BLEED AND PROPELLING NOZZLE AREA INCREASE

TURBINE INLET TEMPERATURE vs L.P. SPOOL SPEED

MB : 8.4 - 9.8 %, ΔA_N : 7.5 %

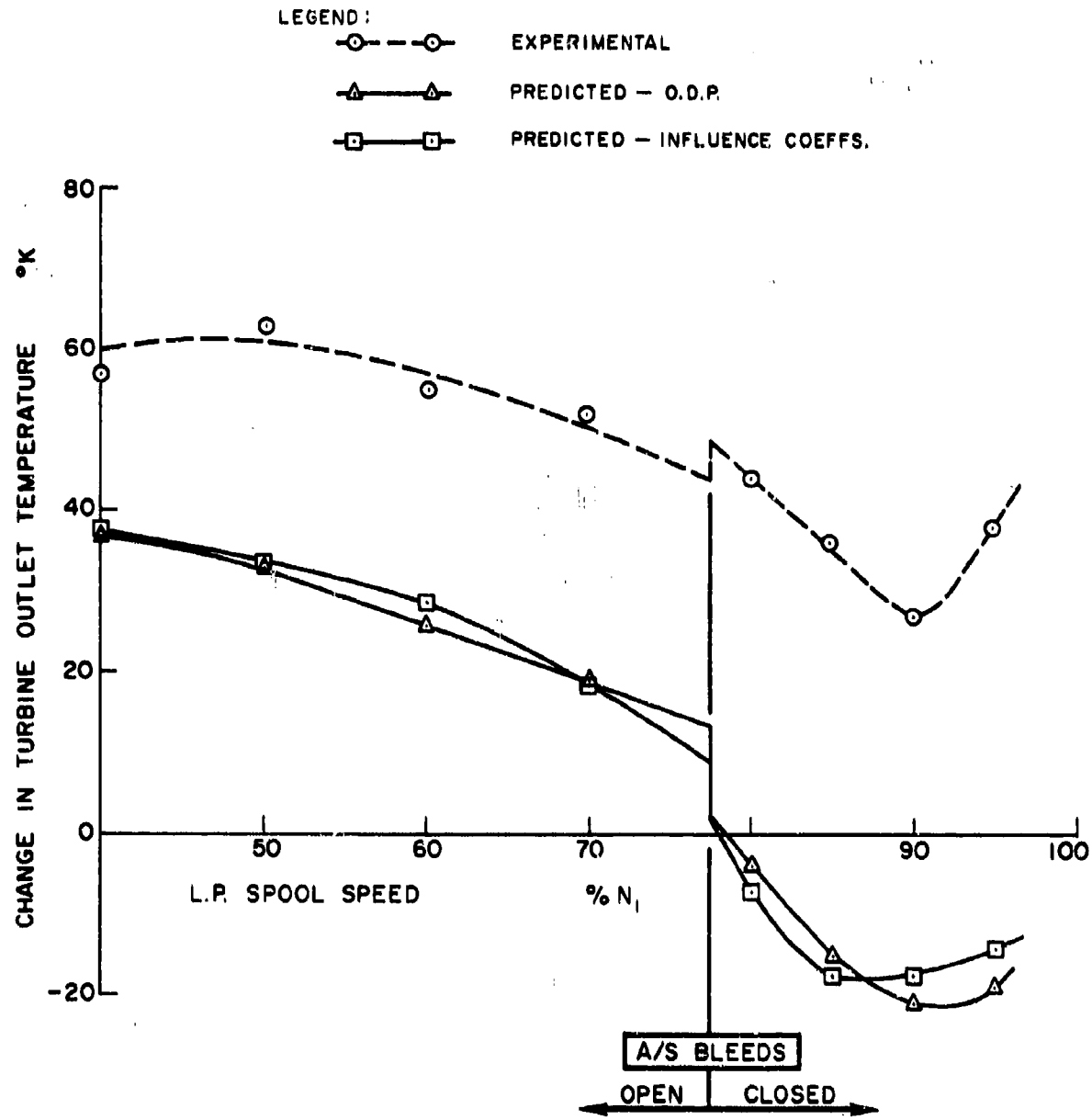

FIG. 42 : COMPARISON OF MEASURED AND PREDICTED EFFECTS OF MAIN BLEED AND PROPELLING NOZZLE AREA INCREASE

TURBINE OUTLET TEMPERATURE vs L.P. SPOOL SPEED

MB : 8.4 – 9.8 %, ΔA_N : 7.5 %

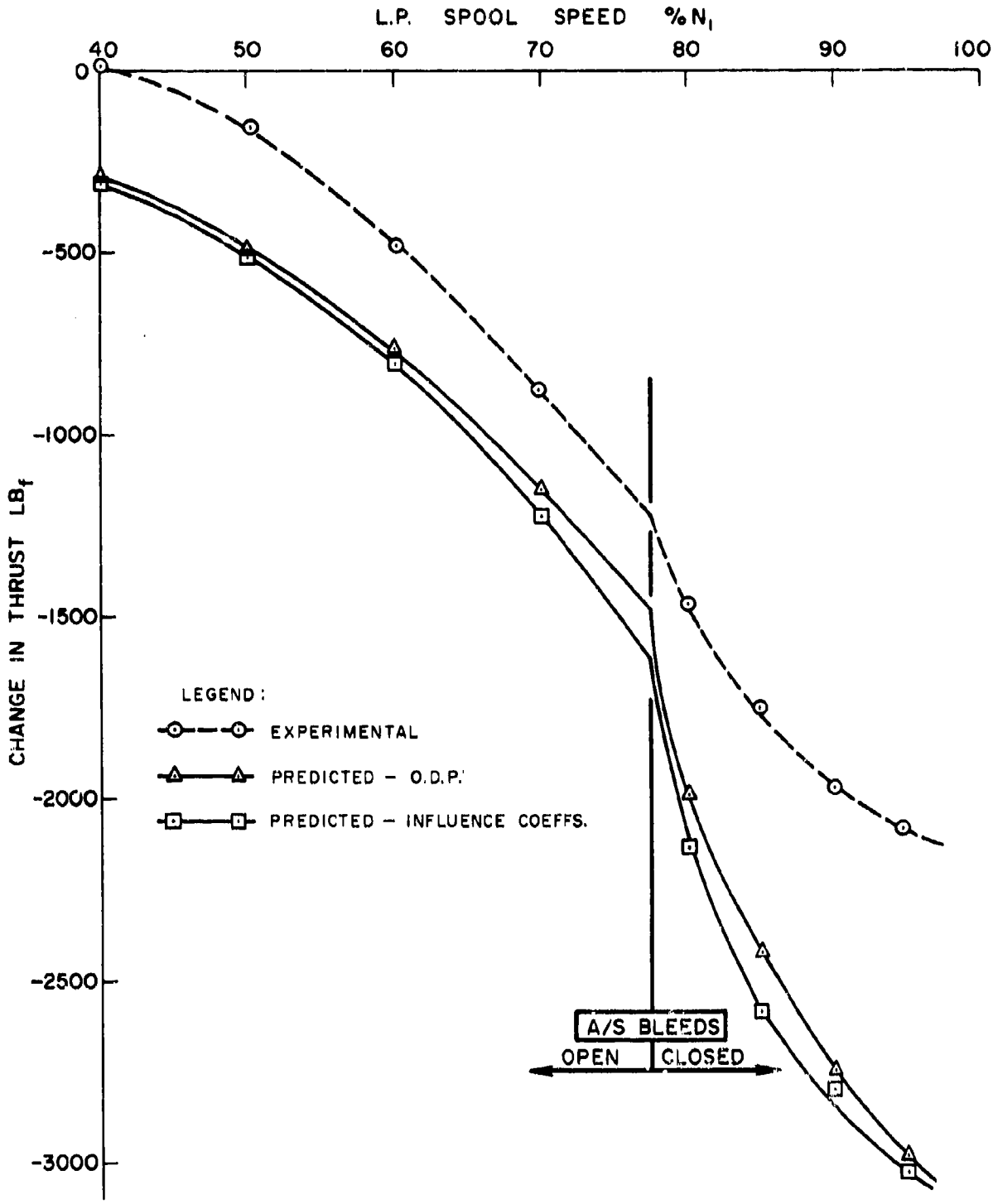

FIG. 43 : COMPARISON OF MEASURED AND PREDICTED EFFECTS OF MAIN BLEED AND PROPELLING NOZZLE AREA INCREASE

THRUST vs L.P. SPOOL SPEED

MB : 8.4 – 9.8 %, ΔA_N : 7.5 %

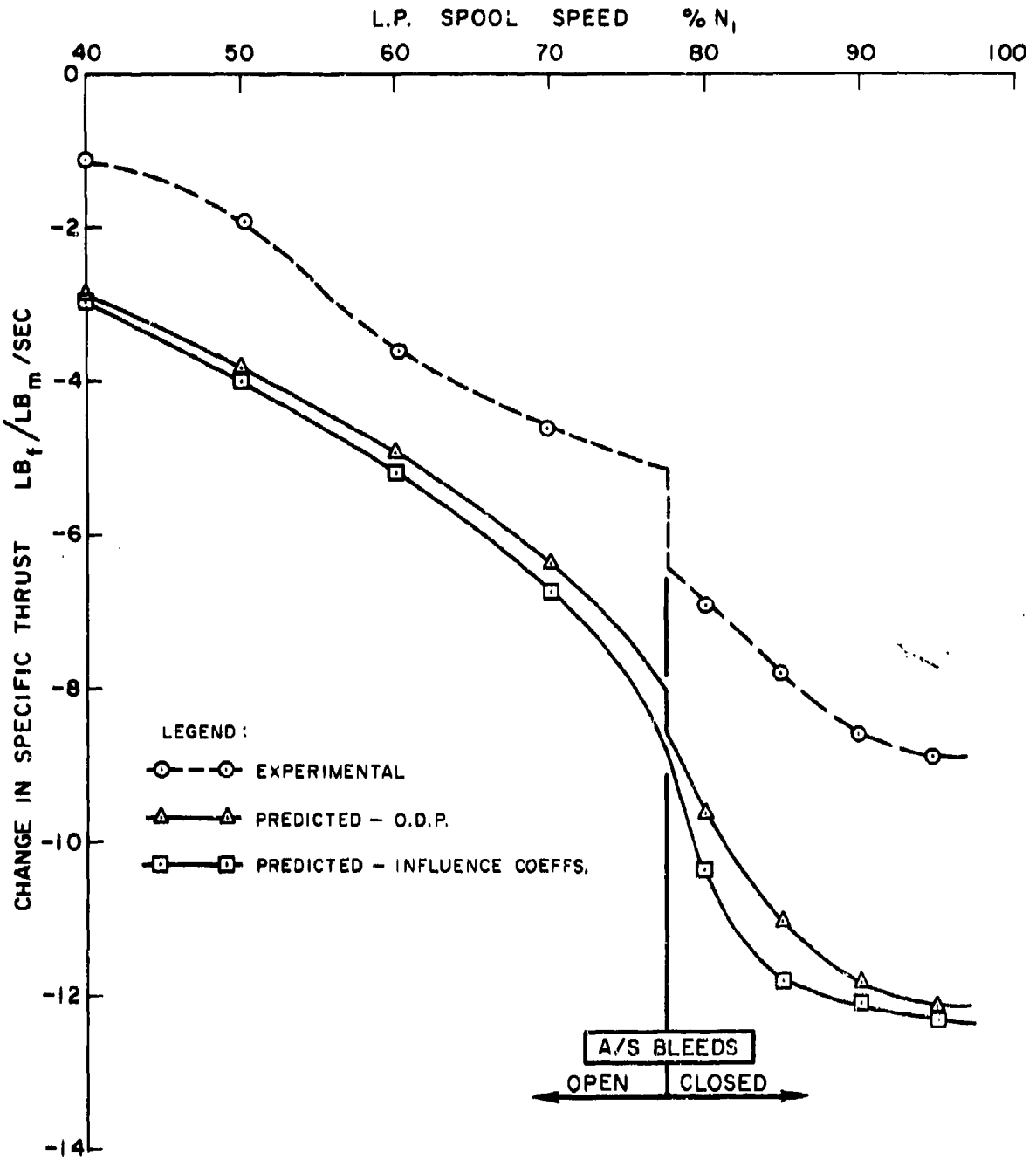

FIG. 44 : COMPARISON OF MEASURED AND PREDICTED EFFECTS OF MAIN BLEED AND PROPELLING NOZZLE AREA INCREASE

SPECIFIC THRUST vs L.P. SPOOL SPEED

MB : 8.4 – 9.8 %, ΔA_N : 7.5 %

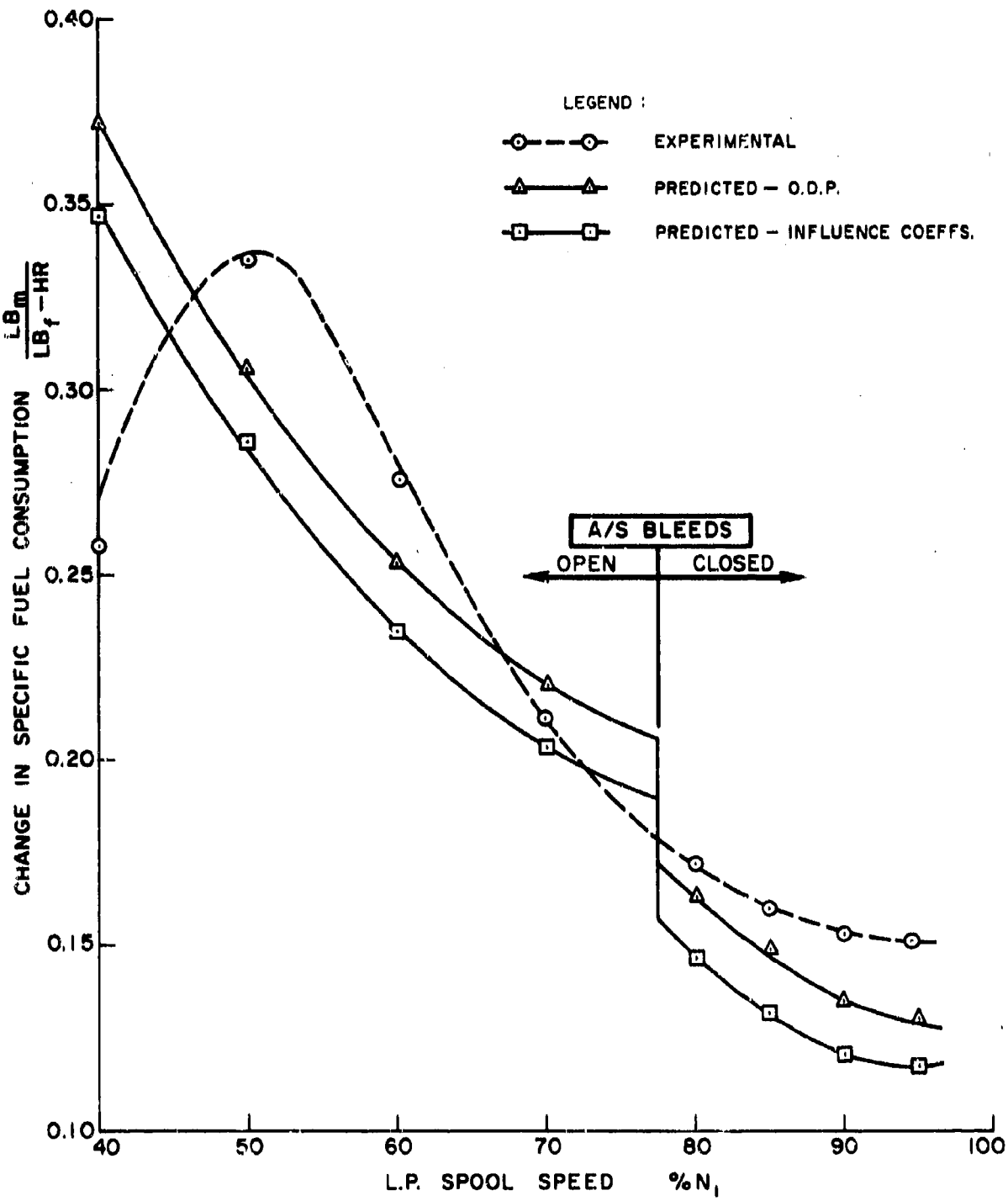

FIG. 45 : COMPARISON OF MEASURED AND PREDICTED EFFECTS OF MAIN BLEED AND PROPELLING NOZZLE AREA INCREASE

SPECIFIC FUEL CONSUMPTION vs L.P. SPOOL SPEED
MB : 8.4 - 9.8 %, ΔA_N : 7.5 %

APPENDIX A

J-75 DATA REDUCTION PROGRAM:

SAMPLE RAW DATA AND OUTPUT SHEETS

J 75 – ENGINE TEST

DATE : 24/3/71 | RUN NO : 029 | SHEET NO : 01

BARO : 29.62 "HG | BARO TEMP. : 22.5 °C

TIME OF READING :			1012	1016	1022	1026	1032	1038	J75 INPR IDENTN
LP COMP. SPEED (N_1)		%	38.75	48.0	58.0	67.9	77.3	82.1	2
HP COMP. SPEED (N_2)		%	64.5	73	79.0	84.0	88.8	91.1	3
ENGINE OIL TEMPERATURE		°C	60	75	80	76	85	92	
FUEL INLET PRESSURE		PSIG	25	22.5	22.0	21.0	19.0	18.0	
JET PIPE TEMPERATURE	1	°C	271	281	309	355	420	453	30
ENGINE OIL PRESSURE (/ATM.)		PSIG	50	50	50.5	51	51	51.0	
FUEL FLOW RATE		LB/HR	1900	2550	3525	4950	7400	8625	28
MAIN BLEED UPST. PRESS. STATIC		PSIG	11.4	18.6	28.2	40.0	57.4	64.7	18
HP COMP. OUTLET PRESSURE		PSIG	25	37.5	54.2	74.0	102	114	15
LP TURBINE OUTLET PRESSURE		"HG	2.75	4.65	7.90	12.9	22	26.4	29
LP COMPRESSOR OUTLET PRESS.		PSIG	4.78	8.2	13.7	20.0	30.3	33.6	9
MAIN BLEED UPST. PRESS. TOTAL		PSIG	12.0	19.0	29.5	41.0	58.5	66.0	22
JET PIPE TEMPERATURE	2	°C	240	252	271	328	391	430	30
	3	°C	220	244	269	300	361	420	30
	4	°C	220	229	802	318	379	425	30
	5	°C	/	/	/	/	/	/	30
	6	°C	/	/	/	/	/	/	30
	7	°C	/	/	/	/	/	/	30
LP COMP. OUTLET TEMP.	STBD.	°C	26	40	60	83	112	120	10
	PORT	°C	26	40	60	82	119	120	10
HP COMP. OUTLET TEMP.	PORT	°C	100	133	174	207	252	267	16
	STBD.	°C	96	128	166	201	241	257	16
A-S BLEED TEMPERATURE	STBD.	°C	26	42	62	84	88	95	12
	PORT	°C	26	42	62	85	67	70	14
MAIN BLEED UPST. TEMPERATURE		°C	94	127	165	201	243	262	20
MAIN BLEED ORIFICE TEMP.		°C	80	105	141	175	220	235	21
ENGINE VIBRATION (DISPLACEMENT)	1		.82	1.0	.6	.8	.7	1.15	
	2		/	/	/	/	/	/	
	3		.6	.6	.85	.85	.8	.8	
	4		/	/	/	/	/	/	
	5		/	/	/	/	/	/	
THRUST		LBF	1180	1925	3150	4970	8225	9575	34
FUEL INLET TEMPERATURE		°C	28.0	7.0	+1.5	+1.0	+.2	0	24
ENG. AIR INLET TEMP.	1	°C	-1.0	-4.0	-4.5	-4.5	-3.0	-3.2	8
	2	°C	-4.0	-6.0	-6.0	-6.5	-2.8	-3.1	8
	3	°C	-3.5	-4.0	-4.0	-3.5	-5.5	-6.0	8
	4	°C	-9.0	-9.5	-3.5	-5.0	+1.1	+2.7	8
CELL DEPRESSION	UPSTR.	"H2O	.05	.10	.20	.3	.5	.6	6
	DWNSTR.	"H2O	/	/	/	/	/	/	6
ENGINE AIR INLET STATIC PRESS.		"H2O	6.4	10.9	19.0	29.8	44.2	51.5	7
A-S BLEED PRESSURE	PORT	"MB	5.25	9.35	18.2	30.4	•	0	13
	STBD.	"MB	5.0	9.10	17.5	29.0	0	0	11
MAIN BLEED PRESS. DIFF.		"MB	10.2	14.9	20.3	27.5	36.0	40.5	19
OIL TANK BREATHER PRESS.		"MB	.6	.85	1.4	2.25	3.9	4.8	

TEST USED IN SAMPLE OUTPUT SHEET

Preceding page blank

J75 DATA REDUCTION AND CYCLE PROGRAM

PCD. NO 3

INPUT DATA

RUN NO 29.1026 DATE 15/06/71

N1	0.674											
N2	0.840		N1 4746.(69.8%)				N2 7610.(87.0%)					
BARO	29.62											
TBARO	23.50		P	T	W	PR	PL	EI	EO	ASBL	MBL	
PLTC	0.30	INLT										
P2S	29.80		1.000	14.70	268.0	178.83			1.0000			
T2T	-4.38	LP										
P3T	20.00	COMP										
T3T	83.00		2.371	34.85	381.7	178.83	2.371	0.00	0.8585	0.0000		
PASTST	29.00									10.07(5.6%)	—— ANTI-SURGE BLEED	
PASTPT	30.40	HP										
TASTST	84.00	COMP										
TASTPT	85.00		6.072	89.23	511.4	168.76	2.561	0.00	0.8914	0.0000		
P4T	74.00										15.38(8.6%) —— MAIN BLEED	
T4T	204.00	COMB										
PUP	40.00		5.768	84.77	873.5	154.83	0.000	0.05	0.0000	0.9800		
DELP	27.50		5.504	80.88	901.1							
TUP	201.00	HP										
TCR	175.00	TURB										
WF	4956.00		2.684	39.45	772.7	154.83	2.050	0.00	0.8500	0.0000		
TFIN	1.00	LP										
PLCC	0.05	TURB										
ETACC	0.58		1.435	21.09	673.3	154.83	1.871	0.00	0.8500	0.0000		
PLAPT	0.60	NOZL										
ETAPPT	0.85		1.000	14.70	615.0	154.83	1.404	0.021	0.0000	0.9600	AREA 535.45 —— INCREASED PROPELLING NOZZLE AREA (x 1.075)	
P7T	12.90											
T7T	355.00											
PLAPT	0.00					MEASURED	CALCULATED	DIFF.(%)				
ETALPT	0.85											
ETAN	0.96				THRUST	5005.02	5367.98	7.25				
XAMC	4970.00											
MBIND	1				SPEC. THRUST	27.99						
PUPT	41.00											
CD	1.0000				FUEL FLOW	5249.52						
					SFC	1.0489	0.9779	-6.76				

BLEED AIR SUPPLY

41.39 PSIG 235.2 C 15.38 LB/SEC 1520.6 HP

N1 69.8 % MBL 8.6 %

APPENDIX B

SAMPLE INPUT AND OUTPUT SHEETS FROM THE OFF-DESIGN-POINT (O.D.P.) PERFORMANCE PREDICTION PROGRAM

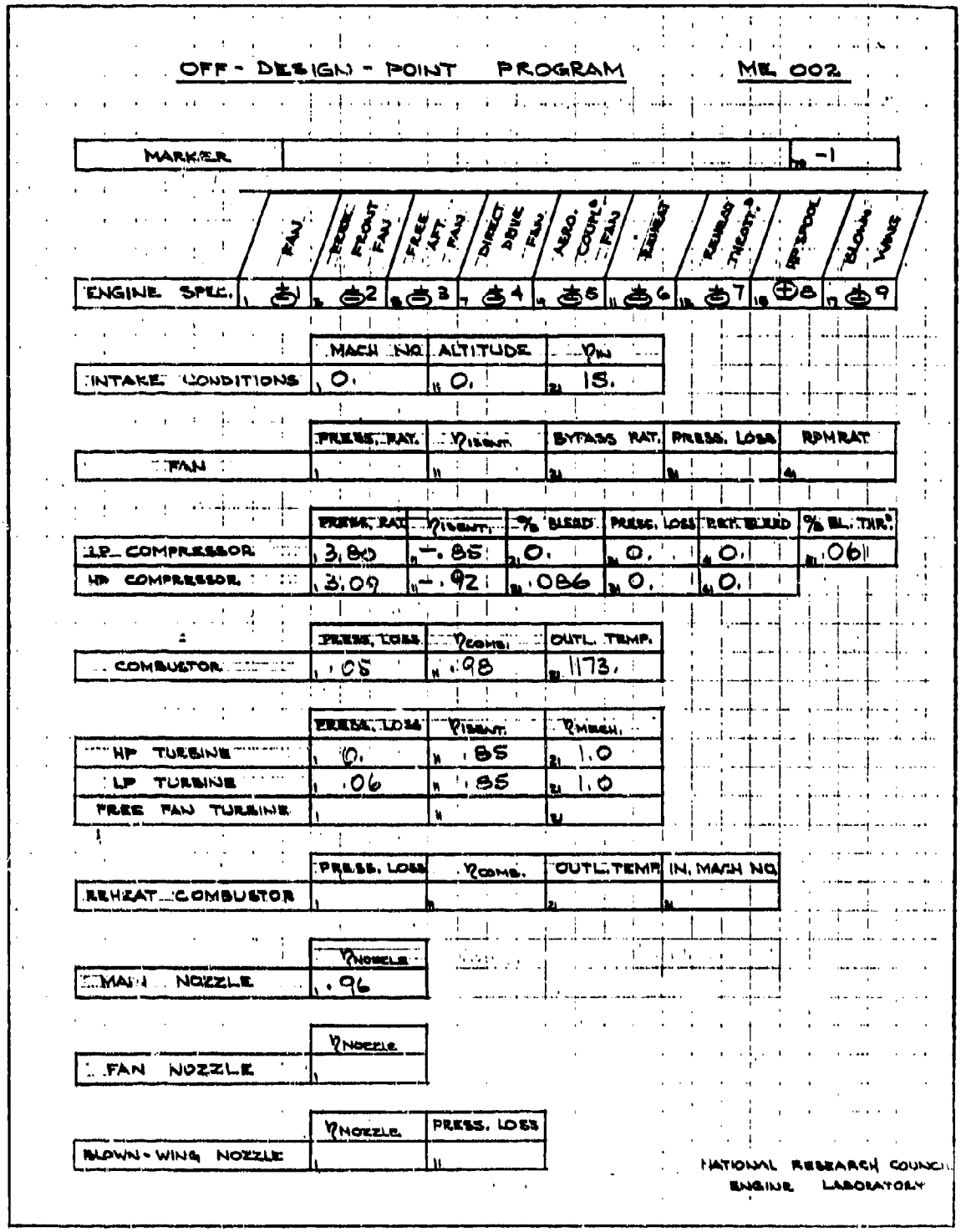

OFF - DESIGN - POINT PROGRAM ME 002

MARKER		-1

ENGINE SPEC.	1 FAN	2 TWIN FRONT FAN	3 FREE LIFT FAN	4 DIRECT DRIVE FAN	5 ASSO. COMP. FAN	6 TURBOJET	7 REHEAT TURBOJET	8 TURBOPROP	9 BLOWN WING

	MACH NO.	ALTITUDE	γ_{IN}
INTAKE CONDITIONS	0.	0.	1.5.

	PRESS. RAT.	$\gamma_{ISENT.}$	BYPASS RAT.	PRESS. LOSS	RPM RAT.
FAN					

	PRESS. RAT.	$\gamma_{ISENT.}$	% BLEED	PRESS. LOSS	REINJ. BLEED	% BL. THR.
LP COMPRESSOR	3.80	.85	0.	0.	0.	.06
HP COMPRESSOR	3.09	.92	.086	0.	0.	

	PRESS. LOSS	$\gamma_{COMB.}$	OUTL. TEMP.
COMBUSTOR	.05	.98	1173.

	PRESS. LOSS	$\gamma_{ISENT.}$	$\gamma_{MECH.}$
HP TURBINE	0.	.85	1.0
LP TURBINE	.06	.85	1.0
FREE FAN TURBINE			

	PRESS. LOSS	$\gamma_{COMB.}$	OUTL. TEMP.	IN. MACH NO.
REHEAT COMBUSTOR				

	γ_{NOZZLE}
MAIN NOZZLE	.96

	γ_{NOZZLE}
FAN NOZZLE	

	γ_{NOZZLE}	PRESS. LOSS
BLOWN-WING NOZZLE		

NATIONAL RESEARCH COUNCIL
ENGINE LABORATORY

Preceding page blank

	P	T	W	AR	MO	MI	PR	PL	EI	EO	BL
INLT											
	0.999	288.1		15.0 FT		0.000				1.000	
LP CCMP											
	2.381	385.5	0.6570	0.0000	0.000	0.000	2.382	0.000	0.8308	0.8500	0.043
HP CCMP											
	6.011	511.8	0.5971	0.0000	0.000	0.000	2.525	0.000	0.9092	0.9200	0.060
CCMB											
	5.711	883.4	0.6029	0.0000	0.000	0.000	0.000	0.050	0.0000	0.9800	0.000
HP TURB											
	2.800	756.0	0.6029	0.5463	0.000	1.000	0.000	0.000	0.8500	1.0000	0.000
LP TURB											
	1.345	653.7	0.6029	1.0287	0.000	1.000	0.000	0.060	0.8500	1.0000	0.000
NOZL											
	0.999	603.7	0.6029	2.2159	0.672	0.000	0.000	0.000	0.0000	0.9600	0.000
BLOW NOZL											
	1.258	321.5	0.0599	0.0849	1.000	0.000	0.000	0.000	0.0000	0.0000	0.000

	HCT	FAN	BLCK	OVERALL NET
SPECIFIC THRUST	30.158	0.000	0.000	27.612

RELATIVE THRUST	100.00%	0.00%	0.00%	XALT/XSLS 0.3015

SFC 1.6881

TURBOJET

NSLS 0.76000 NFPSLS 0.89770 NCSLS 0.69971 NFANSLS 0.00000

4 ECCPS

LP SPOOL SPEED : 70 %

NOZZLE AREA INCREASE : 7.5 %

MAIN BLEED : 8.6 %

ANTI-SURGE BLEED : 6.1 %

AT W_{inj} (100%) = 258 $\frac{Lbm}{Sec}$:

THRUST = 4987 Lb_f

FUEL FLOW RATE = 5426 $\frac{Lbm}{HR}$